Advances in Colloid and Interface Science 302 (2022) 102620

Contents lists available at ScienceDirect

Advances in Colloid and Interface Science

journal homepage: www.elsevier.com/locate/cis

Historical Perspective

A broad perspective to particle-laden fluid interfaces systems: from chemically homogeneous particles to active colloids

Eduardo Guzmán [a,b,*], Fernando Martínez-Pedrero [a,**], Carles Calero [c,d], Armando Maestro [e,f], Francisco Ortega [a,b], Ramón G. Rubio [a,b,*]

[a] Departamento de Química Física, Facultad de Ciencias Químicas, Universidad Complutense de Madrid, Ciudad Universitaria s/n, 28040 Madrid, Spain
[b] Unidad de Materia Condensada, Instituto Pluridisciplinar, Universidad Complutense de Madrid, Paseo Juan XXIII 1, 28040 Madrid, Spain
[c] Departament de Física de la Matèria Condensada, Facultat de Física, Universitat de Barcelona, Avenida Diagonal 647, 08028 Barcelona, Spain
[d] Institut de Nanociència i Nanotecnologia, IN2UB, Universitat de Barcelona, Avenida, Diagonal 647, 08028 Barcelona, Spain
[e] Centro de Fisica de Materiales (CSIC, UPV/EHU)-Materials Physics Center MPC, Paseo Manuel de Lardizabal 5, 20018 San Sebastián, Spain
[f] IKERBASQUE—Basque Foundation for Science, Plaza Euskadi 5, 48009 Bilbao, Spain

ARTICLE INFO

Keywords:
Particle
fluid interfaces
contact angle
dynamics
active particles
rheology

ABSTRACT

Particles adsorbed to fluid interfaces are ubiquitous in industry, nature or life. The wide range of properties arising from the assembly of particles at fluid interface has stimulated an intense research activity on shed light to the most fundamental physico-chemical aspects of these systems. These include the mechanisms driving the equilibration of the interfacial layers, trapping energy, specific inter-particle interactions and the response of the particle-laden interface to mechanical perturbations and flows. The understanding of the physico-chemistry of particle-laden interfaces becomes essential for taking advantage of the particle capacity to stabilize interfaces for the preparation of different dispersed systems (emulsions, foams or colloidosomes) and the fabrication of new reconfigurable interface-dominated devices. This review presents a detailed overview of the physico-chemical aspects that determine the behavior of particles trapped at fluid interfaces. This has been combined with some examples of real and potential applications of these systems in technological and industrial fields. It is expected that this information can provide a general perspective of the topic that can be exploited for researchers and technologist non-specialized in the study of particle-laden interfaces, or for experienced researcher seeking new questions to solve.

1. Introduction

Adsorption and self-assembly of nanoparticles and microparticles at fluid interfaces are widely exploited phenomena on different technological and industrial purposes. This may be understood considering that fluid interfaces provide a suitable environment for the quasi-2D confinement of particles, which results extremely useful for guiding the fabrication of soft and reconfigurable interface-dominated devices [1,2]. In fact, particle-laden interface has been used as support of novel applications which range from the stabilization the stabilization of dispersed systems, including emulsions (Pickering emulsions or bijels), foams, liquid marbles or colloidosomes, to the production of novel nanoporous membranes for filtration or encapsulation [3–6] and the fabrication of functional materials with different electrical, optical, or magnetic properties [7–9]. The accumulation, and quasi-2D confinement, of colloids at fluid interfaces leads to the emergence of completely new behaviors and properties, e.g., intriguing 2D phase transitions or anomalous rheological responses. These cannot be easily explained in terms of the physico-chemical concepts traditionally used in the description of their 3D counterparts, and require to consider thermodynamics aspects acting at the molecular scale with mechanical ones operating at the microscale or even larger distances, which are strongly determined by the characteristics of the particles and the nature of the fluids composing the interface [10,11]. The distinctive features of particle-laden interfaces with respect to those stabilized with surfactants, can be understood considering that: (i) particles are frequently

* Corresponding author at: Departamento de Química Física, Facultad de Ciencias Químicas, Universidad Complutense de Madrid, Ciudad Universitaria s/n, 28040 Madrid, Spain.
** Corresponding author.
E-mail addresses: eduardogs@quim.ucm.es (E. Guzmán), fernandm@ucm.es (F. Martínez-Pedrero), rgrubio@quim.ucm.es (R.G. Rubio).

https://doi.org/10.1016/j.cis.2022.102620
Received 4 December 2021; Received in revised form 22 February 2022; Accepted 23 February 2022
Available online 3 March 2022

chemically isotropic objects (Janus particles and patchy colloids are exceptions that introduce some specificities); (ii) particles do not tend to aggregate in bulk to form well-defined supramolecular systems such as micelles, and (iii) most of the adsorbed partices hardly undergo desorption or bending processes [12–15]. The above aspects, together with the effect of colloidal interactions between particles, some of them arising specifically at interfaces, or between the particles and the interfaces, determine the adsorption kinetics and self-organization of adsorbed particles [16–18].

The understanding of phenomena involving the interactions of particles with fluid interfaces has advanced significantly since the seminal studies of Ramsdem [19] and Pickering [20], in which some of the most fundamental aspects underlying the physico-chemistry of particle-laden fluid interfaces were introduced. Nowadays, the development of new synthesis routes, which have enabled the controlled fabrication of many types of particles that differ in shape, size (ranging from a few nanometers to several micrometers) or surface chemistry has opened new avenues on the understanding of the physico-chemical behavior of particle-laden interfaces [21]. Controlling the physicochemical and structural characteristics of particles also greatly expands the phenomena arising from adsorption and particle assembly at fluid interfaces, while allowing the behavior of particle-laden fluid interfaces to be modulated almost at will [16]. On the other hand, in the last years that the understanding the fundamental aspects of particle adsorption/desorption at fluid interfaces, such as the dynamics of binding, requires experiments that monitor the motion of controllable particles during the process [22]. Nevertheless, there are many aspects of the behavior of particle-charged fluid interfaces that remain unclear, which continues to stimulate the research aimed to the understanding of the processes of particle adsorption at fluid interfaces and the physico-chemical properties of the resulting layers, such as their response against mechanical stresses.

The last decade has been fruitful in advancing the knowledge of particle-laden interfaces, as reflected in the numerous published reviews on specific aspects of this type of systems, e.g., contact angle [23–25], mechanical response [11,26–35], the dynamics of particles trapped at fluid interfaces [36,37], active and externally actuated particles [8,38], the interaction of particle layers with biological interfaces [39,40] or the development of particular applications (stabilization of emulsions and foams, interface-dominated devices or prevention of coffee-ring effect) [1,2,5,14,15,18,41]. This review attempts to provide an integrative view of the behavior of particle-laden fluid interfaces that may help researchers and technologists in the understanding of fundamental and applicative aspects of this type of systems.

2. A brief approach to the adsorption and self-organization of particles at fluid interfaces

This section tries to provide a description of the two processes that are indispensable in the formation of any particle-laden fluid interface, regardless of the specific nature of the colloidal objects or the fluid interface: (i) the transport of colloidal particles to the interface, and (ii) the breach of the interface as a result of particle protrusion. As soon as the particles enter into contact with the interface, their penetration into the interface is mainly driven by the reduction of contact area between the two fluid phases, which leads to the minimization of the unfavorable fluid/fluid interactions and the reduction of the total free energy of the system [13]. This energy reduction in turn contributes to guarantee the interfacial stabilization.

2.1. Interaction between particles and the interface

Particle-interface interactions can be expected to be relevant as soon as the particle is transported to the vicinity of the interface. Since most of the particles of interest hold surface charges that lead to the emergence of electrical double layer forces, and both the water/vapor and water/non-polar fluid interfaces exhibit a negative effective charge [42], the adsorption of negative charged particles at the fluid interface is expected to occur very slowly, or does not occur [43], while the adsorption of positively charged particles is usually strongly favored, although the diffusion process can be very slow. Furthermore, as the particles approach the interface made up of fluid with different dielectric constant, they experience repulsive image charge repulsions and other confinement effects, that distort the electrical double layer of the particles near the interface [43–45]. In fact, when a charged colloidal particle approaches to the interface between fluids having very different values of dielectric constants, a new type of electrostatic interaction emerges. This can be rationalized considering that a particle with a defined charge close to the interface (at a distance d) perceives a force equivalent to that what would be expected for its interaction with a similar particle placed in the other phase at similar distance to the interface, i.e., the particle and the image particle are separated by a distance $2d$ [46]. For charged particles suspended in water near an interface with air or oil, the image charge interactions are always repulsive, independently of the sign of the particle charge. This allows modulating the adsorption by varying the ionic strength of the dispersion [47], because the increase of the electrolyte concentration screens the electrostatic repulsion between the particles and the interface. On the other side, when the sign of the image charge is opposite to that of the particle, the interaction results attractive.

Moreover, short range van der Waals particle-interface interactions arise from the combination of three different contributions (i) interactions between permanent dipoles (Keesom interactions); (ii) interactions between permanent and induced dipoles (Debye interactions), and (iii) interactions involving fluctuating dipoles (London interactions). The overall interaction can be parameterized in terms of the Hamaker constants of the three materials, i.e., those that compose the particle and the two fluids. Thus, for a smooth and chemically homogeneous spherical particle of radius R completely immersed in one of the fluids (fluid 1), but placed very close to the fluid interface, it is possible to define the Hamaker constant for the interaction between the solid particle and the second fluid (fluid 2) through a very thin layer of fluid 1, A_{P12}, as follows [47]

$$A_{P12} \approx \left(\sqrt{A_{PP}} - \sqrt{A_{11}}\right)\left(\sqrt{A_{22}} - \sqrt{A_{11}}\right) \tag{1}$$

where A_{PP}, A_{11} and A_{22} are the Hamaker constants of the particles, and fluids 1 and 2, respectively. Note that A_{P12} is always positive, so the van der Waals particle-interface interactions are always attractive [48]. The different contributions to the Hamaker constant A_{P12} can be related, using Lifshitz's theory, to the dielectric permittivity ε and refractive indices of the two fluid and the particles [49]. Considering dielectric media with identical adsorption frequency (ν_e), it is possible to obtain the following approximate expression,

$$A_{P12} \approx \frac{3}{4}k_B T\left(\frac{\varepsilon_P - \varepsilon_1}{\varepsilon_P + \varepsilon_1}\right)\left(\frac{\varepsilon_2 - \varepsilon_1}{\varepsilon_2 + \varepsilon_1}\right) + \frac{3h\nu_e}{8\sqrt{2}}\frac{\left(n_P^2 - n_1^2\right)\left(n_2^2 - n_1^2\right)}{\sqrt{n_P^2 + n_1^2}\sqrt{n_2^2 + n_1^2}\left(\sqrt{n_P^2 + n_1^2} + \sqrt{n_2^2 + n_1^2}\right)} \tag{2}$$

where h is the Planck's constant; and ε_i and n_i are, respectively, the static (zero-frequency) dielectric constants, and the refractive indices in the visible range, and k_B and T the Boltzmann constant and the absolute temperature, respectively. Here, the sub-indexes P, 1 and 2 refer to the particle and the fluids 1 and 2. In Equation 2, the first term accounts for the Keesom and Debye contribution, and are always lower than ¾k_BT [48,49], while the second term incorporates the contribution of London interactions, which is commonly the most significant.

2.2. Adsorption dynamics of particles to the fluid interface

The different transport mechanisms that promote the approach of micron-sized particles from a bulk phase to the fluid interface can be classified into (i) spontaneous (including Brownian diffusion, sedimentation or flotation) or (ii) externally triggered (field-induced or hydrodynamically guided) [35,36,50–52]. When diffusion is the main mechanism, gravity often plays an important role due to the particle density. In the dilute regime, where interactions between particles can be neglected, the terminal velocity of particle settling is determined by a balance between the gravitational and viscous forces. According to the Stokes' law [53], the terminal velocity of the falling particles is given by

$$v_{St} = \frac{2R(\rho_p - \rho_1)g}{9\eta} \tag{3}$$

where ρ_p and ρ_1 are the densities of the particles and the fluid phase, respectively, g *is* the gravitational acceleration and η the dynamic viscosity. The competition between gravity and diffusion is evaluated by means of the Péclet number, a dimensionless number which evaluates the ratio of convective to diffusive transport defined as

$$Pe = \frac{Rv_{St}}{D} \tag{4}$$

Here, D is the bulk diffusion coefficient of the particles. Péclet number assumes values about 0.1 for silica particles of 1 μm suspended in water, whereas particles of 10 μm presents a Péclet number almost 4 orders of magnitude higher. Therefore, it is clear that the increase of the particle size may favor the ballistic movement of the particles over diffusive transport [29].

If gravitational forces can be neglected, $Pe << 1$, and diffusion occurs in the absence of adsorption barriers and external flow fields, particles transport to the interface can be described by a Fickian-like diffusion law, in a similar manner to the description of molecular surfactant adsorption developed by Ward-Tordai [45]. Thus, the mass transport rate is given by

$$\frac{\partial c(x,t)}{\partial t} = D\frac{\partial^2 c(x,t)}{\partial x^2} \tag{5}$$

with $c(t, x)$ being the bulk concentration, x the distance to the fluid interface and t the diffusion time, respectively. Assuming an initially homogeneous particle bulk concentration $c(x, 0) = c_\infty$, then the boundary condition for the adsorption kinetics is given by

$$\frac{\partial \Gamma}{\partial t} = D\left[\frac{\partial c(x,t)}{\partial x}\right]_{x=0} \tag{6}$$

where $\Gamma(t)$ is defined as the time-dependent interfacial excess of particles adsorbed at the interface, and $\Gamma(0) = 0$. Thus, taking the Ward-Tordai approach under conditions of irreversible adsorption and without the presence of any adsorption barrier, and considering a complete depletion of the particles contained in the sublayer and small change of the bulk concentration, i.e., $c(\infty, t) \rightarrow c_\infty$, the combination of Equations (5) and (6) leads to [45]

$$\Gamma(t) = 2c_\infty\sqrt{\frac{Dt}{\pi}} \tag{7}$$

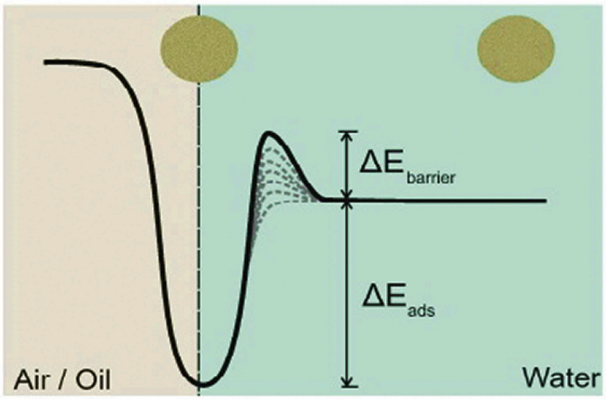

Fig. 1. Simplified representation of the energetic landscape emerging for adsorption of a particle to a fluid interface. The energy barrier $\Delta E_{barrier}$ usually increases with the interfacial coverage due to the increase of the electrical potential and, thus the Debye length. Reprinted from Deshmukh et al. [35], Copyright (2015), with permission from Elsevier.

However, the presence of electrostatic barriers between the particles in the bulk phase and the fluid interface is very common and requires an extension of the framework described above (see Fig. 1). The effect of the electrostatic barrier on the time evolution of the surface concentration can be approximate by including an effective diffusivity [54]

$$\Gamma(t) = -2c_\infty \Delta E_p\sqrt{\frac{D_{eff}t}{\pi}} \tag{8}$$

where ΔE_p is the reduction in interfacial energy associated with the screening of the fluid–fluid interface and D_{eff} is the effective diffusion coefficient, defined as

$$D_{eff} = Dexp\left(-\frac{\Delta E_{barrier}}{k_BT}\right) \tag{9}$$

with $\Delta E_{barrier}$ being the height of the energy barrier of the energetic landscape emerging for adsorption of a particle to a fluid interface [54].

On the other hand, Schwenke et al. [50] found that the adsorption kinetics is also slowed down with the increase of interfacial coverage in agreement with the results by Deshmukh et al. [35]. The latter reported the existence of two distinct regimes in the time evolution of the adsorption of microgel particles at water/vapor interfaces: (i) a short-term regime, where adsorption is controlled by diffusion, and (ii) a long-term slower regime, limited by the increase in coverage and the associated steric barrier. This is similar to what was found for the adsorption of several surface active water-soluble polymers, where a first initial fast diffusion of the molecules from the solution to the subsurface is followed by a reorganization of the molecules, which is limited by the steric hindrance induced by the adsorbed molecules and drives the equilibration of the interfacial layer [55].

2.3. The meaning of the interfacial tension for particle-laden interfaces

Fluid interfaces are commonly considered to be in the molecular scale, with their density profile being analytically described by a hyperbolic-tangent function [56,57]. However, in most of the cases, the size of the particles is much bigger than the interface width, which does not allow one to use the classical microscopic description for explaining the decrease of the interfacial tension of clean fluid/fluid interface γ_{12} as result of the particle trapping at the interface [2]. Instead, it is usually described in terms of the decrease of the free energy associated with the reduction of the contact area between the two fluid phases [58–61]. Considering a particle constituted by a material having the same interfacial tension with both fluid phases, it is expected that its adsorption at the interface occurs because it leads to a decrease of the direct contact

between the two fluids, without any additional energetic costs due to the contact of the particles with the fluids [40].

The above picture requires a description of the interfacial tension using a macroscopic perspective, which considers that the surface tension of a particle-laden interface is not truly a thermodynamic magnitude, and should be defined as an effective one [2,13]. Thus, the reduction of the effective interfacial tension is due to the emergence of a 2D lateral pressure Π, originated from an intricate balance between the entropy and inter-particle interactions, which counteracts the contraction of the interfacial area associated with the interfacial tension. This leads to a decrease of the interfacial tension $\gamma=\gamma_{12}-\Pi$, as the interfacial packing of the particle-laden interface increases, which is measurable using some of the common methodological approaches used for interfacial tension evaluation [2,13,61–65].

Further analysis of the change of the interfacial tension with the trapping of particles point out that the reduction of the area between the two fluids is directly correlated to the interfacial excess of particles, Γ, and, consequently, to the total number of particles, N, which leads to a definition of the effective interfacial tension for a particle-laden interface as

$$\gamma = \left(\frac{\partial G_\gamma}{\partial A}\right)_\Gamma = \left(\frac{\partial G_\gamma}{\partial A}\right)_{N,T,p} \tag{10}$$

The trapping of a particle to a fluid/fluid interface is associated with an energy change ΔE_p, which leads to a reduction of the interfacial tension $\Delta E_p/A$. Therefore, the effective interfacial tension of the particle-laden fluid/fluid interface in absence of any contribution of the inter-particle interactions, i.e., at low interfacial excess concentration, is defined by [66]

$$\gamma = \gamma_{12} - \Pi(\Gamma) \tag{11}$$

with $\Pi(\Gamma) = \Gamma|\Delta E_p|$.

2.3.1. Thermodynamics model for describing particle-laden fluid interfaces

The definition of the interfacial tension for a particle-laden interface as an effective magnitude makes it difficult to obtain a physically insightful thermodynamic description of such systems. The definition of the interfacial tension for a particle-laden interface as an effective magnitude makes it difficult to obtain a physicaly insightful thermodynamic description of such systems. This makes it necessary to consider the role of the interactions between the particles trapped at the interface and between the particles and the interface, together with the wetting and the chemical potential of the particles [2,31,32]. However, this is not trivial for particle trapped at fluid interfaces, because, unlike molecular species, the particle size is very different from that of the solvent molecules [67], so, a new thermodynamic framework is needed.

Henderson [68] proposed the first thermodynamic description of particle-laden fluid interface, considering that the interfacial film was composed of a 2D colloidal fluid of hard disc-shaped particles, in which only the role of the volume interactions was considered. However, this model did not provide a realistic picture because it did not include the changes on the surface pressure at low interfacial coverage due to long-range electrostatic inter-particle repulsions. The simplification adopted in the previous model was partially overcome by the one introduced by Binks [68], who combined Volmer and van der Waals equations were combined. This model accounts for the absence of lateral interactions between particles at low packing density and short-range lateral interactions between them at high packing density, respectively. Besides, it includes two additional assumptions: (i) the behavior of the particles is reminiscent of that expected for a surfactant molecule, and (ii) the area occupied by the adsorbed particle at the fluid interface is the area projected by the adsorbed particle on the fluid interface, i.e., its geometrical area. However, this model did still not consider the role of interactions between particles at long separation distances, so it continued to provide unrealistic predictions on the dependence of the interfacial tension with the packing density. Finally, the different length-scales involved in particle-laden and surfactant-laden interfaces were an additional contribution to the failure of the model, that predicted changes in the surface pressure only at high values of the interfacial coverage (50-70% of the total interfacial area when the monolayer was composed of small particles, diameter < 1nm).

A more realistic thermodynamic description of particle-laden fluid interfaces was proposed by the group of Miller [69,70]. They extended their previous work on the thermodynamic description of protein-laden fluid interfaces [71] by including specific aspects enabling for a description of the behavior of particles trapped at the fluid interface. According to this model, the interfacial pressure of the particle-laden interface is given by

$$\Pi = \frac{k_B T}{\omega_0}\left[ln\left(1-\frac{\omega}{A}\right)+\left(\frac{\omega}{A}\right)\right] - \Pi_{coh} \tag{12}$$

where ω/A and ω_0 are the fraction of area covers by particles and the area of a single particle, respectively, and Π_{coh} is the cohesion pressure, a parameter that accounts for the contribution of the inter-particle interactions to the packing of the particle-laden interface. Application of the above model provides a suitable description of the change in interfacial tension with packing density, regardless of the chemical nature and dimensions of the particles in question, even when the interfacial coverages is far from a close-packed state.

More recently, Hua et al. [72] introduced an alternative model that accounts for: (i) the impact of the reduction of the contact line between the two fluid phases on the interfacial tension, and (ii) the inter-particle interactions. The contribution of the reduction of the contact line on the surface pressure due to particle adsorption, Π_p, was obtained in terms of the particle density at the fluid interface, whereas the contribution associated with the inter-particle interactions, $\Pi_{p\text{-}p}$, was assessed, assuming a linear additivity $\Pi = \Pi_p + \Pi_{p\text{-}p}$, by evaluating the change of the interfacial pressure of the 2D particle-laden interface. Thus, combining these contributions with the Frumkim model [57], which considers the non-ideality of the interactions, and assuming thermodynamic equilibrium, where the Gibbs relationship is fulfilled, the interfacial pressure is given by the following expression [73]

$$\Pi = -k_B T \Gamma_\infty \left[ln(1-\vartheta) - 0.5K\vartheta^2\right] \tag{13}$$

where Γ_∞ and K are the interfacial excess concentration for a close-packed particle-laden interface and an inter-particle interaction constant, respectively. Here, $\vartheta=\Gamma/\Gamma_\infty$ represents the interfacial coverage, i.e., the affinity of the particles for the interface.

Finally, Groot and Stoyanov [74] proposed a model that introduces the dependence of the inter-particle interactions on the interfacial coverage density in the estimation of the interfacial pressure. According to this model, the latter is described by

$$\Pi = \frac{4k_B T}{\pi d^2}\left[\frac{byZ}{\lambda} - b_2\vartheta^2\right] \tag{14}$$

where d accounts for the range of the long-range interactions, Z is the compressibility factor [74], $(\lambda)^{1/2}\sqrt{\lambda}$ is the effective diameter of the particles, and b and b_2 are parameters accounting for the inter-particle interactions. This model has been successfully applied on the description of the collective behavior of soft particles adsorbed at fluid interfaces [75].

2.4. Wettability of particles at a fluid interface

The chemical anisotropy of surfactants, i.e., the existence of two moieties with different polarities and different affinity for fluid phases, is the main driving force for their attachment to fluid interfaces. The entropic penalty associated with the reduction of the degree of freedom in the orientation of the surfactant molecules, is counterbalanced by a

favorable enthalpic contribution, thus reducing the Gibbs free energy of the system. However for describing the entrapment of smooth, spherical and chemically isotropic particles at a fluid interface, particle wettability plays the essential role [29]. Entrapment of a particle at a fluid interface is only possible when the difference between the energies of the particle dispersed in one of the bulk phases and that of the particle trapped at the fluid interface exceeds the energy associated with thermal agitation k_BT. Assuming that the particle is small enough to neglect gravitational forces, the energy of a particle, whose center is located at an arbitrary distance z of the interface, is given by [1,25]

$$E(z) = \pi R^2 \gamma_{12}\left[\left(\frac{z}{R}\right)^2 + 2\left(\frac{\gamma_{P2}-\gamma_{P1}}{\gamma_{12}}\right)\left(\frac{z}{R}\right) + 2\left(\frac{\gamma_{P2}+\gamma_{P1}}{\gamma_{12}}\right) - 1\right] \quad (15)$$

where γ_{P1} and γ_{P2} are the interfacial tensions between the solid particles and the two fluid phases. Fig. 2 shows the dependence of the energy of a particle as a function of $z_0 = z/R$, with $z_0 = 1$ and $z_0 = -1$ corresponding to a particle completely immersed in the fluid 1 and 2, respectively, and $z_0 = 0$ to a particle placed in the interfacial plane.

The equilibrium position ${z_0}^{min}$, which corresponds to a particle mostly immersed in fluid 1 ($0<{z_0}^{min}<1$) or 2 ($-1<{z_0}^{min}<0$), is placed at the distance where the free energy is minimized, i.e., $\partial E/\partial z = 0$, and is given by [76]

$$z_0^{min} = \frac{\gamma_{P1}-\gamma_{P2}}{\gamma_{12}} R \quad (16)$$

At this point, the equilibrium condition of the forces acting at the contact line can be defined in terms of the three characteristic interfacial tensions, the interaction between the particle and both fluids and between the two fluid phases, simplifies to the Young-Dupre equation

$$0 = \gamma_{P1} - \gamma_{P2} - \gamma_{12} cos\theta \quad (17)$$

Here, the contact angle, θ, is defined as the angle between the plane tangent to the particle's surface and the interface at the line where the interface meets the solid, as shown in Fig. 3 [77].

Under these conditions, the equilibrium contact angle is completely determined by the three surface tensions

$$cos\theta = \frac{\gamma_{P1}-\gamma_{P2}}{\gamma_{12}} \quad (18)$$

From the previous equation, it follows that the particle adsorbs at the fluid interface only when the following inequality is met [13,25]

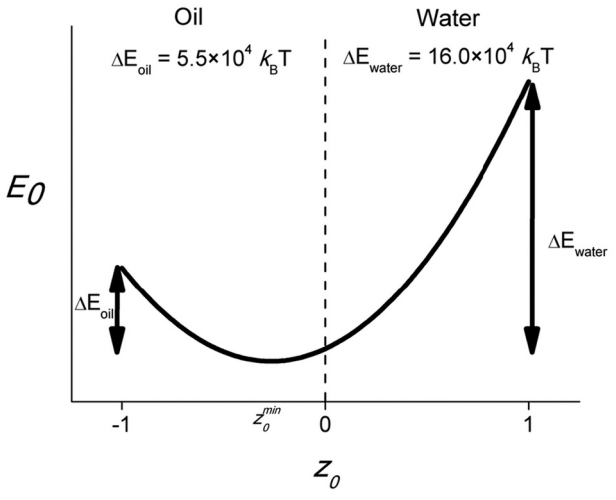

Fig. 2. Free energy of a spherical colloidal particle ($R = 50$ nm) as a function of its center relative to the hexadecane/water interface. The interfacial tensions are γ_{12}= 53.5 mN/m, γ_{P1}= 28.5 mN/m and γ_{P2}= 14.2 mN/m. Reprinted from Ballard et al. [25], Copyright (2019), with permission from The Royal Society of Chemistry.

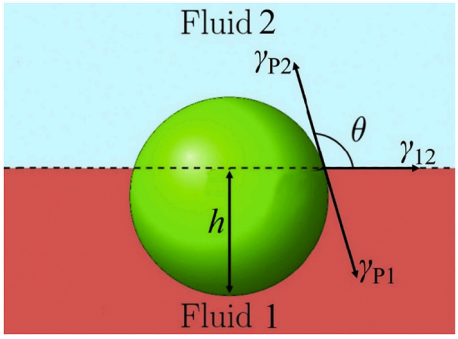

Fig. 3. Idealized representation of the position of a particle trapped at an arbitrary fluid/fluid interface. θ and R represent the contact angle, or relative wettability of the particle by the interface, and particle radius, respectively; γ_{P1} and γ_{P2} are the interfacial tensions between the solid particle and the two fluid phases, and γ_{12} the interfacial tensions corresponding to the fluid interface. Adapted from Davies et al. [77], Copyright (2014), with permission from American Institute of Physics.

$$|\gamma_{P2} - \gamma_{P1}| < \gamma_{12} \quad (19)$$

Hence, the contact angle plays the same role as the hydrophilic-lipophilic balance (HLB) of molecular surfactants [12,23], i.e., a parameter that provides information on the preferential partitioning of particles between the two fluid phases, and results from the different interaction of the particles with the two fluid phases [10,12,78].

It is possible to describe the trapping of colloidal particles at a fluid interface in terms of the intricate balance of interactions, e.g., van der Waals, polar and electrostatic interactions, and hydrodynamics forces that contribute to interfacial equilibrium [48,49]. For example, in charged particles the free energy per unit of area, associated with the formation of the electric double layer, ΔF_{DL}, leads to a change of the surface free energy $\gamma_{1P}=\gamma_{1P,0}+\Delta F_{DL}$ [79], where $\gamma_{1P,0}$ is the surface tension at the point of zero net charge. Introducing the above correction into Equation (18), the following expression is obtained

$$cos\theta = cos\theta_0 - \frac{\Delta F_{DL}}{\gamma_{12}} \quad (20)$$

Considering that in most cases the double layer forms spontaneously, $\Delta F_{DL} < 0$. Therefore, a smaller partitioning of the charged particles between the two media is expected than for an uncharged particle. If one of the fluids is water, particles are considered as hydrophilic when $\theta < 90°$, and they remain mainly submerged in water, while particles are considered hydrophobic when $\theta > 90°$, and they are predominantly submerged in the non-aqueous phase. The case in which the particles show a similar preference for both fluid phases is the so-called neutral wetting and is characterized by a contact angle of 90° (see Fig. 4).

For spherical and perfectly smooth particles, it is possible to find a simple geometrical relation connecting the contact angle and the protrusion height h of the particle into the less polar phase,

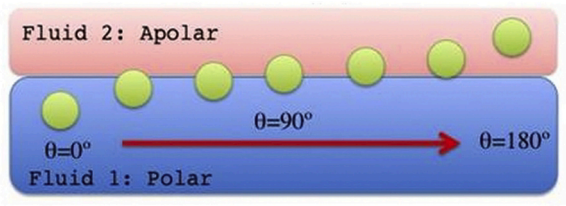

Fig. 4. Schematic showing the relative position of a colloidal particle in relation to the interfacial plane as a function of its contact angle. Reprinted from Maestro et al. [80], Copyright (2019), with permission from The Royal Society of Chemistry.

$$\theta = cos^{-1}[1 - h/R] \tag{21}$$

From equation (15), the energy change associated with the transference of a particle from a fluid phase to its equilibrium position, i.e. the so-called trapping energy, is given by [81]

$$\Delta E_p = -\frac{\pi R^2}{\gamma_{12}}(\gamma_{12} - (\gamma_{P1} - \gamma_{P2}))^2 \tag{22}$$

which for spherical particles can also be defined in terms of the contact angle as

$$\Delta E_p = -\pi R^2 \gamma_{12}(1 \pm cos\theta)^2 \tag{23}$$

where the ± signs in the bracket indicate the position of the particles in relation to the interfacial plane. According to Equation (23) particle trapping at fluid interfaces strongly depends on size. Fig. 5 shows the dependence of the entrapment energy on the contact angle, calculated with Equation (23), for two colloidal particles with different sizes, 10 nm and 1 μm, at an arbitrary fluid interface with $\gamma_{12} = 50$ mN/m.

The energetic landscape, resulting from the analysis of the contact angle and size dependences of the trapping energy, shows that the latter largely exceeds the thermal energy k_BT in most of the cases [82]. Therefore, the adsorption of micron-sized particles to a fluid interface can be considered as an irreversible process, with typical trapping energy values in the range between 10^6 k_BT and 10^7 k_BT. For the mentioned microparticles, adsorption is reversible only at very low values of the fluid/fluid interfacial tension $\gamma_{12,}$ and/or for cos$\theta \sim 1$. On the other hand, in particles with sizes smaller than 10 nm the trapping energy is of the order of several k_BT. This suggests that for particles with a very small size, the low value of the trapping energy can lead to a thermal-activated escape of the particles from the interface. Hence, small nanoparticles exhibit an adsorption-desorption equilibrium like that found in conventional molecular surfactants, polymers and proteins [83]. Fig. 6 shows the dependence of the detachment energy ($-\Delta E_p$) on the particle radius for the trapping of colloidal particles at an oil/water interface with $\gamma_{12} = 50$ mN/m, and a fixed value of $\theta = 90°$. The residence time of particles at the fluid interface is reduced with the decrease of the characteristic size of the adsorbed particles, which explains the facilitated displacement of small nanoparticles from the interface by the adsorption of particles with bigger size [84].

In most cases, micro-sized particles are irreversibly adsorbed, so that

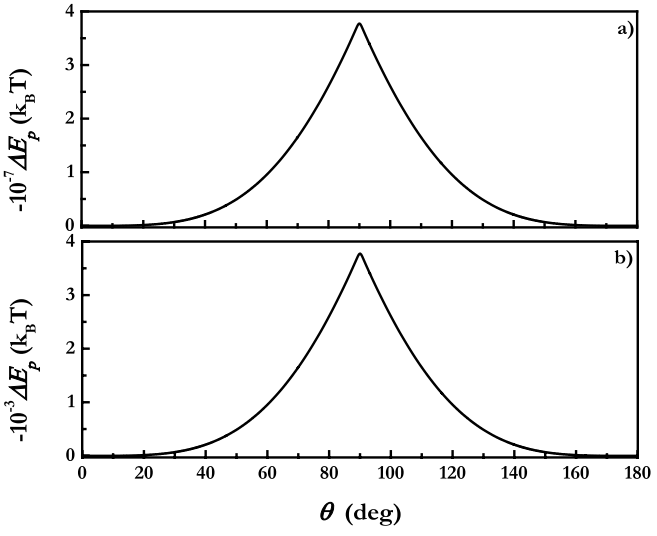

Fig. 5. Trapping energy for two colloidal particles with $R = 1$ μm (a) and $R = 10$ nm (b), at a fluid interface with $\gamma_{12} = 50$ mN/m, as function of the contact angle. Please, note the differences on the energy scales. Reprinted from Guzmán et al. [34], Copyright (2021), with permission from Institute of Physics.

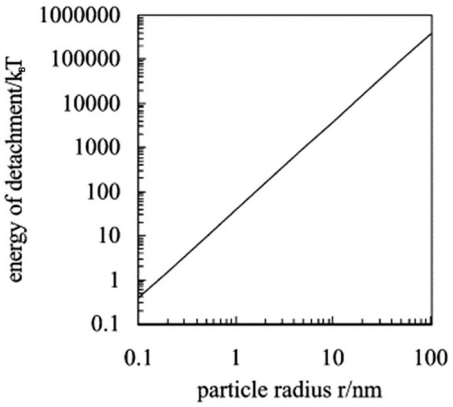

Fig. 6. Dependence of the detachment energy at 298 K for a particle adsorbed at a planar oil/water interface ($\gamma_{12} = 50$ mN/m) at a fixed contact angle $\theta = 90°$. Note the low energies for particles with radii smaller than 0.5 nm (close to that of molecular surfactants). Adapted from Binks [12], Copyright (2002), with permission from Elsevier.

the particles can only move freely within the interfacial plane. The existence of lateral mobility of the particles allows their rearrangement in a diffusive manner or after the application of external stimuli, which lays the foundation for the fabrication of new materials that can be reconfigured by adjusting the particle interactions/organization at the fluid interface [17,37]. This scenario largely differs from the one stablished when particles are set on liquid/solid interfaces [16], or even when particles are in the vicinity of a fluid interface but without actually being adsorbed [85]. The position of particles trapped at fluid interfaces undergoes fluctuations relative to the interfacial plane, when the interfacial and thermal energies are comparable, and deformations induced by interface capillary waves [84,86]. However, the motion of adsorbed particles along the direction perpendicular to the fluid interface induces the emergence of capillary forces that promote the reestablishment of the equilibrium position [87].

The entrapment of a colloidal particle in the interfacial plane separating two fluid phases requires that the interfacial tension forces can overcome the action of gravity [81]. The balance between these two contributions is typically defined in terms of the Bond or Eötvos number

$$Bo = \frac{\Delta\rho g 2R}{\gamma} \tag{24}$$

where $\Delta\rho$ denotes the difference between the density of the particle and the fluid. It should be noted that the gravitational contribution only is relevant for particles of several micrometers. For particles smaller than 10 μm, *Bo* assumes values well below unity, and hence the contribution of interfacial tension forces becomes dominant [88,89].

It should be noted that the reversible/irreversible character of the attachment of particles to the fluid interface, together with the value of the contact angle have an important impact on different physicochemical aspects associated with potential applications of particle-laden interfaces. Among them, the organization of the particles at the interface, the strength and nature of the interparticle interactions, the friction coefficient values in microrheology experiments, or the response of particle-laden fluid interfaces to external mechanical deformations, that govern the ability of particles to stabilize emulsions and foams [27,64,78,80,86,90–93].

2.4.1. Effect of line tension and particle roughness in the wetting of particles for fluid interfaces

The contributions of the particle roughness and/or the line tension to the wetting properties of the particles limit the applicability of Equation (18) to provide an appropriate description of particle entrapment at fluid interfaces [94]. The line tension is caused by the imbalance

between the intermolecular forces that operate within the three-phase contact line [95], and can be positive or negative, with a magnitude in the range between 1-100 pN [25]. The relative importance of its contribution can be assessed in terms of a dimensionless number defined as

$$Li = \frac{\tau}{\gamma_{12} L} \tag{25}$$

where τ and L are the line tension and the length of the contact line, respectively [96]. The role of the line tension in the wetting of particles can be included by modifying the Young's equation with the correction proposed by Bresme and Quirke [97], who introduced a dependence between both interfacial and line tensions on the contact angle of spherical smooth particles as follows

$$\frac{\gamma_{P1} - \gamma_{P2}}{cos\theta} - \gamma_{12} = -\frac{\tau}{Rsin\theta} \tag{26}$$

It follows from the above expression that the line tension influences the wettability of particles only for sizes below 20 nm [10,18,98–100]. Following arguments analogous to those developed in section 2.4, but including the contribution associated with the line tension, the energy change associated with the entrapment of a particle at the fluid interface can be defined as

$$\Delta E_p = \gamma_{12} cos\theta_\infty 2\pi R^2 (1 - cos\theta) + 2\tau\pi R sin\theta - \pi R^2 \gamma_{12} cos^2\theta \tag{27}$$

where θ_∞ is the contact angle provided by the Equation (18). When particles are in conditions of mechanical and thermal equilibrium, with $(\partial \Delta E_P/\partial\theta)_T = 0$, they are in the position dictated by the contact angle

$$cos\theta = cos\theta_\infty \left[1 - \frac{\tau}{R\gamma_{12}}\right]^{-1} \tag{28}$$

It should be noted that the minimization of the line tensionmodifies the wettability of non-spherical particles and their orientation at the interface [88,89,96]. For $\theta \to 90^\circ$, i.e., intermediate wetting conditions, it is possible to neglect the role of line tension, and Equation (28) becomes Equation (18). In such conditions, the line tension applies almost tangentially to the interface, and therefore its impact on the position of the particles in relation to the interficail plane becomes almost negligible [13,25]. When the contact angle differs significantly from 90°, the perpendicular component of the line tension assumes a relatively high value, becoming maximum for $\theta \to 0^\circ$ and $\theta \to 180^\circ$ [101], which leads to a positive contribution to the energy change associated with the trapping of the particle.

The assymetry of the shape and roughness of the particles increase the ratio between the contact line and the characteristic dimension of the particles [98], also modifying the wetting properties of colloidal particles by fluid interfaces [61,102], especially when the roughness of the particles is high and their size is small [103]. This modifications were studied theoretically by Nonomura and Komura [103] using the Cassie–Baxter model, associated to the emergence of pinning–depinning of the interface along the contact line.

2.4.2. *Tuning the contact angle of particles at a fluid interface*

The interfacial organization of the particles within the interface can be modulated by altering the wettability of the particles (see Fig. 7), and consequently the interparticle interactions.

Many physical and chemical tools are currently available to modify the wettability of colloidal particles and tune their interfacial organization. The most widespread strategy to modify the ability of particles to remain trapped at the fluid interface is the addition of different chemical additives, e.g., surfactants, polymers, salts or even low molecular weight compounds (e.g., alcohols), to the particle dispersion. These molecular species can decorate the particle surface through non-electrostatic, e.g., hydrogen bonds, electrostatic or van der Waals interactions [51,58,60,61,102,104–108].

For instance, due to a complex interplay between hydrophobic and non-covalent electrostatic interactions, it is possible to modify the wettability of the particles in situ by modifying the amount of surfactant added in the dispersion containing the colloidal particles, or in the second fluid [109]. The gradual addition of surfactants usually results in the appearance of different surfactant structures and the progressive increase in particle hydrophobicity. The maximum degree of particle hydrophobization is usually found for surfactant concentrations high enough to ensure neutralization of the surface charge of the particles. Any further increase of the surfactant concentration beyond the isoelectric point usually leads to rehydration of the particles. The decrease in contact angle is usually due to the formation of a surfactant bilayer on the surface of the particles through hydrophobic interactions between the alkyl tails of the surfactant molecules. This approach was explored by Maestro et al. [80] and Binks et al. [110], who added two different types of alkyltrimethylammonium bromide surfactants (hexadecyltrimethylammonium bromide, CTAB and dodecyltrimethylammonium bromide, DTAB) to dispersions containing silica nanoparticles to tune the assembly of silica nanoparticles at the water/steam interface. Binks et al. [111] extended the possibility of modifying the wettability of silica particles by the addition of a two tails surfactant (didecyldimethylammonium bromide). Obviously, the impact of the addition of surfactants on the wettability of particles is determined by the chemical nature of the particles. Deleurence et al. [112] studied the modification of hydrophobic anionic polystyrene and hydrophilic silica particles with a cationic surfactant. They found that polystyrene particles underwent a

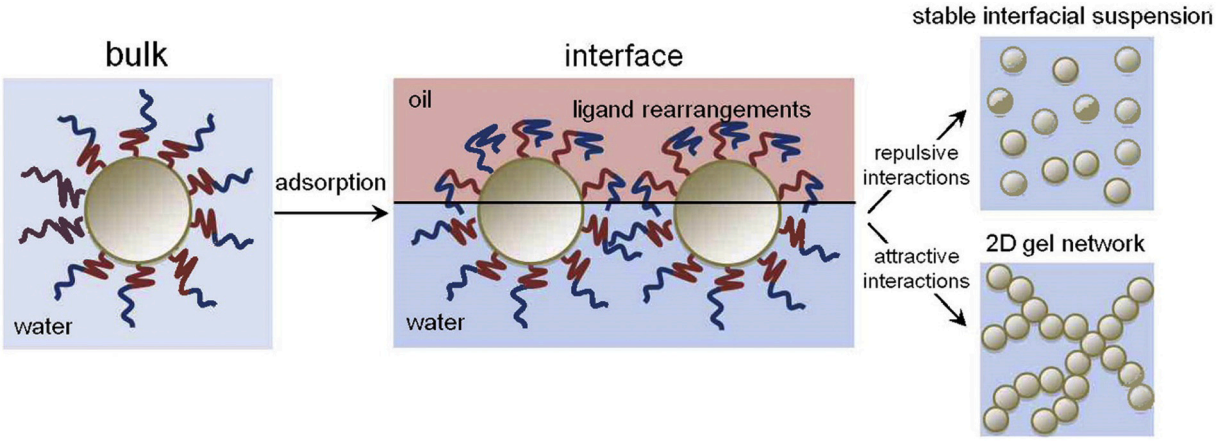

Fig. 7. Sketch showing the effect of the wettability of the particles on their organization at a fluid interface. Reprinted from Garbin et al. [93], Copyright (2012), with permission from Elsevier.

strong change in their contact angle. However, the contact angle of silica particles was not significantly modified, although there was a strong modification of the particle charge. Another example of the strong impact of the additives on the interfacial properties of particles can be found in the work by Perrin et al. [113]. They demonstrated that the addition of diethylene glycol monobutyl ether to silver nanoparticles leads to a strong modification of the ability of particles for adsorption at both fluid/fluid and fluid/solid interfaces, which can be exploited in the fabrication of electronic devices by ink-jet printing [114].

On the other hand, it is also possible to obtain a well-controlled modification of particle wettability by irreversible covalent bonding of specific coating ligands to the particle surface [115]. For instance, silanization of silicon dioxide particles, with a reduction in the percentage of surface free silanol groups from 34% to 20%, leads to an increase in the value of the particle contact angle at the water/vapor interface by a factor of two. [116] Thus, particles with the highest hydrophobicity (those with 20% of free silanol groups) present a contact angle of 113°, whereas this decreases for hydrophilic particles (those with 34% of free silanol groups) down to 55°. Similarly, grafting poly (glycerol-monomethacrylate) chains onto the surface of polystyrene latex particles modifies their contact angle at the fluid interface [117].

The particle wettability control developed in recent years has stimulated significant research efforts on the rational design of wettability-controlled particles, and in particular for the design of colloidal particles with asymmetric wetting properties, e.g., Janus particles and patchy colloids [29,118,119].

2.4.3. Experimental methods for the evaluation of the contact angle of particles trapped at fluid interfaces

Since there is no standard approach to determine the contact angle of particles at fluid interfaces, regardless of their dimensions, shape and morphology, its determination remains a challenge [120–122]. At present, there are different experimental techniques designed for a direct or indirect determination of the contact angle of isolated particles adsorbed at the interface of the fluid (or its assemblies). These methods are usually classified into three different groups: (i) indirect measurements; (ii) direct measurements of multiple particles (ensemble methods); and (iii) direct measurements of individual particles, in which the position of the particle centre is resolved relative to the interfacial plane [23,24,123,124]. Indirect methods the mean value of the contact angle of the particle trapped in a fluid interface by measuring a property associated with it. In single particle methods, colloids are directly visualized by different types of microscopies (optical, electron, atomic force...), so the minimum particle size that can be observed depends on the specific technique. These methods are usually free of assumptions and allow the detection of any interface heterogeneity. However, they require imaging of a large number of particles to ensure good statistics for contact angle determination. On the other hand, ensemble approaches allow determining a very accurate mean contact angle, with very good statistics, by measuring the macroscopic properties of the system, even in smaller objects. However, the use of this type of methods does not give directly information about the possible heterogeneity of the particle contact angle, i.e., the possible variation of the contact angle between individual adsorbed particles resulting from subtle changes on their chemistry, size or morphology (shape and roughness).

2.4.3.1. Indirect methods. The analysis of the profile of a sessile droplet deposited on the surface of a flat substrate, that has the same chemical nature as the particles trapped at the fluid interface, is an indirect method commonly used to estimate the contact angle [125]. However, the assumption that this angle coincides with the particle contact angle fails in most cases because it does not consider the role of curvature, roughness and line tension.

The particle contact angle at the fluid interface can also be determined through the analysis of interfacial pressure-area isotherms (Π-A) of particle-laden fluid interfaces. Two different methods have been described for such purpose: (i) the analysis of the area exclusion induced by the particles in a second component, usually a surfactant, and (ii) the evaluation of the isotherm collapse pressure. The first method is based on the analysis of the area displacement exhibited by the Π-A isotherms of an insoluble surfactant when colloidal particles are adsorbed simultaneously. In this case, the contact angle is estimated by assuming both that the wettability of the particles does not change with the presence of the surfactant, and that such displacement occurs because the particles occupy part of the interfacial area. The latter assumption implies the absence of interactions between particles and surfactant molecules. Otherwise, the area shift could mask the expansion or contraction of available area associated with the interactions [126,127]. The second method, exploited for a long time, calculates the contact angle by surface pressure measurements and geometrical considerations, assuming that once the system reaches the collapse pressure, Π_c, identified by a kink or flat region in the Π–A isotherm,the particles adopt a close packing configuration organized in ideal coplanarity [52,128–131]. On the other hand, if compression provides enough energy to force desorption of the particles the collapse pressure and desorption energy can be correlated as follows [128]

$$\Delta E_p = \frac{\Pi_c}{\Gamma_c} \tag{29}$$

where Γ_c is the surface concentration at the collapse point.

The pendant drop tensiometer is also a technique often used to measure the binding energy of particles trapped at a fluid interface. This technique monitors the time evolution of the interfacial tension of a droplet of the particle suspension during the spontaneous adsorption of the particles at the fluid interface [66]. Thus, neglecting the existence of interparticle interactions at the interface, and assuming that the maximum packing of the particles at the interface corresponds to a perfect 2D hexagonal array, the saturation of the interfacial tension is related to the adsorption free energy as

$$\Delta F = -(\gamma_{12} - \gamma)\pi R^2/\eta \tag{30}$$

with η=0.91 for a close-packed interface.

A very popular alternative approach for indirect contact angle determination is based on the measurement of the upward velocity of a fluid, pushed by capillary pressure, which is contained in a capillary column filled by a packed bed of particles [132,133]. This method, exploited to determine the contact angle of particles with a wide range of sizes, shapes and chemical nature, assumes that particles form a bundle of capillary tubes, of circular cross-section and radius R_{eq}. In this method, the contact angle is assessed using the Washburn equation [134]

$$h_L^2 = \frac{\gamma_{12} R_{eq} cos\theta}{2\eta} t \tag{31}$$

where h_L, t and η are the height of the liquid column, the time and the viscosity of the rising liquid, respectively. According to Equation (31) h_L is defined as a function of the experimental time. However, this method is limited to the determination of the contact angle of rather monodisperse particles, which form bundles where the porosity of the bed of particles is well defined. Furthermore, the Washburn method only provides information of the advancing contact angle, which can be far from the true equilibrium situation due to the wetting dynamics.

As alternative to the Washburn method, Diggins et al. [135] introduced another approach based on the determination of the equilibrium capillary pressure of a packed bed of particles, ΔP, which can be defined as the pressure required for hindering the fluid motion through the packed particles. The latter is related to the contact angle through the Laplace-White equation [136]

$$\Delta P = \frac{\gamma_{12} A \phi cos\theta}{1-\phi} \tag{32}$$

The main advantage of this approach is that only depends on experimentally accesible parameters, such as the specific surface area A, the volume fraction of powder ϕ and the fluid/fluid interfacial tension γ_{12}.

The use of a force tensiometer can also help on the evaluation of the wettability of powders. This evaluation is possible by loading a packed bed of particles, hunged from a precision balance and then dipped into the liquid. Thus, it is possible to determine the contact angle from the change detected in the mass when the liquid progressively penetrates through the bed, as follows

$$cos\theta(t) = \frac{m^2 \eta}{C \rho^2 \gamma_{12} t} \tag{33}$$

where C is a constant characteristic of the material and m the variation of the mass at a given embedding time t [137]. It is should be stressed that the different approaches introduced for replacing the conventional Washburn method can be only used for obtaining the advancing contact angle.

Another approach used to determine the contact angle is based on the use of a heat-flow calorimeter to measure the energy change-associated with the mixing of solid particles and a liquid [138]. In this method, the contact angle is related to the enthalpy of immersion, through thermodynamic consideration, as follows

$$cos\theta = \frac{-KT - h_i}{\gamma_{12}} \tag{34}$$

where K is given by the temperature change associated with the immersion of the particles in the fluid phase, and h_i is the change of enthalpy associated with such immersion. This approach requires the use of two calorimetric cells: the first one filled with dried powder, and the second empty one used as reference. The experimental evaluation of the contact angle relies of the equilibration of both chambers with liquid, and the determination of the differences on the changes of thermal energy during the wetting process. This method is commonly used for particle trapped at liquid/vapor interfaces, with the contact angle for particles at liquid/liquid interfaces being obtained by combination of the data obtained for the individual liquid/vapor interfaces. However, the required assumptions to link immersion enthalpy and contact angle have limited the applicability of this approach.

A last indirect alternative used to determine the contact angle relies on the use of the Atomic Force Microscope (AFM). In this method, the contact angle is estimated by measuring the force-distance curve due to the interaction between a colloidal probe and a liquid bubble [139]. This is possible because during attachment and detachment of the colloidal particle from the interface, it is possible to obtain information of different parameters, including the jump-in and detachment position, the detachment force and the work adhesion, which allows estimating both the advancing and receding contact angles of particles bigger than 2–3 μm. The use of AFM for determining the contact angle is a extremely sensitive methodology which is affected by specific details of the particle surface, e.g. surface topography and chemistry, which can result in displacements of the contact line or local pinning. Furthermore, the complexity of the methodology makes it difficult to obtain a detailed statistical analysis from AFM measurements, even though this technique provides important information related to the mechanics of the wetting of particles.

2.4.3.2. Direct methods for particle ensembles

2.4.3.2.1. Immobilization methodologies. A very popular approach for determining the contact angle of particles trapped at fluid interfaces relies on the immobilization of particles at the interface, commonly by freezing [122] or gelling [140], followed by an analysis of the immobilized surfaces by using a high-resolution microscopy (electron microscopy or AFM). Currently, there is a broad range of immobilization strategies that allow obtaining information on the contact angle of particles at fluid interfaces, with their main advantages arising from the possibility to evaluate many particles from a single measurement. Nevertheless, their application appears limited by the significant interface manipulation, which may modify the locations of the particles, induce particle deformations or change the composition of the system.

The first and probably most popular methodology based on particle immobilization is the so-called gel trapping technique (GTT). It was originally designed for the evaluation of the contact angle of microparticles at a fluid/fluid interface by their transference to a solid matrix, allowing their direct visualization by using Scanning Electron Microscopy (SEM) [140]. It was quickly extended to the determination of the contact angles of nanoparticles trapped at fluid interfaces by using AFM for imaging [99,120]. In the GTT, a particle film is prepared at the interface between a fluid and an aqueous solution of a gellan, maintained at a temperature above its gelling temperature. The temperature is then reduced to force the gelation and the particles are trapped in their fixed position at the interface. This allows the monolayer to be transferred to a poly(dimethylsiloxane) (PDMS) replica, where the relative position of the adsorbed particles can be directly determined by microscopy. From the images it is possible to estimate the contact angle by a simple geometrical analysis. Thus, it is possible to determine the contact angle of particles with sizes in the range 100 nm-100 μm, trapped at both liquid/vapor and liquid/liquid interfaces [102,120,140]. Despite its apparent simplicity and accuracy (contact angle can be determined with a variability of 3-5°), the use of GTT appears limited due to the different aspects. First, the gellan is a non-surfactant active molecule with a characteristic length of 10 nm. This can lead to trapping heterogeneities which makes difficulty to provide a definition of the contact line when particles with a diameter below 100 nm are considered. Furthermore, the aplication of high temperatures limits the applicability of GTT to non-volatile fluids, and can induce deformation on the particles [141].

Vogel et al. [142] introduced an alternative to conventional GTT based on the addition of butylcyanoacrylate to the interface through the vapour phase. The formation of a poly(butylcyanoacrylate) matrix, via an anionic polymerization process that starts upon the contact of the precursor butylcyanoacrylate with the aqueous phases promotes the trapping of the colloids at the water/vapour interface. This approach also creates a solid replica of the interface that can be used for the evaluation of the equilibrium positions of the colloids, using high resolution microscopy.

A more sophisticated immobilization methodology combines freeze-fracture (FreSCa) and shadow-casting cryo-Scanning Electron Microscopy (SEM) [122]. This method relies on the immobilization of the particles at the fluid interface by a fast vitrification, helped by the action of propane jet freezer, that traps the particles at the fluid interface without any significant thermal contraction. The obtained sample are later fractured and uni-directionally coated with a metal layer at a well-defined tilt angle α, and then the contact angle of the particles is determined from the images obtained using cryo-SEM, using simple geometrical assumptions [111,122,143]. This is possible because the presence of a particle-laden layer at a flat interface appears as a weak fracture plane, and allows the exposure of the immobilized particles. Thus, the oblique metal deposition casts the shadow of the particle protruding from the interface. The measurement of the length of the shadow and the projected height make it possible the calculation of the protruding height h, and consequently the contact angle, knowing the value of the shadowing angle α and the geometry of the particles [144]. The use of the FreSCa coupled with cryo-SEM imaging allows evaluating relatively large regions of particle-laden interfaces, which allows an accurate evaluation of the existence of wetting heterogeneities at the interface. Furthermore, this method offers a high accuracy and flexibility for the determination of contact angles of particles at water/oil

interfaces independently of the chemical nature of the particles and the liquid [111]. Furthermore, it is not limited to the determination of the contact angle of model-hard spherical particles but can also be used in the evaluation of the contact angles of ellipsoids, Janus colloids, dumbbells, proteins fibrils or soft particles [96,143]. Despite the many advantages of the above method, it cannot be used for measuring the contact angle of extremely hydrophilic particles, due to the minimum possible value of the accessible casting angle. Furthermore, the determination of the contact angle requires a priori knowledge of the particle geometry to obtain the relationship between the protrusion height and the contact angle.

van Rijssel et al. introduced the use of cryo-electron tomography (ET) to determine the contact angle of small particles trapped at a fluid interface [145]. The method requires freezing the fluid interface on the surface of a Transmission Electron Microscopy (TEM) grid. Then, images of the sample are acquired at different tilt angles (in the range between -65° and 65°) to create tomograms by weighted back projections. This makes it possible to obtain three-dimensional reconstructions of the samples, which provide the contact angle by calculating the distance between the particle centre of mass and the nearest interface. Even when the use of TEM imaging allows for a significant reduction of the minimal size of the particles that can be studied, the use of complex algorithms is often required in the tomogram reconstruction [146]. Furthermore, the introduction of assumptions related to the geometry and symmetry of the particles are essential to determine the protrusion height from the images.

A last alternative based on the immobilization for particles at liquid/vapor interface was proposed by Mc Bride et al. [99]. Their approach relies on the deposition of a dispersion of particles with an excess of chloroform in an interface containing low-glass-transition temperature polystyrene. After the chloroform is evaporated upon heating, the liquid mixture is deposited onto a glass slide. By cooling, the polystyrene melt undergoes a solidification process, which favours the trapping of the particles in their positions. The analysis of the samples, done by SEM or AFM, gives information of the protrusion height. However, this type of method is only applicable for particles that are insoluble in chloroform and are trapped at the interface between polystyrene melt and vapor.

It should be noted that all the above immobilization techniques have limitations associated with the stastistics due to the maximum number of particles that can be imaged and analyzed.

2.4.3.2.2. Optical techniques. Reflectivity techniques are very powerful for assessing the position of the particles relative to the interfacial plane, taking advantage of contrasts in refractive index or scattering density across the interface. Most methods for the determination of the contact angle by reflectivity techniques are based on the comparison of the results obtained for the clean and particle-laden interface.

The use of ellipsometry provides a non-invasive methodology to evaluate the contact angle of sub-micrometer particles trapped at fluid interfaces [121]. In this technique the particle-laden interface is modelled as a bilayer, with the first layer being formed by the fraction of the particles and the layer of liquid that appears just below the interfacial plane, and the second layerby the fraction of the particles and fluid remaining just above the interfacial plane. Later, the ellipsometry analysis considers each layer as an independent media with a homogeneous reflectance, neglecting the role of scattering phenomena. Hence, the relationship between the contact angle of the particles and the thickness of the two layers is established in terms of the Effective Medium Approach (EMA) [80,116,121].

The use of scanning angle reflectometry (SAR) provides similar information than that obtained using ellipsometry [124,147]. This technique is based on the analysis of the reflectivity profile of a p-polarized beam in the viccinity of the Brewster angle. This provides an effective refractive index of the monolayer, n_{eff}, which in turn contains information on the position of the particles in relation to the interfacial plane, and consequently to the value of the contact angle. There are two experimental approaches to extract information of the contact angle of particles trapped at the fluid interface from SAR experiments. The first is applicable for particles smaller that the wavelength of the incident beam and with a refractive index close to that of the fluid phases (uniform layer approach). Here, the effective refractive index of the monolayer is obtained from the profile of the reflected intensity [124]. The second approach considers a gradient layer model that assumes that the effective refractive index depends on the light penetration depth [147]. Despite the differences between the two models, both assume the presence of a laterally homogeneous monolayer of monodisperse particles. Hence, the applicability of ellipsometry and SAR is limited to perfectly ordered assemblies of particles having strong interactions. This condition may have some effect on the contact angle, which could be different to that measured in monolayers of isolated or non-interacting particles. It has to be remarked that, although SAR and ellipsometry determine in situ the average contact angle of particles trapped at a fluid interface, the quality of the fitting procedure is essential to obtain physically reliable values.

The above method relies on the use of visible light. However, x-ray radiation can be also used to obtain information about the location of colloidal particles in relation to the interfacial plane. The measurement of the dependence of X-ray reflectivity (XRR) on the wavevector of the incident beam, followed by the modeling of the obtained reflectivity profiles, has been used to determine, with a sub-nanometric resolution, the position of adsorbed nanoparticles trapped at water/vapor or water/fluid interfaces [148,149]. In parallel, the use of scattering techniques allows a direct determination of the interfacial coverage, which can be related to the contact angle. However, the use of XRR does not overcome the need to include assumptions related to the particle packing. For a better quantification, reflectivity measurements are often combined with in-plane characterization via Grazing incidence small angle X-ray scattering (GISAXS) experiments [150]. Recently, Smits et al. [151] compared the contact angles obtained by measuring the contact angle of a water droplet deposited on flat substrate which the values obtained by XRR for particles directly trapped at fluid interfaces, maintaining the same surface charge, chemistry and roughness in both particles and flat substrate. They found that the wettability of the flat substrate may provide a good representation of the wetting properties of the particle trapped at the fluid interface in absence of adsorption barriers.

Neutron reflectivity (NR) is also a very powerful tool for assessing the organization of small particles within complex particle-laden interfaces [152]. This is possible because the use of neutrons allows adjusting almost at will the optical contrast between the particles and the fluid phase, providing information both on the relative position of the particles in relation to the interface and on the chemical composition of the particle surfaces exposed to both fluid phases. The need of large-scale experimental facilities, together with the need for a complex fitting of an optical model to reflectivity profiles, explain the still limited use of NR for the study of particle-laden interfaces.

2.4.3.3. Direct methods for single particles. This type of methods relies on the analysis of the relative positions of big particles at the fluid interface by optical microscopy observation. This strategy was used by Horvölgyi et al. [153] to determine the inmersion depth of particles adsorbed at an water/vapor interface sandwiched between two glass slides, which makes it possible to obtain directly the contact angle of the particles by a simple calculation. A similar approach can be done using a modified pendant drop device coupled to an optical microscope [154,155]. In this strategy, particles with big dimension settle at the bottom of the drop, where they are imaged. The contact angle is determined, by simple geometrical considerations using the radius of the protruded spherical cap and the total diameter of the particles. The above methodology suffers from limitations associated with the optical resolution limit of the bright-field microscope used for detection. This limitation may be partially overcome by using a fluorescence confocal microscope, in

which fluorescence slices are collected with an optical resolution of about few hundred nanometers [156]. These slices are combined to reconstruct the relative position of particles trapped at the interface, which is possible by adding a dye to visualize simultaneously the position of the interface and the particles. Since the addition of the dye can modify the wetting properties of the particles, the procedure is repeated at different dye concentrations, and the true contact angle is obtained from the extrapolated value of zero concentration. The main advantage of this approach is that can it be applied to both hydrophilic and hydrophobic particles at flat or curves interfaces [157]. A major drawback to the use of fluorescence confocal microscope for contact angle assessment is the lateral and vertical resolutions of the images.

An alternative approach used in the determination of the contact angle of particles based on fluorescence microscopy relies on the exploitation of single-molecule localization microscopy, in particular the so-called interface Point Accumulation for Imaging in Nanoscale Topography (iPAINT) [158,159]. By labelling with appropiate dyes and switching between two different irradiation beams, this method allows selective visualization of both the interface and the particles and, consequently, direct estimation of flotation heights and contact angles.

Microscopy techniques often present vertical resolution problems that can be partially solved by using digital holographic microscopy [86]. In this high spatial and temporal resolution technique, the adsorbed particle position is monitored by fitting the time evolution of the holographic patterns to the Lorenz-Mie model, giving access to dynamic measurements of the contact angle aging [86]. On the other hand, digital holographic microscopy is limited by poor statistics and the large computational effort required to fit the hologram.

The Bessel beam microscopy (BBM) technique combines high vertical resolution and good statistics [123], both of which are essential in the determination of the particle flotation height, being used in the measurement of the contact angle of particles with sizes ranging from 10 nm to several microns.

An alternative to improve the vertical resolution in particle contact angle determination is the use of a wide range of interferometric methods, which provide information on interfacial distortions or thickness of liquid films, helping on the determination of the contact angle. A first interferometric method is the film trapping technique (FTT) [160], in which the particles are captured in a liquid film with a thickness less than the particle diameter. When observed in reflection configuration, the formation of a liquid meniscus around the particles favours the appearance of several interference fringes. The analysis of the reflection pattern, applying Laplace's equation, allows the reconstruction of the meniscus shape, which provides the value of the contact angle with an accuracy of 2-5°. The main advantage of FTT is that the required instrumentation is easily accessible and that its use is not limited to hard particles, but is also open to soft particles or oil droplets. The possibility of forming the meniscus under the required conditions emerges in many cases as the main drawback of FTT.

Another interferometric technique is the film-calliper method [117,161], which takes advantage of the ability of colloids to form stable inter-particle liquid bridges, where they adsorb at their equilibrium positions. The analysis of the interference pattern of the reflected light captured by optical microscopy provides information on the thickness profile in the meniscus, which is determined by the particle contact angle.

Although the use of interferometric techniques provides a significant improvement in vertical resolution, such techniques are diffraction-limited for in-plane measurements and therefore are only applicable with micrometer-sized particles. This limitation can be partially overcome by applying imaging methods based in X-ray microscopy. Finally, it is worth mentioning that Transmission X-ray imaging can be also used to determine the height of the protrusion level of particles (both soft and hard) trapped at fluid interfaces [162,163].

3. Particle dynamics at the fluid interface

The interest in understanding how particles trapped at fluid interfaces move, i.e., their dynamics and transport properties, has received much attention in recent years. Among the different reasons, one can include the role of fluid interfaces as models providingimportant insights on the behaviour of different chemical and biological systems, and the possibility of exploiting the motion of particles to determine the mechanical response of interfaces (e.g., their use as probes in microrheology experiments) [37,40,91,92]. The motion of particles, both in bulk and attached at a fluid interface, is strongly determined by the mechanical properties of the surrounding media, in particular, their viscoelastic properties, which can be described in terms of the Generalized Stokes-Einstein (GSE) relation [164].

On the other hand, the high energy commonly associated with particle entrapment at the interface causes the movement of adsorbed particles to be strongly hindered in the direction perpendicular to the interfacial plane, where only small thermal fluctuations around the equilibrium position are possible. Since fluctuations, flows or external actuations only induce in the particles, in most cases, motions parallel to the interface, they become strongly confined 2D thermal systems [165,166]. The current understanding of the dynamics of particles confined at bare fluid interfaces is far from being clear. On the one hand, these systems present an intricate balance of inter-particle and particle-fluid interactions. On the other hand, the motion of the particles is determined by the heterogeneous hydrodynamic conditions imposed by the interface and the two fluids.

Some authors stated that the quasi-2D confinement of the adsorbed particles leads to an in-plane diffusion coefficient significantly higher than the diffusion coefficient in the bulk, probably due to the lower viscosity of the interfacial region [166]. On the other hand, other authors predict a decrease of the in-plane diffusion coefficient as result of the effect of the out-of-plane fluctuations [167] or the layering of the fluid surrounding these adsorbed particles [168]. Indeed, it has been experimentally proven that the in-plane translational diffusion coefficient is significantly lower than that determined by hydrodynamic predictions, due to contact line fluctuations, which lead to contact line friction [169].

In first approximation, the viscous drag parallel to the interface for the trapped particles can be considered as an average value of those corresponding to the particles dispersed in each fluid weighted by the immersion depth in each of the fluids, i.e., the contact angle θ [37,170], and can be defined as

$$g = f\left(A_{p1}, A_{p2}, A_i, \eta_1, \eta_2, \eta_s, \theta\right) \tag{35}$$

in terms of A_{p1}, A_{p2} and A_i, the portions of the particle surface exposed to fluid 1 and 2 and the cross-sectional area of the particle at the interface, respectively, and η_1, η_2 and η_s, the viscosity of the fluid 1 and 2, and the interface, respectively. It should be noted that since the bare interface itself has no viscosity, η_s should only be included in interfaces containing surface active species [171,172]. For those cases in which the viscosity of the fluid 2 is much smaller than the viscosity of fluid 1 (see Fig. 1) it is possible, in principle, to consider only the contribution associated with fluid 1 [170]. However, as recently pointed out by Villa et al. [37], hydrodynamic models do not allow a complete description of the translational viscous drag of adsorbed particles with sizes below few micrometers [170,171]. These discrepancies arise from the coupling between thermally activated fluctuations of the triple contact line and viscous drag [170].

A detailed analysis of the translational motion of particles at the fluid interfaces evidences the existence of different regimes. At the shortest times, the behavior of the fluids is reminiscent from that observed in a compressible material. In this regime, in the range between 0 and 0.1 ns, the motion of the particles can be described as a sound wave characterized by a time $t_s=R/c_s$, with c_s being the velocity of sound. At longer

times, hydrodynamic interactions start to operate, which leads to a second dynamic process defined by a characteristic time t_h of up to 10 ns. This second process appears as a transverse momentum that diffuses away from the particles, leading to a drag force between the particles. Here, the motion can be considered as the diffusion of a transverse momentum within the inter-particle distance. In addition to the motion associated with the hydrodynamic interactions, the particle motion induces a decay of the initial velocity of a colloid as result of the time-dependence of the velocity field. This motion appears dependent on the diffusion coefficient of the transverse momentum of the fluid.

Typically, the translational motion of isolated colloids adsorbed at a fluid interface over a distance as the particle radius occurs in the time range between 1-1000 ms^{-1}. Therefore, the colloidal diffusion can be separated from the faster dynamics previously defined, and the long-time motion of particles emerges as an uncorrelated Brownian motion. A simplified description of the dynamics of particles considers a diffusion-controlled motion defined by a characteristic diffusion constant, which is given by the Stokes-Einstein relationship

$$D = \frac{k_B T}{g} \tag{36}$$

For non-deformable spherical particles dispersed in a bulk fluid, the drag coefficient is $g = 6\pi\eta R$. However, the drag coefficient of particles trapped at a fluid interface must consider the contribution of the two fluid phases, which is determined by the immersion depth of the particles in each fluid phase (contact angle) [173], and the viscous drag generated by the activated fluctuations of the triple contact line. However, the above definition does not account for the presence of neighbors surrounding each single particle, which leads to the modification of the particle dynamics as result of the inter-particle interactions [36,37].

Video-microscopy techniques have made it possible to track the trajectories of particles trapped at fluid interfaces, and thus to directly observe the dynamics of the system. A first approximation to the dynamics of the monolayer is usually made in terms of the mean square displacement, MSD ($<\Delta r^2(t)>$), defined as

$$\langle \Delta r^2(t) \rangle = 2dDt^{\alpha} \tag{37}$$

where α is a scale exponent, and d defines the number of degrees of freedom of the translational motion, assuming a value of 2 for the interfacial motion. At interfaces with low interfacial coverage, the MSD dependence on t is commonly linear [36,170]. However, the increase in interfacial coverage leads to a more complex dynamics, characterized by the dependence of the motions occurring at short and long times leading to $\alpha \neq 1$. In the shortest time, the motion of each individual particle is constrained within the cage defined for its nearest neighbors, which drives the system to an arrested dynamics [174]. The presence of inter-particle interactions as result of the increase of the surface coverage, ϑ, hinders the diffusion of particles in the short-time limit, and

$$D_s = \lim_{t\to 0} \frac{\langle \Delta r^2 \rangle}{4t} = \alpha D_0 (1 - \mu\vartheta) \tag{38}$$

where μ is a dimensionless parameter that introduces the contribution of the inter-particle interactions [172]. At longer times, the long-term diffusion coefficient, defined as

$$D_m = \lim_{t\to\infty} \frac{\langle \Delta r^2 \rangle}{4t} \tag{39}$$

reflects the collective motion of the particles. The long-time regime is determined by the escape dynamics of the particles from the cages formed by their closest neighbors, the so-called α-relaxation [175,176].

The complexity of the dynamics makes it difficult to obtain an analytical expression of the diffusion coefficient. As a first approximation, a model based on an independent Brownian harmonic oscillator (BHO) has been applied, where the motion of the particles is described by an extended Langevin equation that includes an elastic term [177]

$$m\frac{dv}{dx} = -gv + F(t) - kx \tag{40}$$

where m and v are the mass of a particle and its velocity, respectively, k the force constant characteristic of the elastic force acting on the particle, and $F(t)$ is a term accounting for the time-dependent random force. For an overdamped motion, in absence of inertia, the mean-square displacement is given by [175,176]

$$\langle \Delta r^2(t) \rangle = 2d\delta^2 \left[1 - e^{-D_0 t/\delta^2}\right] \tag{41}$$

with $\delta^2 = k_B T/k$. Under this conditions, the dynamics has a characteristic time defined as

$$t_{BHO} = \frac{\delta^2}{D_0} = \frac{g}{k} \tag{42}$$

The interactions between Brownian particles are generally considered through *ad hoc* corrections, which introduce the non-exponential character of time decay [178]

$$\langle \Delta r^2(t) \rangle = 2d\delta^2 \left[1 - e^{-\left(D_0 t/\delta^2\right)^{\varphi}}\right] \left(1 + \frac{D_0 t}{\delta^2}\right) \tag{43}$$

The introduction of both the stretching exponent φ and the term including the escaping dynamics of a single particle from the cage defined by its closest neighbors (long time dynamics) allows recovering the linear dependence of the MSD with time. It is worth to mention that the stretching exponent appears as a fitting parameter with a value less than 1, defining the width of the relaxation spectrum. This model is not appropriate for describing the motion of particles in very dense, solid-like, monolayers. These systems are better described by the Over-damped Bead-Spring model (OBS), which only considers interactions involving the closest neighbors [179]:

$$m\frac{dv_i}{dt} = -gv_i(t) + F_i(t) - k\sum_{j}^{nn}\left[u_j(t) - u_i(t)\right] \tag{44}$$

where $u_i(t)$ is the displacement of the particle i at time t, and nn provides the number of the nearest neighbors to i. In dense monolayers, the motion associated with the escape of single particles from the cage formed for its closest neighbors appears hindered due to high coverage. This causes the increase in MSD at long times, becoming far from linear. The long-time solution of the OBS model is

$$\langle \Delta r^2(t) \rangle = \frac{2dk_B T}{kN} \sum_b \frac{1}{L(q_b)} \left[1 - e^{-kL(q_b)t/b}\right] \tag{45}$$

Here, the lattice factor $L(q_b)$ is defined by

$$L(q_b) = \sum_{j}^{nn} \left[1 - cos\left(q_x n_j\right)\right] \tag{46}$$

with q_b being the b^{th} wave vector of the relaxation mode q, and n_j accounting for a vector pointing from the point i of the lattice to its closer neighbor j. For the long-time limit, the OBS model gives a limiting value, determined by both the strength of the harmonic force and the lattice factor as

$$\lim_{t\to\infty} \langle \Delta r^2(t) \rangle (t\to\infty) = \frac{2dk_B T}{kN} \sum_b \frac{1}{L(q_b)} \tag{47}$$

In the short time limit, the OBS model recovers the MSD time dependence predicted by the BHO one in the initial stages.

The quantitative analysis of the motion of particles at fluid interfaces must consider the contribution of different aspects: (i) the mechanical properties of the fluid phases; (ii) the mechanical coupling between probe and environment, and (iii) the distribution of the probe within the

interface [180,181]. The previous factors control the time-scales on which the motion of particles trapped at the fluid interface occurs [92,182–184], which differs from those involved when particles diffuse into the bulk. This is especially important when considering the dynamics of active particles. The most common approach to describe the mean-square displacement of active colloids at interfaces is to include a contribution associated with the directed propulsion, giving a mean-square displacement defined as [185]

$$\langle \Delta r^2(t) \rangle = 4Dt + \frac{V^2\tau_R^2}{3}\left[\frac{2t}{\tau_R} + e^{-2t/\tau_R} - 1\right] \tag{48}$$

where V and τ_R are the propulsion velocity and the characteristic time of the rotational motion. The latter is defined, as $1/D_R$, by the rotational diffusion coefficient D_R. In the long-time limit, the expression for the mean-square displacement of active colloid can be simplified as

$$\langle \Delta r^2(t) \rangle = 4Dt + \frac{V^2 t}{D_R^2} \tag{49}$$

Both the passive and active motions contribute to an overall effective diffusion and the effective active motion arises by reducing D_R or increasing V.

4. Inter-particle interactions

The wealth of the interactions arising from confining particles at fluid interfaces is probably one of the most important aspects of the physics of 2D colloidal systems. Besides the forces appearing between particles suspended in a solvent, the trapping of particles at interfaces leads to the emergence of new interactions, which depends on the chemical and morphological features of the considered particles and the specific physico-chemical properties of the fluid phases conforming the interface [10,78,186]. Thus, the particle organization and dynamics within the fluid interface results from an intricate balance of interactions with different origin [10,27,32,93], which can be roughly defined in terms of the difference between the standard values of the chemical potential of particles trapped at the fluid interface, μ_{int}, and those dispersed in the bulk, μ_b,

$$\Delta\mu = \mu_{\text{int}} - \mu_b \tag{50}$$

This difference contains the contributions of the different types of interactions operating within the particle-laden layers

$$\Delta\mu(\phi,\vartheta) = \Delta E_p + \mu_i(\phi,\vartheta) + \mu_e(\phi,\vartheta) \tag{51}$$

where ΔE_p accounts for the trapping energy due to the particle wettability and introduces the contribution of the contact angle to the energetic landscape (see Equation (23)), μ_e accounts for the unfavorable entropic contribution associated with the reduction of the translational degrees of freedom of the particlesdue to the trapping at the interface, and μ_i all the interactions operating between particles within the interfaces, e.g., van der Waals, electrostatic, capillary, density fluctuations or hydrophobic ones. These inter-particle interactions emerge from the particle coupling, which depend strongly on the inter-particle distance, and are determined by the interfacial coverage ϑ and the volume fraction of particles in the bulk ϕ. Fig. 8 presents a sketch with the most common types of interactions that appear between particles at particle-laden fluid interfaces.

Any discussion of the interactions operating in particle-laden interfaces requires to consider the differences arising from the existence of the interface acting as a confining environment in relation to that what occurs in their 3D counterpart systems. The presence of the interface makes it necessary to consider the particles as objects attached to a fluctuating surface that separates two continuous fluids with different physico-chemical properties. Furthermore, the behavior of the system depends on specific characteristics of the attached particles, e.g., particle size and shape; charge density and wettability, or surface chemistry [10,27,61,78,93].

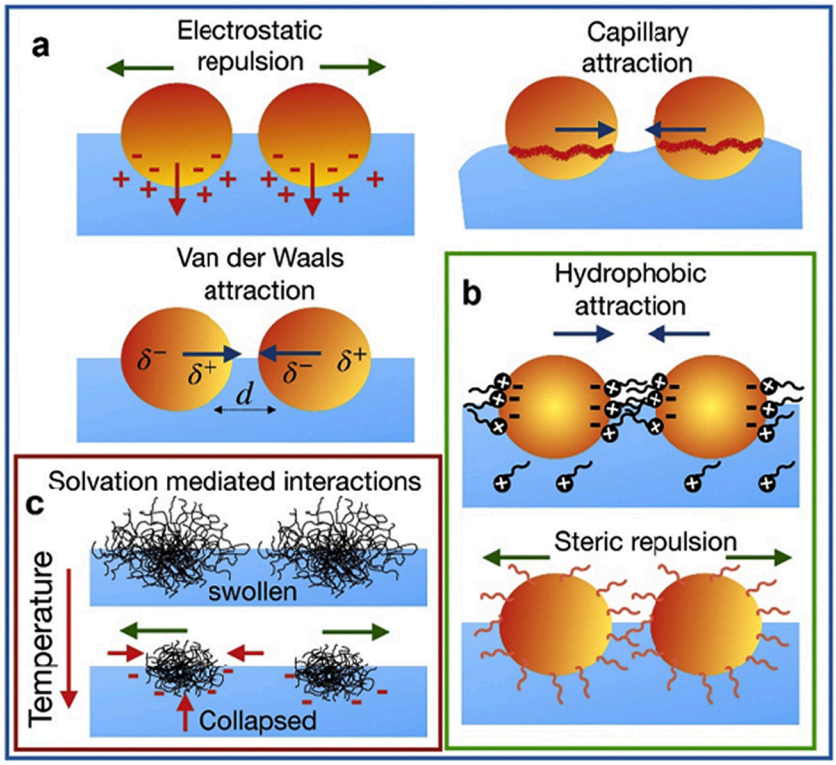

Fig. 8. The sketch shows an idealized picture of different types of inter-particle interactions that can emerge in particle-laden fluid interfaces: (a) Repulsive dipolar and Coulombic, van der Waals and capillary attractive interaction, (b) attractive hydrophobic forces and steric repulsions, and (c) solvation-mediated interactions. Adapted from Maestro et al. [27], Copyright (2019), with permission from Elsevier.

It should be noted that the above discussed inter-particle interactions (sketched in Fig. 8) occurring in particle-laden fluid interfaces can be rationalized in terms of three main contributions to μ_i. The first one accounts for the direct interactions between particles, e.g. electrostatic, hydrophobic and van der Waals, which are determined by the specific characteristics of the particles [27]. Although this type of interactions also appears in bulk systems, they are strongly modified by the presence of the interface. The second type of interactions emerges as result of the confining role played by the interface, e.g., capillary interactions. The last type of interactions emerges upon the presence of external fields acting on individual objects or ensembles of them.

Currently, there are different methodologies for measuring the interaction potentials arising in particle-laden interface. The use of passive methods, such as video-microscopy, provides information about the averaged potential, in diluted monolayers, through the analysis of the pair correlation functions [187,188]. Active methods, some of them based on the use of magnetic particles, allow one a quantitative characterization of the attractive capillary forces, even in conditions far from the equilibrium [189,190].

However, the most popular approach to assessing particle-particle interactions is their direct measurement using optical tweezers [189,191,192]. In a typical experiment, two particles adsorbed at the interface and located at a long separation distance are simultaneously trapped by using optical traps with a well-controlled stiffness. Then, one of the particles is moved towards the second particle, while monitoring the change of position of the stationary particle as a consequence of the approach of the second particle, and measuring the force experienced by the particles at the different values of the inter-particle separation. Most recent devices allow one to trap several particles, thus allowing one to explore many particle effects.

4.1. Direct interactions

The current knowledge of direct interactions remains poor due to the difficulties associated with the quantitative analysis of the different repulsive and attractive contributions, which in many cases include many-body interactions [189].

4.1.1. Van der Waals interactions

The van der Waals, London-van der Waals or dispersion forces are ubiquitous in chemical systems, and appear as result of the interaction between the individual components of the particles [18,35,193]. However, their introduction into the energetic landscape of particle-laden interfaces is less straightforward than when considering the interactions of particles dispersed in a bulk fluid. An approximate treatment makes it necessary to introduce an effective Hamaker constant, H, that depends on the fractional height of the particle immersed in the fluid 2, i.e., the volume fraction of particle immersed in the fluid 2 [f=(1-cosθ)/2] [10,16,93,194],

$$H = H_{P1} + f^2(3-2f)(H_{P2} - H_{P1}) \tag{52}$$

where H_{P1} and H_{P2} are the Hamaker constants of the particles across fluid 1 and fluid 2, respectively. This results in a situation in which the strength of van der Waals interactions will depend on f, i.e., the particle wettability and the relative values of H_{P1} and H_{P2}. The use of an effective Hamaker constant accounts for the differences in inter-particle interactions between particles dispersed in a bulk fluid and those trapped at a fluid interface to be introduced into the energetic balance. Thus, the average van der Waals interaction between a pair of particles trapped at an arbitrary fluid interface is given by the following expression

$$E_{vdW} = -\frac{H}{12}\left(\frac{2R}{r-2R}\right) \tag{53}$$

where r is the separation distance between the centers of two adjacent particles. Van der Waals interactions between particles adsorbed at a fluid interface appear to be similar to the interaction potential accounting for the growth of anisotropic particle domains as result of an asymmetrical distribution of the interactions within the interface [195–197]. It should be emphasized that van der Waals interactions between two identical objects are always attractive, and may lead to the irreversible aggregation of particles, unless other interactions counteract them. On the other side, van der Waals interactions between bodies with different chemical nature can be either attractive or repulsive [198].

Even when the van der Waals interactions in particle-laden interface are always stronger than those found when the particles are completely immersed in one of the fluid phases [10,35], their impact in the energetic landscape of particle-laden interactions is often negligible (0.1-1k_BT) [10], and their role is only important when the particles are located in close proximity to each other. At particle-laden interfaces, due to strength of the repulsive contributions, this is not the most common situation.

4.1.2. Electrostatic interactions

When charged particles are present, electrostatic interactions are a very important contribution to the energetic landscape of particle-laden fluid interfaces. Despite the electrostatic interactions also appears between charged particles dispersed in a bulk fluid, their contribution for particle-laden interactions presents a much longer range than that of the screened Coulomb interactions in bulk [82]. Therefore, the electrostatic contribution to the energetic landscape of particle-laden interface results from the combination of a short-range interaction, similar to that for particles suspended in a bulk fluid. The involves the part of the particles submerged in the polar phase, and is associated with a screened coulombic repulsion between the double layers of the colloidal particles, and long-range attractive dipole-dipole interaction, dues to the confinement of the particles at the interface and is strongly dependent on the chemical nature of such phases (dielectric constant) [43,193–197,199]. Thus, the overall electrostatic potential between particles separated a distance r can be calculated by simultaneously solving the Poisson–Boltzmann equation in the polar phase and the Laplace equation in the non-polar phase, under conditions in which the Derjaguin approximation is satisfied and the overlapping of the double layers can be considered negligible [191,200]

$$E_{electrostatic} = \frac{a_1 k_B T}{3r} e^{-\kappa r} + \frac{a_2 k_B T}{r^3} \tag{54}$$

Here, κ is the inverse Debye screening length, and a_1 and a_2 are prefactors that weight the relative importance of the contributions of the screened Coulomb potential and the dipolar interaction, respectively. For inter-particle distances long enough,$\kappa r >> 10$, the contribution of the screened Coulomb interaction can be neglected, and the dipolar component becomes the main contribution to the electrostatic interaction [200].

It was stated above that the distribution of the electrostatic interactions across the interface is not symmetrically distributed, i.e., the presence of the interfacial plane is associated with an asymmetry in electrostatic interactions [82]. If a water/non-polar fluid interface is considered, the dipolar interaction occurs between the dipoles formed by the dissociated groups on the surface of the particles and the dissociated counterions existing in the bulk, for the portion of particles immersed in water, and the surface charges and their image charges appearing in the water for the portion of particles immersed in the oil phase [10]. Therefore, the dipolar contribution is strongly influenced by the position of the particles relative to the interfacial plane, i.e., the wetting properties of the particles, but also by the dielectric constants, and the degree of screening in the aqueous phase (e.g., the ionic strength). For a particle that is transported from the aqueous continuous phase to a fluid interface, the interaction across the aqueous phase does not undergo any significant modification. On the other side, in the part of the particles immersed in the non-polar phase the neutralization of

the surface groups is energetically favored, which results in the emergence of an asymmetric double layer. This plays a very important role in the control of the interactions across the interface because it is known that the interactions between surfaces having the same charge always appears as repulsive, whereas the interactions between surfaces with different charges depend on their relative separation, and may be attractive or repulsive [18]. Hence, the overall interaction between particles trapped at a fluid interface can be modified by changing different parameters, e.g., the volume fraction of particle immersed in each fluid, or the ionic strength [201].

4.1.3. Hydrophobic interactions

The necessity to minimize the unfavorable contacts between hydrophobic surfaces and water leads to an important attractive hydrophobic interaction between the surfaces. Since there are no systematic studies dealing with this type of interactions at particle-laden interfaces, their theoretical description remains an open challenge. Hydrophobic interactions are highly dependent on the molecular details of the particles and fluid phases, and their strength increases with decreasing particle size. This can be understood by taking into account that the molecular details of the continuous phases and the interface introduce a contribution to the energetic landscape that increases as the characteristic length scale of the particle decreases [132,202].

4.1.4. Steric interactions

The addition of different species is often used to increase the stability of colloidal particles [108]. These additives, in particular polymers, form a capping shell that decorates the surface of the particles and creates an osmotic pressure on the confinement experienced when two particles approach each other [198]. The formation of a capping shell occurs either by a chemical grafting of the molecules to the particle surface, through covalent or hydrogen bonds, or by a direct adsorption mediated through physical interactions. The configuration and structure of the formed shell are governed by the coverage and the quality of the solvent, so that changes in the medium allow for the modulation of the interaction between the particles [93]. Due to the unfavorable entropic contribution due to the compression of the solvated chains, the steric interactions are always repulsive. Besides, the osmotic pressure that emerges in the region where the capping shells overlap leads to a minimization of the aggregation phenomena [198]. Using the Derjaguin approximation, this energy contribution can be described as follows

$$E_{steric} = RL^2\sigma^{3/2}\left(\frac{2L}{r-2R}\right)^{1/4} \tag{55}$$

where L and σ represent the effective length of steric repulsions and the maximum brush length, respectively. It is worth mentioning that the brush of the particles trapped at a fluid interface becomes asymmetric, so the value of L cannot be homogeneously defined. The steric repulsions present a big interest in the design of tunable particle-laden interfaces, with structures that can be easily adjusted by changing the organization of the capping shell [93].

4.2. Interactions mediated by the presence of the interface

4.2.1. Capillary interactions

Capillary interactions are probably the most important contribution to the energy landscape among those that only arise under particle confinement [203]. These interactions are promoted by the interface deformations resulting from particle adsorption at the fluid interface [44,204]. Fig. 9 presents a schematic representation of the different types of capillary forces that arise between particles trapped at a fluid interface.

The strength of the capillary interactions in particle-laden interfaces is strongly dependent on the particle properties. When the adsorbed particles are large enough, the gravity induces a significant deformation of the interface, which, in turn, leads to the appearence of the flotation forces. These forces depend on the shape, buoyancy, and wetting properties of the particles, and favor their approach or separation. The importance of the flotation forces significantly diminishes when the size of the trapped particles is reduced, becoming negligible for particles with sizes smaller than the capillary length of the fluid interface ($l_c=\Delta\rho g/\gamma_{12}$, where $\Delta\rho$ is the density difference between the two fluid phases) [191]. From a practical point of view, their impact on the energetic landscape of a particle-laden fluid interface can be considered negligible for particles smaller than 5-10 μm, with a Eötvös number not much less than 1 [see Equation (24)]. In this range, the weight of the particles is too low to induce a significant deformation of the fluid interface, and the lateral flotation forces become smaller or comparable to the thermal energy k_BT. In systems where the flotation forces contribute substantially to the total energy, the interactions are attractive when the interfacial deformations induced by the two neighboring particles present the same orientation (both menisci are concave or convex), whereas they are repulsive when particles induce deformations with opposite curvatures [186,205].

As above mentioned, the effect of the lateral flotation forces emerging at a liquid interface laden with small micro-particles can be considered almost negligible. However, this does not mean that this type of capillary forces does not influence the energy of the particle-laden interface [205]. [186]. The fluid interface maintains its shape upon the adsorption of the particles, and their position, in relation to the

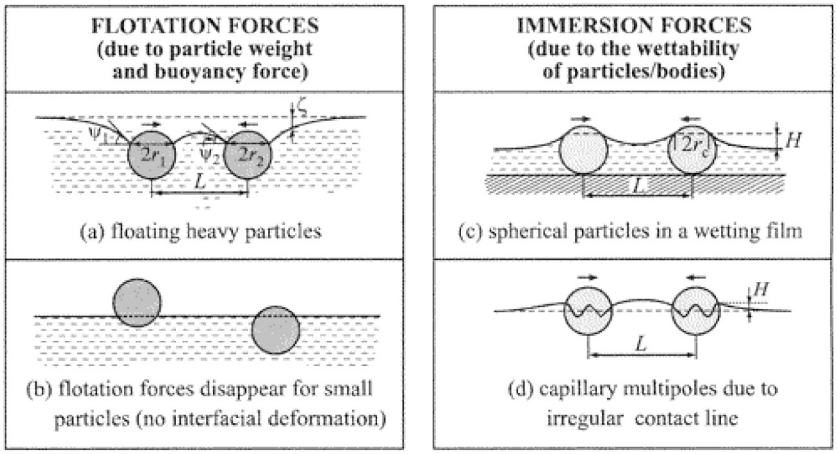

Fig. 9. Scheme showing the different types of capillary forces that can appear between particles trapped at a fluid interface. Reprinted from Kralchevsky et al. [203], Copyright (2001), with permission from American Chemical Society.

interfacial plane, is mainly defined by the wetting properties of the particles [206]. However, their adsorption can lead to local deformations of the fluid interface around the particles, thus leading to long-range capillary immersion forces. Roughness and/or chemical heterogeneities on the surface of the adsorbed particles surface promote the formation of a non-smooth, wavy or irregularly shaped, three phase contact lines, deformed enough to promote strong capillary interactions [10,40,207].

The capillary interaction between two identical neighboring spherical colloids can be expressed through an effective potential [207]

$$E_{capillary}(R) = -12\pi\gamma_{12}K^2\zeta\frac{r^4}{R^4} \tag{56}$$

where ζ is a factor that defines the dependence of the capillary interaction on the particle orientation and K a function accounting for the deformation amplitude of the interface.

The deformation of the interface, and thus the strength and dominant mode of capillary forces, can be modified by the application of electric or magnetic fields [208], or the addition of different additives (salts, surfactants, or polymers), that allow fine-tuning of particle wettability and interfacial tensions. The adsorption of charged colloids at a fluid interface between non-polar and polar fluids promotes extra interfacial deformations. These deformations are produced by the vertical interfacial electric force directed towards the fluid with higher dielectric constant, resulting from the combination of any external vertical force acting on the colloid and an inhomogeneous stress field. The latter presents different components of the above and below the fluid interface, which are induced by the electric dipolar field of the particles, and can be described in terms of the Maxwell pressure tensor [10]. These conditions lead to the electrodipping and electrocapillary forces that involve multiple or single particles, respectively [18,205]. It should be noted that electrocapillary and electrodipping forces can induce interfacial deformations that are often comparable to those resulting from the action of gravity on interfaces laden with large particles [78].

When the capillary interactions engage a larger number of particles, they can induce self-assembly through the so-called "Cheerios" effect, similar to that what is observed in cereal bowls [88]. Therefore, the control of capillary interactions, by adjusting the shape or wetting properties of the particles, can be used in the fabrication of complex interfacial structures [188]. If the apparent weight of the adsorbed species becomes larger than the interfacial forces, which is often the case of monolayers with a high interfacial coverage, the collective effects may modify the simple pairwise interactions, determining the deformation of the surrounding interface. This affects the organization of particles at the interface such that the entire aggregate sinks to the heavier phase ("collective sinking mechanism") [192,209].

4.2.2. Hydrodynamic interactions

Capillary forces are not the only contribution to the energetic landscape emerging in particle-laden fluid interfaces appearing as result of the presence of the interface, with the hydrodynamic interactions, stimulated by the motion of the particles through the viscous media, being strongly distorted by the particle adsorption. The adsorbed particles move in an overdamped regime, in which the applied forces and torques are constantly balanced by their viscous counterparts. The flow generated by the random or directed motion of the adsorbed particles, which can be modified by the possible presence of other particles or objects and surfaces, transports energy through the two media and can be described by the linearised Stokes equations. Therefore, apart from other possible direct interactions, the particles always exhibit solvent-mediated forces which, unlike the interactions described above, cannot be described by a potential. Complex and indirect hydrodynamic interactions have a tensor character, as they are strongly determined by the shape, orientation and relative velocity of the agents involved.

These interface-mediated hydrodynamic interactions control the steering of swimmers along defined trajectories [210], their attraction towards the interface [211], the circular path found in the motion of *Escherichia coli* [212], can be exploited on the transport of cargos along fluid interfaces [9], or the rectification of rotation into translational motion [213], where the local flow induced by the slip boundary condition imposed by the liquid-air interface differed from the one generated by the stick boundary condition characteristic of a solid wall. On the other hand, the balance between attractive interactions and hydrodynamic repulsive interactions emerging between rotating disks, floating at a liquid/air interface, leads to the assembly of dynamic lattices [214]. The relative importance of the hydrodynamic interactions is given by the capillary number

$$\mathrm{Ca} = \frac{\eta v_p}{\gamma_{12}} \tag{57}$$

where v_p is the particle velocity. It is commonly accepted that for $\mathrm{Ca} < 1$, the role of the hydrodynamics interactions may be neglected [40,208].

4.3. Externally actuated interactions

The adsorption of particles at a fluid interface is associated with a restriction of their mobility with respect to the interfacial plane. However, in-plane mobility is not limited, and in principle particles are free to move within the interfacial plane [215]. This motion can be boosted by the mechanical deformation of the interface, which can induce changes on the interfacial area (dilatational deformations) or shape (shear deformations). So, these perturbations can be exploited in the control of the interfacial assembly or the modulation of 2D phase transitions, which allows to adjust almost at will different mechanical, optical or electronic properties [104,216,217]. The application of magnetic or electric fields leads to similar effects when considering assemblies of responsive particles and is also a very powerful tool for tuning the assembly of colloids at fluid interfaces [7,208,218]. When adsorbed particles respond appreciably to the application of a magnetic field, while dispersive fluids do not show a strong response, the presence of the interface has essentially no effect on the nature of the magnetic interaction between the particles. However, the mobility constraints imposed by the high adsorption energy force the particles to restrict their motion to the adsorption plane. Consequently, the angle of application of the external field becomes a fundamental parameter determining the response of the particle monolayer. Alternatively, the applied field can be used only to force the rotation of the particles along the axes parallel to the confining surface, which is strongly hampered by the occurrence of interfacial pairs. The induced rotation can be used to change the extent and nature of capillary interactions at will [10,97].

An alternative way to modulate the interactions between particles, and thus the organization of particle assemblies at fluid interfaces, is by modifying the environmental conditions (pH, temperature or ionic strength). For example, changing environmental conditions has proven to be a very powerful tool for controlling the assembly of microgel particles at fluid interfaces [35,75,182].

5. Chemically isotropic particles at fluid interfaces

As developed previously, the surface chemistry of particles influences the self-assembly of particles at the fluid interfaces [75]. This results from the specific wetting properties of the particles [117], the shape of the contact line and/or the inter-particle interactions operating between the adsorbed particles [219]. In particular, chemical heterogeneities on the particle surface can lead to an undulated contact line. Furthermore, the presence of surface charges on the particles may modify the electrostatic and capillary contributions to the inter-particle interactions [219], and consequently the self-assembly of particles at the fluid interfaces. Therefore, the importance of the surface chemistry on the control of the properties of particle-laden fluid interfaces makes

necessary to distinguish between at least three different situations: (i) chemically isotropic particles; (ii) particles capped with ligands, and (iii) chemically anisotropic particles. This section focuses on the interfacial behavior of chemically isotropic particles.

5.1. Hard particles at fluid interfaces

Colloidal hard particles are a category including a broad range of particles with different chemical nature (polymeric, metallic, metal oxide compounds or ceramic), which present as main characteristic that their maximum deformation upon trapping at the interface remains on a length scale much smaller than their diameter, and hence they behave at the interface as solid-impenetrable objects for neighboring particles. This property determines the maximum packing that these particles can achieve at the fluid interface.

5.1.1. Spherical particles

The equilibrium trapping of chemically isotropic spherical particles at fluid interfaces is characterized by the existence of a single energy minimum, determined by the interfacial tension, particle size and contact angle, which also rule on the organization and properties of the adsorbed assemblies.

5.1.1.1. Interfacial organization. The understanding of the organization and self-assembly of colloidal particles at fluid interfaces requires to consider both the distribution of the particles within the quasi-2D fluid interface, and the position of the particles with respect to the interfacial plane, i.e., contact angle of the particles or immersion height. Both aspects are strongly correlated to the complex interactions that occur between particles both through the bulk and the fluid interface [220]. For instance, Zang et al. [221] reported that the change in the wettability of the adsorbed nanoparticles allows tuning the packing of the structures formed at the fluid interface, and consequently the interfacial morphology, in agreement with studies by different authors [64,80]. In a different work, the increase of the hydrophobicity of particles was described as the driving force for to a transition from loose-packed to close-packed arrays of particles [61], which appears strongly correlated to the complex interplay of interactions occurring between particles both in the bulk and upon trapping at the fluid interface [220].

Bonales et al. [222] studied the self-assembly of polystyrene sulfate latex particles, with a broad range of diameters (in the range 1.0-5.7 μm) at water/oil interfaces (in particular at water/octane interfaces). They found that the increase of the interfacial coverage drove the emergence of transitions between phases with different degree of ordering as was also found for nanoparticles [221]. It should be noted that the transitions between the different phases were not find independent of the particle dimensions, and only a shift of the critical density for the onset on a specific phase was observed with the change of the particle size. These finding were in accordance with the results obtained by Parolini et al [223] in a similar work. Fig. 10 reports a set of optical microscopy images corresponding to polystyrene sulfate latex particles microparticles of different sizes trapped at the water/octane interface, at different surface densities, together with the corresponding Fast Fourier Transform (FFT) of the images.

The images obtained using an optical microscope shows that the increase of the density of the particles trapped at the fluid interface enhances the order within the monolayer, in such a way that should be considered as reminiscent to that what happens in traditional 3D systems. The increase of the interfacial order is also reflected in the FFT images (see insets in the optical microscope images). The fluid phases, both gas-like and liquid-like films, are characterized by a random distribution of points in the FFT images. The hexatic phase, and more clearly the solid one, shows the formation of well-defined hexagonal arrays of dots in the FFT images as the monolayer density increases. The authors obtained further information related to the organization of the particles at the fluid interface by calculating the structure factor. Thus, at low interfacial coverage, the gas-like character of the monolayer was evidenced from an initial increase of the value of the structural factor from 0 to 1, followed for a region of constant value. The increase of the interfacial coverage pushes the monolayers to the onset on the liquid-like phase. This presents a structure factor characterized for the presence of a few oscillations which undergo an exponential damping with the increase of the separation between particles. This may be considered the result of the weakening of the positional order with the increase of the separation between particles. Therefore, the gas-like and liquid-like monolayers are characterized by the absence of orientational and positional order. The order in hexagonal 2D solid is evidenced by the presence of a narrow and intense peaks followed by another set of peaks, which appears at the position expected for a hexagonal array. The hexagonal 2D arrays present positional and orientational orders. On the other side, the hexatic phase presents only orientational order, appearing as an intermediate state between a liquid-like system and a perfectly order solid-like one as is predicted for the KTHNY theory [224]. Bonales et al. [225] also explored the interfacial organization of mixtures monolayers composed of particles having different sizes. They found that independently of the size difference between the particles the inclusion of particles of different size promotes disorder, and the stoichiometry in the mixture determines the emergence of arrested glassy states or polycrystalline regions, leading to an interfacial organization which appears as intermediate between those what correspond to each individual set of particles.

Rahman et al. [226] analyzed the possible correlations existing between the inter-particle interactions and the different phases emerging in particle-laden interfaces as the coverage increases. They found that the order at the interface is dependent on the strength of the interactions. Weakly repulsive or strongly attractive interactions promote the formation of disordered phases, whereas the emergence of a strong repulsion between the particles at the interface is associated with the formation of a highly ordered hexagonal array. The formation of the hexatic phase occurs when the repulsive and attractive forces are counter-balanced.

The important role of the interactions in the organization of particles

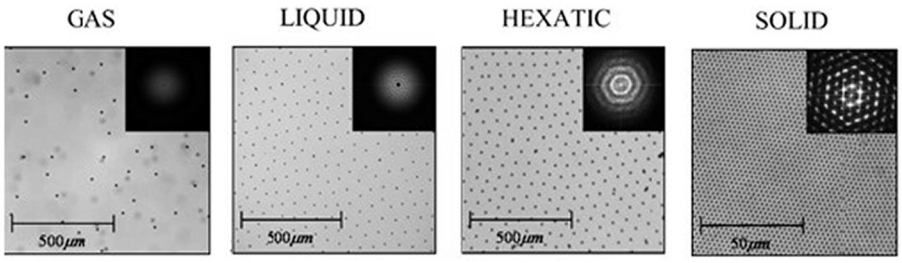

Fig. 10. Images and FFT images for charged polystyrene sulfate latex microparticles trapped at the water/octane interface. From left to right: microparticles with diameter of 2.9 μm; microparticles with diameter of 5.7 μm; microparticles with diameter of 1.6 μm, and microparticles with diameter of 1.0 μm. Adapted from Bonales et al. [222], Copyright (2011), with permission from American Chemical Society.

at fluid interfaces was also revealed by the results obtained by Reynaert et al. [227]. They found that the modulation of the electrostatic and capillary interactions, by adding electrolyte or surfactant, may induce the aggregation or percolation of perfectly ordered monolayers formed by polystyrene sulfonate latex microparticles adsorbed at the water/decane interface. Thus, under conditions characterized by strong capillary and/or hydrodynamics interactions, percolation can occur, resulting in the formation of networks formed by particles formin chains that span the boundaries of the interface [130]. The emergence of percolation in particle-laden interfaces offers a very interesting tool for modulating the mechanical resistance of the film [228].

5.1.1.2. Interfacial rheology. The adsorption of particles to fluid interfaces is widely used in the design and optimization of new materials and technological processes [65,70,183,229], e.g., phase transfer catalysis, encapsulation, enhanced oil recovery or emulsification and foaming [230]. In particular, these systems can be introduced to control the thicknesses of films in coating flows [231,232], the dispersion of surface waves [30,233], the dynamics and thicknesses of spreading films [113,234] and the lifetime of foams and emulsions [235–237]. The latter occurs because the adsorbed particles induce an additional energetic barrier to the coalescence of droplets and bubbles, due to electrostatic or steric repulsions, which slow or stop the thinning of liquid films. [238]. These processes are also governed by the dynamics of the system, since the particles advected by film thinning introduce gradients (Marangoni stresses) that oppose film drainage [239]. On the other hand, particles trapped at fluid interfaces can induce excess surface viscosity, elasticity or viscoelasticity that delays or modifies the film thinning [235]. Therefore, the understanding of the mechanisms involved in the relaxation of particle-laden interfaces after a mechanical deformation is a problem with a marked multidisciplinary character [240–242]. In this framework, interfacial rheology explores the deformation and flow that occur at interfaces when mechanical perturbations are applied to them.

The interfacial response of particle-laden fluid interfaces is characterized by the surface pressure, which is opposed to the surface tension and contributes to the in-plane deformations of the interfacial plane, dilations that cause changes in the material area, and shear stresses that induce changes in shape, generated by the coupling between the flows occurring at the interface and those of the bulk. On the other hand, under specific stress conditions, complex fluid interfaces exhibit out-of-plane deformations that push the monolayers or parts of the monolayers out of the interfacial plane (splaying or bending), inducing phenomena such as buckling of the monolayer, expulsion of material into the bulk or the formation of multilayers. Fig. 11 displays an idealized image of the different types of deformation that a particle-laden interface can undergo as result of the application of a mechanical stress.

The study of the rheological response of a particle-loaded interface requires consideration of the role of thermodynamic and hydrodynamic interactions between the particles and the surrounding fluids. The solution to this complex problem is only straightforward when the mechanical response of the bulk fluids is decoupled from that of the interface, i.e., when the mechanical response of the fluid phases is negligible with respect to that corresponding to the interfacial layer [235,243]. If the above condition is fulfilled, the deformation of a particle-loaded fluid interface can be considered the result of two concurrent processes that govern the mechanical properties of the interface: (i) the change of the size and/or shape of the fluid interfaces, and (ii) the deformation of the interfacial layer. Hence, the energy input required for the interfacial deformation can be expressed as

$$\sigma_{ij} = \gamma\delta_{ij} + T_{ij} \tag{57}$$

where δ_{ij} is the Kronecker delta and σ_{ij} the interfacial stress tensor, that is comprised by two contributions: (i) the interfacial energy, which is related to the energetic cost of the existence of a fluid interface with a fixed area. This contribution also includes any adsorption/desorption phenomena, that modify the interfacial tension, and (ii) the Marangoni stresses resulting from the existence of spatial surface tension gradients. The second contribution, the so-called anisotropic tensor (T_{ij}), includes the energetic cost associated with the deformation of the particle layer [2,244].

5.1.1.2.1. Interfacial dilational rheology. The trapping of particles at fluid interfaces does not influence only to the interfacial tension, but also leads to an increase of the resistance to compression that is characterized by the interfacial dilational viscoelastic modulus ε [27]. This magnitude provides information on changes in surface tension as a result of the modification of the area available for the distribution of the particles, which can be determined from the temporal evolution of the surface pressure $\delta\Pi(t)$ as result of the change of the interfacial area $\delta A(t)$ upon the application of an uniaxial stress [245]

$$\delta\Pi(t) = \Pi(t) - \Pi_0 = \frac{\partial\Pi}{\partial A}\delta A = -\varepsilon(t)u(t) \tag{58}$$

Here, $u(t)$ and $\varepsilon(t)$ are the temporal evolution of the compressional strain and dilational viscoelastic modulus, respectively, and $\Pi(t)$ and Π_0 the temporal evolution of the surface pressure and the initial surface pressure, respectively. The time dependence of the viscoelastic dilational modulus is given by

$$\varepsilon(t) = -A_0\left(\frac{\partial\Pi}{\partial A}\right)_T \tag{59}$$

and that of the compression strain by

$$u(t) = \frac{\delta A}{A_0} \tag{60}$$

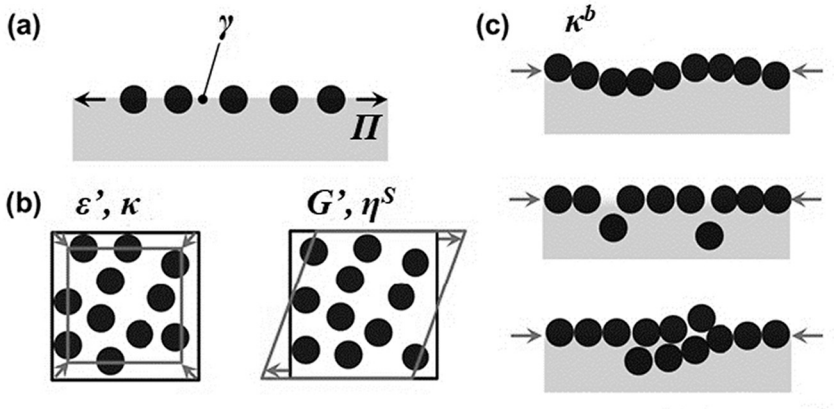

Fig. 11. Idealized representation of the different types of deformation that can appear at particle-laden interfaces as result of the application of a mechanical stress. (a) Equilibrium particle-laden interface characterized by its values of surface tension γ and surface pressure Π. (b) Particle-laden interface subjected to dilational (left panel) and shear (right panel) deformations, characterized by surface dilational elasticity ε' and viscosity κ, and shear elasticity G' and viscosity η^S, respectively. (c) Particle-laden interfaces subjected to out-of-plane deformations (from top to bottom): buckling (characterized by the bending elasticity κ^b), expulsion of material to the bulk, and multilayer formation. Adapted from Garbin [26], Copyright (2019), with permission from Elsevier.

Considering a fluid layer under equilibrium condition, the limit value of the dynamic modulus at zero frequency can be defined as the static modulus in terms of the Gibbs elasticity ε_0 as

$$\varepsilon(t)\rightarrow\varepsilon_0 = \Gamma\left(\frac{\partial\Pi}{\partial\Gamma}\right)_{eq} \tag{61}$$

where $\Gamma=1/A$ is the interfacial concentration. For an oscillatory deformation of small-amplitude and characteristic frequency ω, the complex dilational viscoelastic modulus is defined as

$$\varepsilon(\omega) = \varepsilon'(\omega) + i\omega\kappa(\omega) \tag{62}$$

where the real part $\varepsilon'(\omega)$ is the storage modulus or interfacial dilational elasticity and the imaginary part $\varepsilon''(\omega) = \omega\kappa(\omega)$ the loss modulus. Here, κ represents the surface dilational viscosity. The above definition of the viscoelastic interfacial dilational modulus considers that the stress associated with the interfacial deformation can change both the adsorption state of the particles and the interfacial structure. Under these conditions, the modification of the interfacial area can promote other different relaxation processes, with different characteristic timescales [36,229,246,247].

One of the first attempts to shed light on the response of particle-laden fluid interfaces to dilational deformations was made by Miller et al. [247]. They provided a theoretical description for the relaxation mechanisms emerging in particle-laden interfaces upon the application of a dilational stress following a similar approach to that was previously reported for the description of the dilational rheology of proteins and proteins–surfactant systems [65,248]. This allows describing the dilational response of particle-laden interfaces in terms of the information provided by the adsorption isotherms. Despite the interest in obtaining models that combine equilibrium information with dynamic one, the above model was not further extended, mainly because of the difficulties associated with determining a true equilibrium isotherm.

The particle wettability is probably the most important parameter for defining the trapping of particles at fluid interface, and hence the contact angle of the particles may modify decisively the performance of particle-laden interface against dilational stresses as was demonstrated by Safouane et al. [249]. They studied the rheological response against dilation of monolayers of fumed silica nanoparticles at the water/vapor interface using measurements of the damping of capillary waves in the frequency range 200–1000 Hz), and found the existence of important correlations between the interfacial morphology and the interfacial rheological response. The elastic component of the dilational viscoelastic modulus was found to increase with the particle hydrophobicity and the interfacial coverage, whereas the loss modulus remained almost. This leads to a situation in which the compressibility modulus of hydrophilic particles trapped at the water/vapor interface emerges close to 0, increasing its value up to values close to 200 mN/m with the increase of the hydrophobicity of the particles. This rigidification mediated for the particle hydrophobicity may be understood considering a densification of the interfacial layer coupled to the strengthening of interactions between the particles at the interface [250]. Kirby et al. [251] showed that the inter-particle interactions play a very important role on the control of the interfacial mechanical response. They found that the screening of the electrostatic repulsion between particles leads to a strong hysteresis on the dilational response of the particle-laden interface, which may be explained considering the formation of rigid incompressible films at the interface mediated for the aggregation of the particles.

Safouane et al. [249] also found that the storage modulus appears always higher than the loss one, irrespectively of the particle hydrophobicity and the interfacial coverage. Zang et al. [252] enlarged the frequency range explored by Safouane et al. [249], including data corresponding to the low frequency range. This study provides information on the relaxation processes emerging at the interface as result of the application of the dilational stress. Thus, it was found that the reorganization of the particles at the interface leads to a relaxation process with a characteristic time of about 1000 s. The importance of this relaxation process was found to increase as the particle hydrophobicity decreases, which may be understood considering the reduction of the interfacial coverage, and hence the reduction of the steric hindrance associated with the reorganization of the particles at the interface which favors the motion of particles at the interface.

The response against dilation of particle-laden interface formed by polymer particles presents some differences with the above discussed for silica nanoparticles as it was reported by Kobayashi and Kawaguchi [253]. These differences may be ascribed to the partial deformability of the polymer particles. Kobayashi and Kawaguchi [253] showed that the dilational response of latex particles at the water/vapor interface presented a mostly viscoelastic character, independently of the strain rate. Furthermore, the elastic and viscous dilational moduli undergo an increase with the interfacial coverage up to reach a critical value at a surface pressure of about 15 mN/m, and then both start to decrease steeply. This may be explained considering the emergence of out-of-plane deformations (buckling) of the monolayer upon the application of the dilational stress, which leads to a distortion of the quasi-2D organization of the particle-laden interface. Analyzing the frequency dependences of the viscoelastic moduli, it was possible to observe the emergence of a transition from a fluid-like behavior to a solid-one as the interfacial packing density increases, which agrees with the structural picture extracted from the studies by Bonales et al. [222]. Therefore, the dilational rheological response may be considered strongly dependent on the specific region of the phase diagram analyzed [222,253,254]. It is worth to stress that the rigidity of spread layers appears in most of the cases higher than that obtained for particle-laden interfaces with the same interfacial density obtained upon compression of the area. This may be the results of the emergence of non-equilibrium arrested states which add some additional relaxation process to the response of the particle-laden interface against dilational stresses [252].

The understanding of the interfacial organization-rheological response correlations in particle-laden interfaces were further explored by del Rio et al. [255], confirming the importance of the nature of the monolayer, i.e., its phase, on the control of the dilational viscoelastic modulus of particle-laden interface. Furthermore, their results confirmed the finding by Safouane et al. [249] in relation to the mainly elastic character of the monolayers, i.e., the storage modulus appears higher than the loss one. The storage modulus was found to increase with the interfacial coverage within the region of low surface pressure of the isotherm, whereas the loss modulus appears similar to that expected for the pristine water/vapor interface. This results from the contribution of the electrostatic repulsion between the particles trapped at the fluid interface. Furthermore, when the interfacial coverage is pushed beyond a threshold value, the storage modulus undergoes a sharp increase up to a value close to 350 mN/m, which can be explained considering the formation of a close-packed particle film at the interface, as was evidenced by using Brewster Angle Microscopy (BAM). It is worth mentioning that the screening of the electrostatic interaction, i.e., in presence of weak repulsive electrostatic interactions, the storage modulus can reach values close to 600 mN/m, which is the results of the minimization of the number of defects remaining in the close-packed monolayer [256]. It should be noted that emergence of out-of-plane deformations at the highest values of the surface pressure makes dropping both the storage and loss moduli in agreement with the results previously reported by Kobayashi and Kawaguchi [253]. On the other, the rheological response against dilation of latex monolayers can be considered qualitatively similar for particles adsorbed at both water/vapor and water/oil interfaces [254,256].

The size of the particles is a very important parameter to be considered when the rheological response against dilational stresses of particle-laden interfaces is analyzed. Vella et al. [257] reported that the Young's modulus of monolayers monodisperse particles with the same

chemical nature at fluid interfaces is inversely proportional to the size of the particles.

It should be noted that the interfacial dilational flows induced in common laboratory experiments are smaller than those what are expected in industrial processes. This was demonstrated by Hilles et al. [258], who explored the dilational response of latex particles at the water/octane interface against oscillatory deformations with different deformation amplitudes and found that particle-laden interfaces present a very narrow region of low strain in which the interfacial response appears as linear.

5.1.1.2.2. Interfacial shear rheology. The existence of bulk flow can induce the emergence of interfacial shear deformations at particle-laden interface involving mass and momentum transport [216]. For shear deformations, the amplitude and time evolution are not coupled to any of the other interfacial modes [259]. This leads to a situation in which is possible to provide a definition of the shear elasticity corresponding to an in-plane shear deformation as a constant that defines the proportionality between the applied strain (u_{xy}) and the stress (σ_{xy}). In a solid like-film, considering a Hookean-like behavior, the shear elasticity is given by $\sigma_{xy}=Gu_{xy}$. On the other side, the behavior of fluid-like layers is dominated by the viscous character of the layer, and the shear stress can be expressed as

$$\sigma_{xy} = \eta^{s}\frac{du_{xy}}{dt} \tag{63}$$

where du_{xy}/dt and η^{S} are the strain rate and the interfacial shear viscosity, respectively. In most of the systems the viscoelastic parameters (G, η^{S}) are higher when the system presents strong interactions between the particles, which can be explained by considering the flow induced in the surface elements as result of the energy required to overcome interfacial interactions [27]. For an oscillatory deformation, the complex shear modulus G^{*} is defined as

$$G^{*}(\omega) = \acute{G}(\omega) + i\acute{\acute{G}}(\omega) \equiv G' + i\omega\eta^{S} \tag{64}$$

with G' and G'' being the storage or shear elastic, and loss moduli, respectively. For experiments in which the amplitude of the oscillatory deformations at fixed frequency ω remains small, it is possible to define the shear viscosity as $G''=\omega\eta^{S}$.

The study of the response of particle-laden fluid interfaces to shear has gained importance in recent years, especially because of the implication of the shear process in different aspects related to the stability of emulsions and foams [28,36,247]. This has stimulated significant research work attempting to unravel the correlations that arise between the interfacial micro-structure and the shear response of particle-laden fluid interfaces, with inter-particle interactions playing a key role in modulating these correlations [260]. It should be noted that the differences between the inter-particle interactions that arise when the particles are dispersed in bulk and at fluid interfaces give rise to important differences in the shearing behavior of 3D particles suspensions and their interfacial counterparts [261].

The seminal work on the characterization of particle-laden interfaces against shear stresses was done by Cicuta et al. [262]. They compared the behaviour of polystyrene latex particles (3 μm of diameter) at the water/decane interface with that of β-lactoglobulin layers. While the interfacial rheological response of the particle monolayers presented a mainly viscous character ($G'' > G'$), the β-lactoglobulin laden interface turned out to be mainly elastic. The difference can be attributed to the possibility that the protein undergoes deformation and compression processes when shear deformations are applied. At low coverage, the response against shear was found to be dominated by the viscous contribution, which can be considered reminiscent of what is expected for liquid-like films. On the other hand, it was found that the viscoelasticity of particle-laden interface undergoes a sharp increase for surface coverage above 75-80% as a result of particle jamming. This agrees qualitatively with the findings by Yu et al. [263] for monolayers of silica particles. In the limiting conditions, at higher coverages, the response is dominated by the elastic contribution, and the monolayers can be considered as solid-like films.

It should be noted that the transition from viscous-like to solid-like behaviour can be modulated by changing the ionic strength, i.e., by modifying the inter-particle interactions. The increase of the ionic strength does not significantly modify the dependence of the viscoelastic moduli on the interfacial coverage. However, the transition from viscous to elastic-like behaviour occurs at lower values of the interfacial coverage as the ionic strength increases, which can be understood considering that the screening of the electrostatic repulsions between particles favours interfacial aggregation [263].

The role of interfacial coverage in the response of particle-laden fluid interfaces to shear stresses was also analysed by Imperiali et al. [264]. They showed that the reorganization ability of the particles plays a central role in controlling the interface response against shear, which qualitative agrees with the results of Barman and Christopher [265] for polystyrene latex at water/vapor interface. They used a double-walled interfacial shear rheometer that allowed characterization of the interfacial microstructure, and found a transition from shear thinning behaviour, characterized by the breakup of particle clusters, to one of yielding with increasing interfacial coverage. The origin of this transition was attributed to differences in the mechanism of viscous stress dissipation. The occurrence of yielding at interfacial coverages well below that corresponding to interfacial jamming, suggested that the solid-like behaviour can occur prior to reaching close-packing or jamming conditions. In addition, the authors found that monolayers with high interfacial coverage can undergo a shear-induced ordering phenomenon.

Barman and Christopher [265] found that increasing interfacial coverage reduces the range in which the rheological response is linear, with the coverage dependence of the viscoelastic shear modulus being described in terms of a power law. The above studies were extended, leading to the conclusion that the viscoelastic response of particle-laden interface is governed by constrains on particle motion. These constrains were associated with the inter-particle capillarity attraction and the caging-effects emerging from the local micro-structure. Furthermore, Barman and Christopher [266] reported the important role of meso-structural organization in determining the elasticity and yield. They found that the formation of aligned domains of hexagonally packed particles gives rise to elastic-like particle films, and that decreasing domain size leads to interfacial flows and viscous-like behaviour.

The study of the effect of the interfacial packing on the response of particle-laden interfaces against shear stresses was extended by Reynaert et al. [267]. They provided further evidence of the influence of inter-particle interactions in modulating the interfacial rheological response, showing that particle aggregation leads to an interfacial shear response reminiscent of that found in bulk counterparts. This agrees qualitatively with the results obtained by Wijmans and Dickinson [268] using Brownian dynamics simulations. The role of the inter-particle interactions in the response of particle-laden interfaces to shear stresses was also studied by Beltramo et al. [247]. They found that the existence of strong lateral interactions between the particles promotes the emergence of interfacial yield stress, and that the elastic modulus and the yield stress increase tenfold when the interfacial coverage increases from 0.47 to 0.88. For interfacial coverages below 0.64 the viscoelastic modulus was almost negligible, while above that threshold the viscoelastic modulus of the particle films increase. For interfacial coverages in the range 0-75-0.80 the viscoelastic modulus reached a plateau, which was attributed to the emergence of interfacial jamming.

Muntz and Thijssen [269] have recently delved into the correlations between the structure of particle-laden interfaces and their rheological behaviour. For this purpose, they studied poly(methyl metacrylate) particles at water/dodecane interfaces using a shear rheometer coupled to a confocal microscope. The results obtained showed that, at low surface coverage, the particle-laden interface behaves as a two-

dimensional Newtonian fluid, which undergoes aggregation when a shear stress above a threshold value is applied. The increase in interfacial coverage leads to an interfacial behaviour dominated by the elastic contribution, and above the yield stress, the interface undergoes plastic deformation.

As was mentioned above, particle roughness plays a very critical role in the entrapment of particles at fluid interfaces and thus in their interfacial organization. Hence, it is necessary to consider its impact on the response of particle-laden interface upon the application of shear stresses. The role of the particle roughness in the shear response of the particle-laden interfaces is closely correlated to the interfacial coverage [270], which can be explained in terms of inter-particle friction [271]. At low interfacial coverage, the interfacial shear viscosity of the particle-laden interfaces decreases as the surface roughness increases, while the response is the opposite as jamming approaches [272].

This behaviour can be understood considering the trapping of the particles at metastable positions as result of the contact line pinning [273]. The emergence of contact line pinning may lead to a situation in which particles behave very differently to that what was expected considering their wettability, i.e., hydrophilic particles may behave upon trapping at fluid interfaces as hydrophobic ones, and the latter as hydrophilic ones. This offers the possibility for stabilizing both water-in-oil and oil-in-water by using a single type of particles, without needing any change of its wettability. Therefore, it is clear that the shear response of particle-laden interfaces appears strongly influenced by the hydrophilic-lipophilic balance of the particles. Safoune et al. [249] confirmed such picture. They studied monolayers of fumed silica particles having different hydrophobicity degrees, and found that the increase of the hydophobicity of particles for a similar value of the interfacial coverage leads to monolayers with higher values of the shear elastic and viscous moduli. The particle monolayers were found to present a behavior governed mainly by the elastic contribution for particles with a low hydrophobicity degree, becoming purely viscous when the hydrophobicity degree is high. Thus, a cross-over between elastic and viscous films was found, i.e., a gel point ($G' = G''$), for particles with an intermediate wettability which are trapped at the fluid interface with a contact angle around 90°. The above studies were extended by Zang et al. [90,252,274], who explored the effect of the particle hydrophobicity on the response against shear stresses. They studied monolayers of fumed silica particles at the water/vapor interface, and did not find any dependence of the elastic modulus on the strain amplitude when the latter was small. Furthermore, an elastic modulus with values ten times higher than the viscous one was found. On the other side, Zang et al. [90,252,274] reported the possible appearance of a melting transition for particle monolayers when the strain amplitude overcomes a threshold value (yield stress). Under such conditions, the loss modulus reaches its maximum value, whereas the storage modulus drops. The response of the particle-laden fluid interface to the application of small deformations of low frequency evidences a viscous character, whereas for deformations of high frequency the behavior becomes mainly elastic. Furthermore, a quasi-linear dependence of the relaxation time on the shear rate was found. This may be considered analogous to that what is found in 3D softs solids, and may be explained considering the reduction of the characteristic time of the structural relaxation that occurs because of the increase of the strain-rate amplitude [275], in agreement with the results reported by Vandebril et al. [276].

A further important aspect to be considered, for the response of particle-laden fluid interfaces to the application of shear stresses is related to the analysis of its time evolution. For elucidating this aspect, Krishnaswamy et al. [277] studied, by using shear rheology, the adsorption kinetics of silver nanoparticles (in the range 10-50 nm) at toluene/water interfaces by using shear rheology, and found an increase of both the storage and loss moduli with time. This is due to the densification of the monolayer during the adsorption process. Furthermore, upon interfacial equilibration it was found that the particle-laden interface has a behavior that presents some reminiscence to that what may be expected for a 2D glassy material, with the shear response depending strongly on the stain amplitude. On the other side, the use of strain sweep measurements evidenced a shear thickening behavior of G'' upon deformations with a large strain amplitude, whereas no dependences of G' on the strain amplitude were reported up to the shear thickening point. Furthermore, it was found that the shear thickening may be described using a power-law in which the exponents for describing the storage and loss moduli assumed values of 2 and 1, respectively. The behavior found for silver nanoparticles may be considered very different to that for gold nanoparticles at the water/vapor interface [278]. The latter shows a behavior reminiscent of a gel-like systems undergoing strain induced softening. Furthermore, for gold nanoparticles the rheological response does not present any dependence on the applied stain for values below a threshold corresponding to 0.1%, and then the storage modulus drops. On the other side, the viscoelastic moduli can be described as a function of the interfacial coverage using a power law with an exponent around 0.65. This seems a reminiscence from that what is found in percolating systems [246].

5.1.1.2.3. Out-of-plane deformation. The deformation of particle-laden fluid interfaces upon the application of large compressional stresses may induce the emergence of elastic instabilities in the monolayer, which leads to out-of-plane deformations of the quasi-2D particle layer [11,26]. This may be explained considering the emergence of different types of phenomena in particle-laden interfaces upon compression. An initial compression of the particle-laden fluid interface leads to the formation of close-packed films, which can undergo in and out-of-plane deformation upon further compression. This results in monolayer buckling, expulsion of material from the interface or multilayer multilayer formation [279].

The buckling in particle-laden interfaces occurs when the surface pressure is high enough to cause a dropping of the effective interfacial tension down to a quasi-null value. However, under specific conditions the expulsion of particles from the interfacial layer may be favored with respect to the buckling. This may be rationalized considering the differences existing between the trapping energy ΔE_p, and the mechanical work required for compressing the interface $dW=\Pi dA$. This allows one to consider that the expulsion of particles from the interface is only possible when the work associated with the compression exceeds to the trapping energy. Therefore, it is possible to define a boundary condition which defines the expulsion of particles as $W=\Delta E_p$. This provides a definition for the force balance associated with the particle expulsion as [280]

$$\Pi = \gamma_{12}(1 \pm cos\theta)^2 \tag{65}$$

It should be stressed that the above expression does not include the role of the interfacial interactions, which may modify the deformation profile. Thus, the presence of attractive inter-particle interactions may induce the formation of elastic solid-like films, in which the emergence of particle expulsion upon compression is not possible [93].

Leahy et al. [281] found that the compression of monolayers formed for gold nanoparticles beyond the close packing leads to the folding of the monolayer followed by the formation of multilayers. The wavelength of the wrinkles allows obtaining information related to the bending modulus of the particle monolayers and multilayers by applying the elasticity theory. The emergence of wrinkles on particle-laden interfaces was ascribed by Vella et al. [257] to the formation of particle clusters at the fluid interface, which allows considering that the compression of particle-laden interfaces beyond the collapse leads to an elastic behavior characterized by a buckling length defined as

$$\lambda = \pi\left[\frac{4}{3(1-\vartheta)(1-\nu_P)}\right]^{1/4}\sqrt{2Rl_c} \tag{66}$$

where ν_P represents the Poisson ratio, which provides information about the deformation of the interface following the direction perpendicular to

the direction of application of the stress. In this particular case, the Poisson ratio evaluates the ability of the interface for undergoing out-of-plane deformations. It should be noted that the above model provides a good description of the interfacial behavior for particles with diameters in the micrometer range (above 1 μm). However, for smaller particles, it provides an underestimation of the buckling wavelength, which may be the result of a high bending elasticity, κ^b [282]. In the case of monolayers of anisotropic particles, the compressive stress can be released by their interfacial rearrangements, which may induce a flipping transition upon compression. Further compression of bucked particle-laden interfaces may result in the expulsion of some particles to one of the adjacent fluid phases [283].

Most of the phenomena occurring at particle-laden interfaces when the monolayer is compressed beyond the collapse may be modulated by changing the particle contact angle [284]. This may be understood considering the important contribution of the inter-particle interaction on the control of the interfacial microstructure and rheological response. Thus, hydrophilic particles lead to the formation of fluid-like particle-laden interfaces which may undergo an irreversible collapse with a noticeable expulsion of particles from the interface to the bulk. On the other side, solid-like films formed by hydrophobic particles present a high compressional elasticity due to the strength of the cohesive interactions between particles. This commonly leads to the emergence of a reversible collapse through the formation of wrinkles and folds. This can be understood considering the arrest of the mechanisms guiding the expulsion of particles from the monolayer to the bulk fluids as result of inter-particle interactions with attractive origin.

5.1.2. *Anisotropic particles at fluid interfaces*

The above discussion has been focused on the analysis of the behavior of spherical or nearly spherical particles trapped at fluid interfaces. However, the adsorption of particles may be modulated by the chemical and geometrical characteristics of the particles [285,286], which has stimulated the interest for studying the interfacial behavior of particles with anisotropy in their shape or in their chemistry [287,288].

5.1.2.1. Chemically homogeneous non-spherical particles. The shape anisotropy of particles presents a key role in the attachment of particles to the fluid interface. This is clear considering that, whereas for spherical particles the position in relation to the interfacial plane can be defined exclusively by the contact angle, the analysis of the trapping of non-spherical particles, including ellipsoids, dumbbells or cylinders, need to consider both the shape and wettability of the particles [289,290]. Particles with a relatively high degree of anisotropy, i.e., particles with a large aspect ratio, adsorb commonly at fluid interfaces orienting their major axes parallel to the fluid interface. Fig. 12 is a sketch showing the orientation of particles with different aspect ratios (S_I) trapped at fluid interface. It should be noted that the aspect ratio provides a relationship between the two main radiuses of the anisotropic particles.

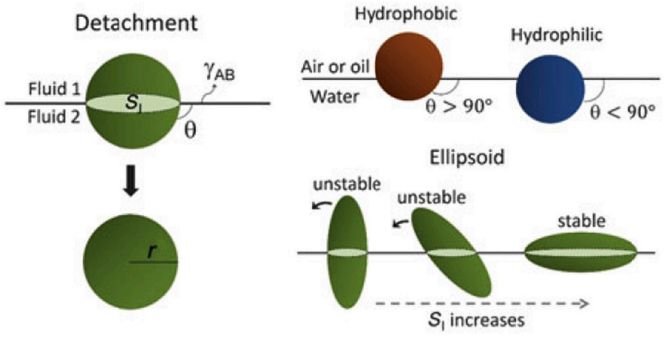

Fig. 12. Sketch representing the adsorption of different chemically homogenous particles with different degree of shape anisotropy trapped at fluid interfaces. Reprinted from Park and Lee [285], Copyright (2014), with permission from Springer-Nature.

The existence of different possible configurations for the trapping of a specific type of particles at a fluid interface influences the balance of interfacial inter-particle interactions, which in turn modifies the assembly of particles at the interface, and consequently the properties of the particle layers. On the other side, the ability of particles with anisotropic shape to remain trapped at the fluid interface is strongly dependent on their geometries. A critical aspect ratio exists beyond which the adsorption of anisotropic particles becomes unstable. The emergence of adsorption instabilities results from the high values of the line tension [10]. The correlations between the line tension and the aspect ratio have driven important research efforts trying to optimize the adsorption of different anisotropic particles, e.g., carbon nanotubes, at fluid interfaces. Thus, for particles with similar volume, the trapping energy changes according to the following order disks>rods>spheres. On other side, the maximum differences of the trapping energy in relation to that what are found for spherical particles can be found at the extreme wetting conditions, i.e., close to 0 and 180 degrees [291].

For cases in which the wetting conditions are fulfilled, ensuring the attachment of chemically homogeneous but geometrically anisotropic particles to the fluid interface, it is possible to find a deformation of the fluid interface in the vicinity of the particles, that leads to attractive capillary interactions that overcome the repulsive electrostatic contributions [188]. Furthermore, the short-range interactions, e.g., van der Waals or steric, are also strongly modified as result of the shape anisotropy of particles [10].

The impact of the shape anisotropy on the assembly was evidenced from the work by Loudet et al. [187]. They explored the assembly of micron-sized particles with ellipsoidal shape at a fluid interface, and found that the asymmetric distribution of the interactions within the interface leads to the association of the particles in open branched aggregates of particles which tends to be oriented forming particle chains as a result of the directionality of the interactions [287]. This behaviour is very different to that what is found for spherical colloids trapped at fluid interfaces which form well-defined close-packed film structures [222]. The differences on the interfacial assembly of particles resulting from the specific particle shape should be ascribed to the capillary interactions. Thus, non-spherical particles interact through long-range capillary interactions with quadrupolar origin, which exceed by several times the thermal energy (k_BT), leading to a complex interfacial assembly [10,187,287,288]. In particular for ellipsoidal particles trapped at the water/vapour interface, the quadrupolar interface deformation characterized by depression and ascension of the interface around the tip and side regions, respectively lead to the assembly of side-to-side or tip-to-tip structures as was reported by Loudet et al. [309]. The quadrupolar deformation of the interface was also reported for the adsorption of cylindrical particles at both water/vapour and water/oil interfaces [188,292]. Thus, for cylinder-like particles trapped at fluid interfaces, the interface deflects upward on the planar end surface and downward around the sides. The prominent interfacial deformation on the end surfaces leads to the formation of linear chain-like structures.

The above differences on the organization of anisotropic particles at fluid interfaces depending on their shape are due to the very different energetic landscapes [292]. Thus, the side-to-side chains obtained from the assembly of ellipsoidal particles present a certain degree of flexibility, whereas the end-to-end configurations obtained from the assembly of cylindrical particles present a high rigidity. This confirms the important directional character of the capillary interactions in monolayers of anisotropic particles at fluid interfaces. The ability for self-organizing of anisotropic particles can lead to a rich interfacial phase behaviour, including the formation of isotropic, 2D nematic, 2D smectic and 3D nematic phases, as was evidenced by Kim et al. [293] for $BaCrO_4$ nanorods and by Hernández-López et al. [294] for carbon nanotubes.

The differences in the assembly induced by the anisotropic shape also affects the interfacial response against mechanical stresses. Madivala et al. [289] explored the interfacial behavior of ellipsoidal particles

made of polystyrene at water/decane and water/vapor interfaces, and found that the assembly of the particles at the fluid interfaces may be tuned by changing the electrostatic interactions within the systems. This leads to the formation of arrangements of individual particles coexisting with linear aggregates at water/decane interfaces, and flower-like aggregates at water/vapor one. The different organization of the particles depending on the nature of the interface leads to very different responses upon the application of shear stresses. This agrees with the general picture that correlates the interfacial packing and the mechanical response of the particle-laden fluid interfaces. In particular, ellipsoidal particles at the water/decane interface behave as an elastic system, with its viscoelastic modulus increasing with the interfacial coverage. Such increase was found to be governed by a strong increase of the elastic component of the shear modulus. It should be noted that the importance of the elastic component on the behavior of ellipsoidal particles is just the opposite situation that what reported by Cicuta et al. [262] for spherical particles, which may be due to the existence of very different relaxation mechanisms [283]. Furthermore, on the contrary to that what was found for spherical particles, ellipsoidal particles trapped at a fluid interface can undergo buckling processes when the interfacial coverage is relatively high. Therefore, it is possible to assume that the differences on the rheological response due to the shape anisotropy of particles may be understood considering the broad range of interfacial packings that can appear for non-spherical particles. This is strongly correlated to the specific degree of anisotropy of the considered particles, which modifies the balance of interfacial interactions, and hence changes the aggregation pattern and interfacial rheology of the particle-laden interface. The effect of the morphology of the particles on the response of the interface upon the application of shear stresses was extended by Brown et al. [271]. They studied particles with different aspects ratios, and found a shear thickening phenomenon independent of the anisotropy degree of the particles. However, the anisotropy becomes a critical parameter for controlling the jamming of the particles at the fluid interface. Thus, the increase of the degree of the anisotropy of the particles reduces the threshold value of the coverage for the onset of the jamming region. On the other side, it has been reported that the asymmetry of the particles may induce the formation of kinetically trapped films, which modifies the shear flows at the interface [295,296].

5.1.2.2. Chemically anisotropic particles. The interest in exploiting chemically anisotropic particles for stabilizing interfaces was originated from the Nobel Lecture of Pierre-Gilles de Gennes, in which the use of colloidal particles with two separated regions with different chemical nature, the so-called Janus particles, was proposed for replacing molecular surfactants [297]. However, the advances in the synthetic routes used for the fabrication of colloidal particles has allowed to introduce other types of chemical anisotropic particles, e.g., dumbbells, patchy colloids or shape anisotropic Janus particles [118].

The adsorption of spherical Janus particles tries to ensure the energy minimization condition. This leads to a situation in which particles with two symmetric domains of different wettability adsorb to the fluid interface in such a way that each domain is paired with its preferred fluid phase, i.e., the phase of higher affinity, and their trapping occurs with the Janus boundary pinned at the interface. This means that particles having a non-polar domain and a polar one will adsorb to water/oil interfaces with the non-polar and polar regions placed in contact with the oil and the aqueous phases, respectively. This conformation leads to the largest decrease of the interfacial energy [298]. Furthermore, the adsorption of Janus colloids in which the domains of different wettability are not symmetric, i.e., present different size also adopts the configuration at the fluid interface that allows minimizing the interfacial energy, which may not correspond to the pinning of the Janus boundary at the interface [299]. It should be stressed that the trapping energies for Janus colloids at fluid interface can be several times higher (up to 3-fold higher) than that corresponding to homogeneous particles [300]. According to the above discussion, the equilibrium position of Janus particles at fluid interfaces may be predicted using similar approach to that used above for defining the contact angle (see Section 2.4) [301]. However, the dual chemistry of Janus particles makes necessary to define two contact angles, the first one in relation to the polar phase θ_P and the second one in relation to the non-polar phase θ_A [299]. This allows defining a degree of amphiphilicity for a Janus particle as $\Delta\theta = (\theta_A - \theta_P)/2$. Thus, it is possible to define the Janus boundary using the angle α, which is placed at 0 and 180 degrees for polar and non-polar particles, respectively, whereas for particles with two patches of the same size assumes a value of 90° [302]. Therefore, it is possible to modify the amphiphilicity of Janus particles by changing the wettability of each patch, i.e., modifying θ_P and θ_A, or the value of the Janus boundary α. Thus, assuming the absence of rotation of Janus particles at the interface, the equilibrium contact angle may lead to up to three different equilibrium positions defined for their equilibrium contact angle θ_E. Fig. 13a-c reports different situations for the equilibrium positions of different Janus particles in relation to their chemically homogeneous counterparts [301,302].

The above discussion clarifies the orientation of spherical Janus particles upon the adsorption to fluid interfaces. However, the situation is less clear when Janus particles with anisotropic shapes (ellipsoids, dumbbells or cylinders) are considered in which the anisotropy provides extra degrees of freedom for modifying the orientation of the particles upon the adsorption at the fluid interface, which influences significantly the interaction between particles at the interface [303]. It has been reported that Janus particles with large aspect ratios adsorb preferentially in a tilted configuration, i.e., with the Janus boundary parallel to the interface. However, the increase of the wettability differences between the two domains of the Janus particle may induce the adsorption in an upright orientation to maximize the contact between each region and its preferred fluid phase. On the other hand, for particles with domains of similar wettability, it is possible to find the coexistence of upright and tilted orientations, which may be considered as a metastable orientation at a secondary energy minimum [303]. Therefore, the rotational freedom of Janus particles emerges as an essential aspect governing their stability at fluid interface [286,298,302]. This was confirmed by Bon and Cheung [304] using Monte Carlo simulation. They reported that neglecting the rotational freedom of Janus particles at the interface underestimates the trapping energy. Furthermore, different studies demonstrated the role of the amphiphilicity of the Janus particles on their orientation at fluid interfaces [190,298]. The adsorption of dumbbells is more straightforward because the narrow neck hinders the secondary energy minimum, which limits the possibility to absorb in the tilted configuration [303]. The existence of this preferred direction for the adsorption was evidenced by the contact angle measurements by Isa et al. [305]. The situation for the adsorption of patchy colloids is analogous to that what appears for dumbbells, with their adsorption occurring in a preferential orientation defined for the opening angle of the patches [199,306]. Fig. 13d shows an example of the different orientations that can emerges for Janus particles for which a combination of shape and chemical anisotropies exists.

The above discussion has evidenced the importance of anisotropies on determining the equilibrium position of particles at fluid interfaces. However, a more detailed analysis allows evidencing that the equilibrium position of Janus particles is defined for the balance between shear- and capillarity induced torques. The former emerges from the shear forces occurring at the particle surface, wherear the latter are a result of the preferential wetting of the particles for one of the fluid, and the equilibrium orientation of Janus particles is given for the point in which the net torque assumes a null value [118].

5.1.2.2.1. Inter-particle interactions. The contact angle pinning of Janus particles trapped at fluid interfaces leads to irregular deformations of the interface which induce attractive interactions between particles [298]. This is because inter-particle interactions are governed by the minimization of the interfacial energy, which requires a reduction

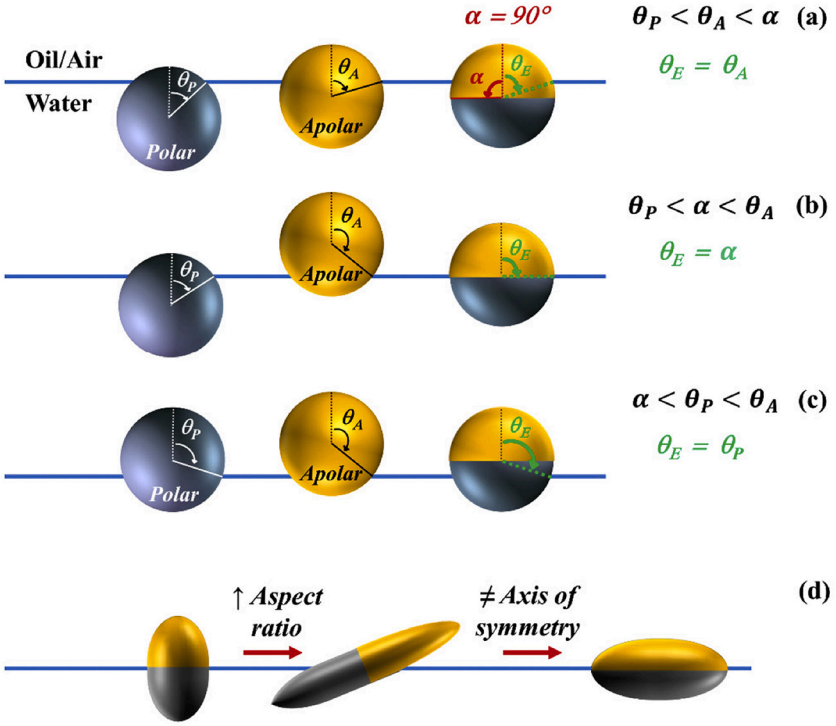

Fig. 13. Equilibrium position of Janus particles at fluid interfaces. (a) Equilibrium contact angle defined for the contact angle of the non-polar phase. (b) Equilibrium contact angle defined for the Janus boundary. (c) Equilibrium contact angle defined for the contact angle of the polar phase. (d) Impact of shape and chemical anisotropies. Reprinted from Correia et al. [29], with permission from MDPI under Attribution License Creative Common 4.0 (2021).

of the contact area between the two fluids. Thus, the reduction of the inter-particle distance between particles placed at the interface with different orientations leads to the overlapping of the interfacial distortions, which leads to strong capillary interactions. On the other side, for particles having similar orientation angles, the interfacial deformations do not overlap and hence the interfacial energy increases as particles are closer. This leads to strong repulsions between particles, which contrast with the situation for particles with opposite orientation angles. As a consequence, the approaching of particles with opposite orientation angles trongly decreases the interfacial energy, thus inducing the formation of capillary bridges as result of the strong attractive interactions between particles [290].

The above picture may be also applied for the description of the inter-particle interactions of patchy particles trapped at fluid interfaces [306]. Thus, for hydrophilic particles containing hydrophobic patches, a capillary attraction may be expected upon approaching. However, the situation changes when the patches of the approaching particles present different amphiphilicity. In this case, the menisci of the particles appear deflected in opposite direction which is translated in inter-particle repulsion.

5.1.2.2.2. Interfacial rheology

5.1.2.2.2.1. Dilational rheology

The response against dilational stresses of Janus particles trapped at fluid interface has been explored for different types of Janus colloids, and many times the results have been put in comparison with those what were found for chemically homogeneous particles. Kadam et al. [307] studied the response of different biofunctionalized silica Janus nanoparticles at the water/vapor interface, and found that the elasticity increases in relation to monolayers of bare silica, with the elastic modulus appearing for monolayers of some specific Janus particles up to six-fold higher than that what was found for bare silica. The increase of the elastic contribution of monolayers of Janus particles in relation to monolayers of non-Janus counterparts was confirmed by Fernández-Rodríguez et al. [308] for monolayers of polymeric Janus particles. They studied the compressional elasticity of such particles at both water/vapour and water/decane interfaces, and found that Janus particles leads to monolayers with higher compressional elasticity than those of homogeneous particles, which may be ascribed to the ability of Janus particles to form particle networks at the interface. Furthermore, an increase of the dilational storage and loss moduli with the increase of the interfacial coverage was reported. Razavi et al. [302] expanded the above studies in relation to the interfacial dilational response using Janus particles of different degree of amphiphilicity. They found that the increase of the amphiphilicity of the Janus particles leads to an increase of their ability for remaining trapped at the water/vapour interface, and enhances the elasticity of the particle-laden interface. Furthermore, it was found that monolayers of highly amphiphilic Janus particles undergo a reversible collapse through interfacial bucking with a reduced number of particles expelled to the subphase after successive compression/expansion cycles. On the other side particles with low amphiphilicity undergo an irreversible collapse upon compression. This difference on the rheological response may be ascribed to the differences on the orientation of particles at the fluid interface. Thus, particles with low amphiphilicity appear trapped at the fluid interface with a random orientation, whereas those with high amphiphilicity are placed at the interface in such a way that they have paired their different regions with the more favourable fluid.

5.1.2.2.2.2. Shear rheology

The study of the response of Janus particles against shear stresses is currently a very active research field [29]. Yin et al. [309] explored the rheological response of silica-based Janus nanosheets at water/oil interfaces by means of frequency sweep experiments performed at small strain amplitude (around 1%), and found a strong increase of the interfacial viscosity up to 1000 $mN \cdot s \cdot m^{-1}$. Furthermore, the increase of the shear rate up to 2.5 rad/s results in a reduction of the interfacial viscosity followed by a plateau region, which may be rationalized in terms of a disruption of the interfacial network.

Rezvantalab et al. [310] explored the response of interfacial layers of Janus particles at fluid interfaces against shearing by calculations using a multicomponent Lattice-Boltzmann method, which allows the study of

the interfacial ordering induced upon shearing for monolayers of different sizes and intermediate interfacial coverage (in the range 32-65% of the total interfacial area). They found that the capillary induced interactions emerging from the overlapping of the interfacial deformations induced by the shear flow induced the formation of particle chains aligned in the direction normal to the shear deformation, independently of the characteristic of the particle-laden interface, i.e., the type of particles and the interfacial coverage. The chain-like structures remain intact upon the removal of the flow field, with the only modification being associated with the rotation of the particle for adopting an upright orientation. Rezvantalab et al. [311] extended their studies for understanding the combined role of chemical and shape anisotropies in the behaviour of Janus particles at fluid interfaces against shear stresses. They found the existence of two rotational dynamics (smooth tilt and tumbling), which depends on the particle shape, degree of amphiphilicity and shear rate. Despite the existence of two type of dynamics, all the particles reach a steady-state orientation at the interface which depends on an intricate balance between torques induced by shear and capillarity. Therefore, it is possible modulate the orientation of Janus particles at fluid interface by controlling the shear rate and the surface chemistry of the particles.

Further studies on the shear induced assembly of Janus particles at fluid interfaces were performed by Paiva et al. [312]. They found that anisotropic Janus particles exhibit tumbling behaviour upon the application of shear stresses that allows overcoming the capillary torques. This leads to the formation of a Janus antiparallel configuration or stacked aggregate sheets. Wang et al. [313] studied the correlation between the interfacial morphology and the shear response of Janus particles of poly(vinylidene fluoride)/poly(L-lactide) at fluid interface, and found that the obtained films present a high elasticity (several times that corresponding to homogeneous particles) and low interfacial tension. This solid-like behaviour was ascribed to the formation of ordered arrays of Janus particles at the fluid interface.

5.2. Soft particles

A paradigm of soft colloidal particles are those made up by microgels (i.e., chemically cross-linked polymers forming networks of colloidal size) that can undergo swelling in liquid environments. The degree of swelling depends on the density of cross-linking and the solvent quality [314]. Microgel particles have properties that can be considered intermediate between those corresponding to colloidal particles, and those that are expected for polymer chains [35,314].

The most common microgel particles are those obtained from poly (N-isopropyl acrylamide) (PNIPAM), a thermosensitive polymer that undergo a reversible swelling/shrinking transition at a temperature around to the physiological temperature of the human body [315,316]. In some cases, it is possible to add some co-monomers that change their ionization state by pH changes, e.g., acrylic or methacrylic acid, which allows obtaining pH responsive microgels [317].

The dual character of the microgels plays a very important role in their trapping at fluid interface. On one side, they are particles and hence they remain trapped at the fluid interface very strongly. On the other side, they present a polymer character which favors their attachment from dispersion to the fluid interfaces [35]. Therefore, the softness is not a limitation to the adsorption of particles at fluid interface. However, it introduces a competition between the bulk elasticity and surface tension, which leads to the particle stretching at the fluid interface. This leads to a change of the energetic landscape associated with the trapping of the particles at the interface, which is characterized by an increase of the trapping energy [75,182,318]. Furthermore, the deformability of the particles enhances the contribution of the capillary interactions and reduces that corresponding to the direct interactions [319]. This results in the formation of interfacial mesostructures, which can be exploited for the stabilization of dispersed systems, mainly emulsions [320–323]. The enhancement of the contribution of the capillary interactions to the global balance of the interface may be understood considering that the capillary interactions are related to the deformation of the interface upon particle adsorption. Therefore, the modification of the wetting properties of soft particles as result of the change of their conformation may induce very different contribution of the capillary forces in such a way that depends on the specific size of the particles [324]. This leads to a degree of propagation of the particle in each phase depending on the quality as solvent of the specific fluid, resulting in very different deformation profiles of the fluid interface. In fact, for small particles the role of the capillary forces can be considered almost negligible, and the interfacial behavior is reminiscent from that expected for monolayers of polydisperse soft disks, whereas monolayers of big particles undergo strong attractive capillary forces, appearing clustering between the particles from the lowest values of the interfacial coverage.

5.2.1. Trapping of soft particles at fluid interfaces

The trapping of soft particles at fluid interfaces, both water/vapor and water/oil, is aimed to reduce the interfacial energy between the two fluids, similarly to that what happens for hard particles [325]. However, the softness of microgels allows its deformation upon adsorption at interfaces, which determines two main aspects of the interfacial organization of the microgels at the interface: (i) the surface activity of most microgels induce that in contact with the interface, microgels can appear stretched out at the interface to maximize the interfacial coverage, and (ii) microgels protrudes into the two fluid phases according to their respective affinities. The latter results in an asymmetric distribution of the microgels between the two phases. It should be noted that the extension of the in-plane deformation and the asymmetry across the interface depends on the specific structure of the microgel and the nature of the fluid phases [326].

Different studies have evidenced that microgels at interfaces between a polar fluid and a non-polar one adopt “fried-egg” morphologies. These result from the lower cross-linking of the external region of the microgel (corona) in relation to the inner one (core), which determines a higher deformability [143,318,323,327]. It should be stressed that the bulk elasticity of the microgels emerges as a restriction to their deformation upon adsorption at the fluid interface. This may be understood considering the balance between two contributions: (i) reduction of the interfacial energy between two immiscible fluids, and (ii) the elastrocapillary length $L_{EC}=\gamma_S/E$ defined as the ratio between the surface tension of the solid γ_S and its Young’s modulus E [318]. Thus, particles with radius larger than the elastocapillary length can be considered effectively as non-deformable particles, and only slight deformations close to the contact line may be expected. On the other side, for particles with radius smaller than the elastocapillary length, particles behave almost as a liquid.

It may be expected that the deformation of soft particles upon adsorption at a fluid interface can appear strongly dependent on the interfacial coverage. At low coverage, the adsorption of the particles occurs with the particles adopting a stretched-out conformation at the interface. This may be understood considering that such conformation ensures the maximization of the fraction of interfacial area occupied by the particles. This introduces a favorable entropic contribution, allowing overcoming the energy penalty associated with the elastic deformation of the particle. Under the above conditions, the major portion of the particles remains immersed in the polar phase, and only a very small fraction appears protruding to the non-polar phase [328]. On the other side, the increase of the interfacial coverage leads to a situation in which the particles at the interface start to touch each other. This drives the collapse of particles at the interface, reducing the contribution of the elastic energy [35]. The above picture can be interpreted considering that at low coverage, microgels can appear forming either monolayers resembling a liquid-like state or clusters mediated through capillary interactions [327,329]. On the other side, the increase of the coverage induces a crystallization of the microgels forming a hexagonal array

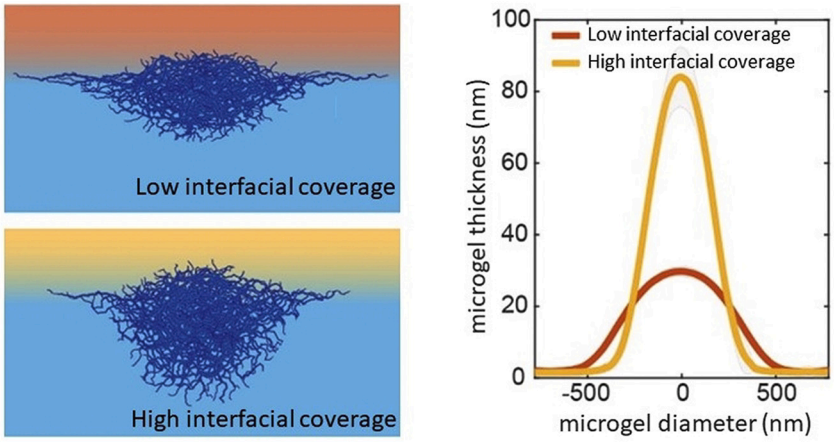

Fig. 14. Conformation and dimensions of single microgels at a fluid interface as function of the interfacial coverage. Adapted from Vialetto et al. [331], with permission from Elsevier under Attribution License Creative Common 4.0 (2021).

where the coronas of adjacent particles appear in contact, and the cores are separated due to the coronas acting as spacers. The increase of the coverage leads to the reduction of the inter-particle separation, which drive the formation of well-defined solid-like hexagonal packing [330,331]. Fig. 14 represents a sketch of the conformation of single microgels trapped at fluid interfaces depending on the interfacial coverage together with the change of microgel dimensions at the interface with the interfacial coverage.

5.2.2. Interfacial interactions

The characteristics of microgels as colloidal particles with a behavior intermediate between hard particles and polymers leads to a situation in which the interactions operating between the particles trapped at the fluid interface emerge very different to that what is found for hard particles [35]. Thus, the swelling of microgel particles leads to a very weak van der Waals attraction, and the absence of appreciable charges. Therefore, the interactions that appears dominant for hard particles may have a negligible role for soft particles. Furthermore, the deformability of microgels introduces new degrees of freedom to the system [143,322,328,332].

The existence of additional degrees of freedom (embedding and deformation) for soft particles trapped at fluid interfaces in relation to that what occurs in common hard particles influences the interaction potentials between soft particles trapped at fluid interfaces. Geisel et al. [329] showed that charged microgels collapse more easily upon compression than uncharged one. This suggested that the compressibility of microgels does not depend directly on the electrostatic interaction. This may be understood considering that the internal structure of the particles, e.g., cross-linking density or their responsiveness to physical stimuli, controls the compressibility of the microgels. Despite the inter-particle electrostatic repulsions do not influence directly the compressibility of soft particles, the charge of the microgels appears as a very important parameter for controlling the swelling degree of microgels, which results from the presence of charges.

Soft particles present a strong capillary attraction with respect to hard particles. This may be easily understood considering the larger contact line, and its roughness and heterogeneity associated with the particle deformability [319]. The importance of the capillary interactions in microgel layers at fluid interfaces was demonstrated in the study by Cohin et al. [333]. They found that microgels undergo a clustering process upon their attachment at fluid interface, which was not observed in bulk dispersion. Therefore, they conclude that the clustering was mediated by the emergence of long-range capillary interactions. It should be noted that once particles are close to each other, they can also interact through short range forces.

5.2.3. Response of microgels layers upon mechanical deformations

The response of soft particles trapped at fluid interface is mainly dictated by their deformability [334]. In particular, the corona region dominates the stress relaxation of microgel layers as result of their rearrangements [321]. Brugger et al. [332] pointed out that the response of microgel-laden fluid interfaces against dilation is closely correlated to the conformation of the particles upon trapping at the interface. Thus, for swollen microgels, the monolayer behaves as a mostly elastic film, whereas the shrinking of the microgels leads to a reduction of the storage modulus and increase of the loss modulus. The analysis of the response against shear deformation of the above layers shows that layers of swollen microgels present a behavior reminiscent from that what is expected for a soft gel-like material undergoing an elastic response against a mechanical deformation. However, the shrinking of the microgels drives the formation of compact and brittle films, which undergo an easy rupture upon deformation.

Varying the surface pressure by compression in a Langmuir trough yields a very rich phase diagram of PNIPAM particles at liquid/liquid interfaces, including an isostructural solid-solid phase transition, described by the emergence of shell-shell and core-core inter-particle contacts in each phase, respectively [335]. Increasing the temperature above the lower critical solubility temperature (LCST) of the constituent PNIPAM chains yields the deswelling of the microgel particles and a potential reduction of their size. This is known as a volume phase transition temperature (VPTT). The existence of a transition from solid to fluid around the VPTT of PNIPAM particles adsorbed at the air/water interface was recently addressed [182]. In detail, a solid-like behavior was found below 30°C, in agreement with the behavior reported by Cohin et al. [336] and Huang et al. [337]. Increasing the temperature above 30°C, towards 38°C, a transition to a fluid-like layer that can flow under stress was observed and rationalized the shrinkage of the particles in the direction perpendicular to the interface, which is consistent with ellipsometry measurements [182,326].

As a corollary of this subsection, the stimuli responsiveness of most of the soft particles, and in particular of those of PNIPAM and their derivatives, leads to a rich interfacial behavior with interesting morphological transitions which impact decisively on the interfacial rheology of their monolayers [35].

6. Effect of the capping ligands on the assembly of particle-laden interfaces

The introduction of capping ligands to colloidal particles can influence the magnitude of the attractive and repulsive inter-particle interactions, which in turn modify the interaction potential and hence the final structure and organization of the assembled particle-laden

interface. In particular, the introduction of surface-active capping ligands can alter the assembly of particle-laden interfaces at many levels [108]. They can bind to the surface of the particles providing a capping shell modifying the way in which particles interact with each other. Furthermore, the introduction of capping ligands leads to a modification on the wetting properties of the colloids, i.e., their contact angle, and their ability for modify the interfacial tension of the fluid interface [16,18,27,93].

6.1. Effect of the capping ligands on the interfacial organization of particle at fluid interfaces

6.1.1. Reversibly capped colloids at fluid interfaces

Very common additives for modulating the ability of particles for assembly at fluid interfaces is the addition of surfactants. They can screen or suppress the particle surface charge [107,111,112,338], tune the particle wettability [64,80] or modify their ability in the stabilization of emulsions and foams [4,6,60,61,106,111].

The combination of oppositely charged particles and surfactants has become a very popular strategy for obtaining surfactant-decorated particles, which allow obtaining a modulated adsorption and assembly of the particles at the fluid interface. Thus, it is possible to reduce the effective charge of the colloidal particles, which reduces the strength of the repulsive electrostatic interaction, fostering the colloidal aggregation. This limits the formation of structures with long-range positional order [339]. However, Velikov et al. [340] demonstrated that it is possible to obtain long-range 2D crystals by capping particles with a surfactant at a concentration which ensures the particle hydrophobization, avoiding their bulk aggregation.

Santini et al. [64] exploited the addition of the cationic surfactant CTAB for tuning the interfacial organization of negatively charged hydrophilic silica particles at the water/vapor interface, and their results pointed out the ability of the surfactant for capping the surface of the particle. This allows modifying the wetting properties of the particles, which in turn controls the immersion of the particles in the fluid phases, i.e., their position in relation to the interfacial plane [80]. Therefore, it may be expected that as the wetting properties of the particles are tuned, their packing at the fluid interface as well as the interfacial morphology of the particle-laden interface should change. This agrees with the result by Zang et al. [221] for silica particles capped through a chemical process with silanes, which confirms the important role of the wettability of the particles in the control of the packing of particles at fluid interfaces.

Santini et al. [61] explored furtherly the impact of the wetting properties of the surfactant decorated particles on their ability for assembly at fluid interfaces, and found that particles with a reduced hydrophobicity tend to assemble forming isolated particles rafts at the interface. The increase of the particle hydrophobicity drives the coalescence of the particle rafts to form close-packed films constituited by 3D particle clusters. These results are in agreement with the strong decrease of the interfacial tension and the sharp increase of the interfacial excess determined by ellipsometry, with this latter parameter being compatible with the formation of particle films thicker than a monolayer. The above results are compatible with those obtained independently by the group of Noskov [62,63,256,341] for micro- and nanoparticles of polystyrene sulfate latex and silica nanoparticles decorated with CTAB at both water/vapor and water/alkane interfaces. Li-Destri et al. [220] using GISAXS reported that the surfactant concentration used for capping oppositely particles plays a key role in the control of the energetic landscape involved in the assembly of the particles. Independently of the surfactant concentration, they found the existence of long-range electrostatic interactions. Furthermore, their found the emergence of short-range interactions which appears dependent on the surfactant concentration and their ability for reorganizing around the particles. At low surfactant concentration, particles capped with oppositely charged surfactant molecules have steric repulsions due to the intermingling of the surfactant molecules on the surface of the particles. However, the increase of the surfactant concentration introduces a repulsive electrostatic contribution due to the formation of surfactant bilayers with the charged moieties exposed to the aqueous phase on the particle surface. This leads to an increase of the inter-particle separation at the fluid interface. In a similar work combining GISAXS and *in situ* AFM studies, Costas et al. [342] demonstrated that the surfactant concentration also plays a very important role on the organization of silica particles at water/oil interfaces. Thus, the results showed that the higher the surfactant concentration the higher the interfacial coverage, and the shorter the inter-particle separation.

Anyfantakis et al. [343] deepen the understanding of the organization of colloidal particles decorated with oppositely charged surfactants at the interface as function of the concentration of both particles and surfactant. They found that, for surfactant concentrations very far from the critical micelle concentration (CMC) of the surfactant (3 or 4 orders of magnitudes lower), particles capped with the oppositely charged surfactant can assemble at the interface following different patterns. In this case there is an electrostatic repulsion between the particles and the capillary force arising from the deformation of the interface around particle clusters defining the organization of the particles at the interface. Thus, tuning the ratio between the concentrations of surfactant and particles, it is possible to obtain different disordered and 2D crystal phases [344].

Li et al. [345] tried to gain further insights on the ability of surfactants for modifying the adsorption of oppositely charged particles at a fluid interface. In particular, they study the adsorption of negatively charged gold particles decorated with CTAB at the water/dichloromethane interface by combining zeta potential measurements and Surface-Enhanced Raman Spectroscopy (SERS). The results evidenced that at low surfactant concentration, the adsorption of surfactant on the particle surface is not high enough for modifying neither the surface charge of the particles nor their wettability. However, the increase of the surfactant concentration enhanced their deposition on the particle surface as evidenced by SERS spectra and the reduction of the zeta potential until quasi-null values (originally around -30 mV). This results in a modification of the lateral organization of the particles at the interface. Thus, for similar particle concentrations highly charged particles (low surfactant concentrations) leads to the formation of more ordered monolayers than particles with a reduced charge density (high surfactant concentration), with the latter evidencing a high tendency to the formation of monolayers of 3D particle clusters.

6.1.2. Irreversibly capped colloids at fluid interfaces

Another approach for tuning the interfacial organization of particles at fluid interfaces is by binding specific molecules using covalent bonds. Park et al. [346] exploited this concept for ensuring the formation of monolayers of gold nanoparticles at the water/hexane with a high degree of order. For this purpose, they linked 1-dodecanothiol molecules to the gold surface, and found that in absence of the capping agent, the obtained monolayers presented a disordered structure, which was ascribed to the electrostatic repulsions between the particles. These repulsions were strong enough to hinder the formation of close-packed monolayers. However, the addition of alkanethiols at intermediate concentrations leads to a decrease of the surface charge density of the particles, which minimizes the unfavorable electrostatic repulsions and favors the ordering of the particles within the interface. On the other side, the addition of alkanethiol at a high concentration drives the aggregation of the particles. It should be noted that the length of the capping agent allows modulating the organization of particles at the fluid interface. Kim et al. [347] pointed out that the increase of the length of the ligands, and in particular, the length of the hydrophobic moiety, allows passing from ordered liquid 2D phases to disordered 2D solid one. This may be explained considering the role of the steric contribution associated with the restriction of the particle mobility due to the capping ligand shell, i.e., entropy-driven transition. This

transition occurs through the formation of a hexatic phase, which allows considering the ligand-induced melting process similar to that of the temperature-induced one, with the ligand length being the control parameter. The role of the length of the tethered chain on the interfacial organization of particles at the fluid interface was also explored by Isa et al. [348]. They studied the assembly of Fe_3O_4 particles capped with poly(ethylenglycol) at the water/decane interface, and demonstrated that the molecular weight of the tethered chains determines the in-plane separation of particles at full interfacial coverage, which agrees with the results by Kim et al. [347].

6.2. Rheological response

6.2.1. Dilational rheology

6.2.1.1. Reversibly capped colloids. It is common to assume that the interaction of oppositely charged particles and surfactant leads to the emergence of different types of synergetic effects between the components [70,240]. This means that the association of particles and surfactants is commonly associated with a stronger modification of the interfacial tension than those expected for the individual components. However, this is not the case when silica particles are capped by the addition of a cationic surfactant such as CTAB. Ravera et al. [51] showed that the dilational viscoelastic response measured in the low frequency limit (0.005–0.2 Hz) using an oscillating drop tensiometer for layers of silica particles capped by CTAB present a strong dependence on the deformation frequency. Furthermore, the elasticity of the particle-laden interface was found to be enhanced in relation to that obtained for surfactant-laden interfaces, which is in agreement with the results obtained by Tambe and Sharma [243] for mixtures of graphite particles and stearic acid at water/decane interface. Furthermore, it was found that the effect of the formation of a particle-laden interface using particles-capped by using surfactants is stronger for water/oil interfaces than for water/vapour one. It should be noted that the interfacial dilational viscoelatic modulus of layers of surfactant-decorated colloidal particles at fluid interfaces increases upon compression. This may be explained considering the increase of interfacial excess of particles [30,63,349].

The seminal work by Ravera et al. [51] was furtherly extended by enlarging the accesible frequency range (from 10^{-3} Hz to 10^{3} Hz) by combining three different experimental techniques (oscillatory drop tensiometer (OD-DS), capillary pressure tensiometer (OB-CPT) and an electrocapillary wave devices (ECW)). This allowed inferring the existence of two different relaxation processes at the interface as response to dilational stresses. Such relaxation processes have well-differentiated origins: (i) a diffusion-controlled adsorption of particles from the bulk to the interface, and (ii) reorganization of the adsorbed material at the interface [30,105]. The former process appears at the lowest frequencies, whereas the second one governs the dilation response for the highest frequency. The above results were well described by using a theoretical model combining a diffusion-controlled adsorption with an arbitrary kinetics processes occurring within the interface [30,241,242]. For the sake of example, Fig. 15 displays a set of data corresponding to the experimental points and the theoretical curve obtained for the dilational response in the frequency range 10^{-3}-10^{3} Hz of a layer of CTAB-decorated silica particles at the water/vapour interface [30]. It should be stressed that a detailed analysis of the interfacial dilational response of CTAB-decorated silica particles evidenced the existence of an intricate balance of interactions, mainly electrostatic and hydrophobic one. This governs the equilibration of the interfacial layers, which includes processes involving the exchange of CTAB molecules from the particles surface to the water/vapour interface, resulting in a modulation of the particle wettability and the inter-particle interactions both in the bulk and upon adsorption at the fluid interface [64,80].

An important issue to consider in the dilational rheological response

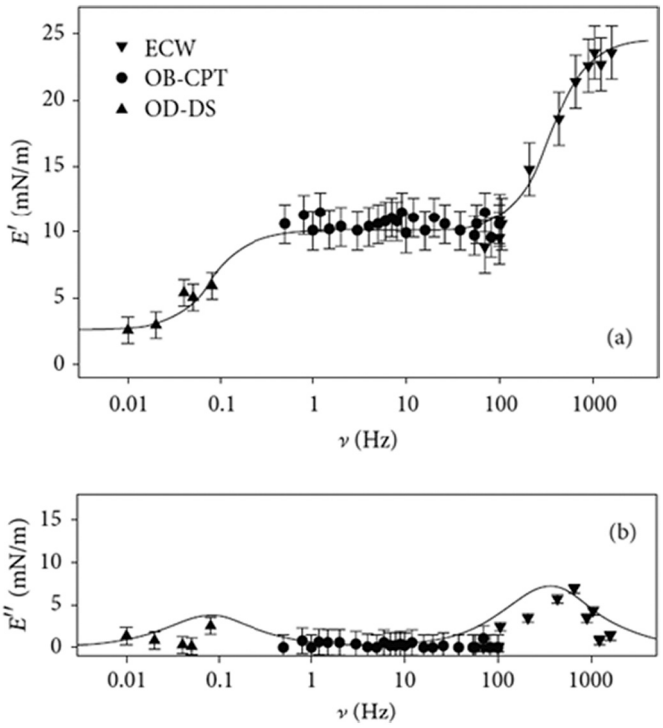

Fig. 15. Wide-frequency interfacial dilational response of silica nanoparticles (1 wt%) decorated with CTAB (0.05 mM) at the water/vapor interface as were obtained by combination of three different experimental techniques. (a) Dependence of the elastic modulus on the deformation frequency. (b) Dependence of the viscous modulus on the deformation frequency. The symbols correspond to the experimental data and the solid lines to the theoretical prediction. Reprinted from Liggieri et al. [30], with permission from The Royal Society of Chemistry. Copyright (2011).

of layers formed by surfactant-capped particles is the effect of the interfacial aging. The interfacial aging leads commonly to a significant increase of the dilational elasticity for layers at interfaces between water and air or oil [63,105,254]. However, the aging induced rigidification is not associated with a change of the interfacial tension. As a consequence, once the maximum interfacial coverage is reached, the exchange of particles between the bulk and the interface is almost negligible or occurs through a very slow kinetics [63], which may be considered as evidence of the irreversible trapping of the particles at the fluid interface. The rigidification process leads to the formation of solid-like films at the interface as was evidenced by Brewster Angle Microscopy (BAM) imaging [63]. This agrees with the finding by Santini et al. [61,64] and Whittby et al. [349] for other surfactant-decorated particle systems. It is worth mentioning that the elasticity of the solid-like films formed upon interfacial aging is comparable with that what was found by Zang et al. [252,274].

6.2.1.2. Irreversibly capped colloids. Da et al. [350] have recently studied the dilational rheology of silica nanoparticles silanized by a combination of two silanes (3-glycidyloxypropyl trimethoxysilane and dimethyloxydimethyl silane) trapped at air/brine interfaces, finding the formation of elastic, yet ductile particle-laden interfaces as result of the combination of the adsorption process and the inter-particle interactions. This leads in some case to a certain degree of reversible aggregation at the interface due to the emergence of weak inter-particle attractive interactions. Furthermore, the increase of the interfacial coverage increases the strength of the van der Waals, capillary and hydrophobic interactions, which leads to an interfacial rigidification characterized by the increase of the elastic contribution.

It should be stressed that the complex rheological response found for

particles capped with ligands upon trapping at fluid interfaces results from the interplay beteween the rearrangements of the particles within the interface, and the molecular rearrangaments of the ligands on the particle surface as was demonstrated by Huerre et al. [351]. They combined GISAXS with pendant drop tensiometry to analyze the organization under compressional stresses of gold nanoparticles capped with mercaptoundecyl tetra(ethyleneglycol) at the water/ octafluoropentyl acrylate interface, and found a very different role of the rearrangaments of the particles and ligands depending on the amplitude of the dilational stresses. Thus, for dilational stresses of small amplitude, the change of the inter-particle distances can be mainly due to the compression of the ligand brush. On the other side, the strain response to dilational stress of large amplitude emerges strongly dependent on the compression rate, which may be the result of out-of plane reorganizations of the particles. Furthermore, the role of the ligand rearrangamentes upon dilational stresses of large amplitude is almost negligible because they do not have enough time for rearranging or migrating.

6.2.2. *Shear rheology*

The shear response of monolayers at fluid interfaces formed by particles capped with different types of ligands has been much less explored than that of their counterpart monolayers containing bare colloidal particles. Despite this limited attention, several studies have pointed out the strong correlations existing between the response of the monolayers to shear deformations and flow, and the interfacial microstructure and inter-particle interactions. One of the seminal works addressing this problem was performed by Orsi et al. [278]. They explored the response of monolayers of dodecanethiol capped gold nanoparticles at the water/vapor interface against shear deformations, and found a mainly elastic response. Such elastic response is characterized by the scaling of the mechanical moduli with the interfacial concentration, which is characteristic of a percolated network. The latter agrees with their previous findings obtained using X-ray Photon Correlation Spectroscopy [352]. On the other side, the frequency dependence of the complex modulus was found to be described by the rheologycal behavior of a soft glass [353], which is a signature of a fractal nature of the film, in agreement with the microscopic observations.

Maestro et al. [104] explored the effect of the surfactant concentration on the shear response of CTAB-decorated silica particles at water/vapor interfaces by combining strain- and frequency-sweep oscillatory shear experiments. The strain-sweep shear experiments showed that at high surfactant concentrations the monolayers undergo a solid-like response below a yield point of a 2D glass, with the shear modulus being in the range 0.1-1 N/m, which is similar to that what was reported for monolayers of silica particles [252,274]. Furthermore, the detailed analysis of the shear response showed that both the storage and loss moduli follow a power-law with respect to the frequency which is reminiscent of a soft glassy material [353]. On the other side, the application of a strain-rate frequency superposition methodology,

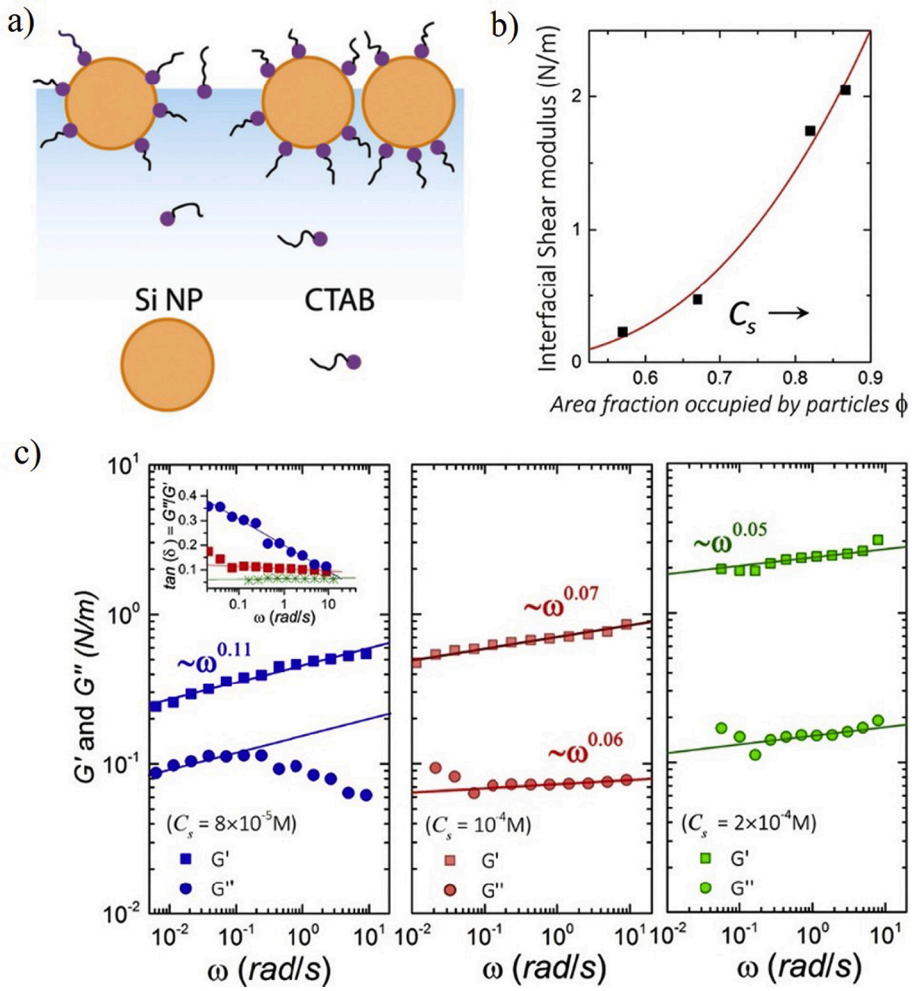

Fig. 16. (a) Sketch of the interfacial assembly of CTAB-decorated silica nanoparticles at a water/vapor. (b) Power-law dependence of the interfacial shear modulus on the area fraction covered by particles. (c) Power-law showing the dependence of the shear viscoelastic moduli on the oscillation frequency. The lines represents the fitting of the data using a Soft Glass Rheology model. Adapted from Maestro et al. [104], Copyright (2015), with permission from American Chemical Society.

similar to that reported by Wyss et al. [354] for 3D rheology, evidences a slow relaxation process which was found almost independent of the strain-rate amplitude. This was atributed to a transition from a fluid-like interface to a solid-like one, similar to that discussed by Zang et al. [274] for monolayers of fumed silica with different hydrophobicity. Fig. 16 shows results obtained for shear experiments of CTAB-decorated silica particles at the water/vapor interface.

The above discussion evidenced that the presence of capping ligands increase the rigidity of particle-laden fluid interfaces as well as their resistance against deformations [27]. It should be noted that solid-like particle-laden interfaces undergo a deformation beyond a yielding point upon a shear strain ramp deformation, which leads to a plastic flow [276]. The yield stress τ^* follows a power law on the interfacial coverage ($\tau^* \sim \Gamma^{\alpha}$). The molecular mechanism of such dynamic response requires to consider all the particle-level and many-body physics as was proposed by Maestro and Zaccone [217]. They introduced a description of the response against shear deformations by including the local connectivity between particles, and their temporal evolution in terms of cage breaking, as well as the dynamics of the microstructural heterogenity of the elastic response. The combination of the two contributions leads to the emergence of non-affine deformations. The power of the model was evidenced in the analysis of data from oscillatory shear measurements, which requires the use of only two fitting parameters: (i) relaxation time of the "cage", and (ii) viscous relaxation time. Furthermore, the model includes an inter-particle spring constant accounting for the strength of the interactions between particles, which can be controlled by changing the hydrophobicity of the particles, i.e. by the amount of surfactant. In summary, the model provides a connection between the concept of non-affine deformation, the rearrangaments of the local cage and the emergentce of a plastic flow, opening the possibility to explain the mechanical response of colloidal particles (both capped and uncapped ones) trapped at the water/vapor interface.

The interfacial shear rheology can be also exploited for evaluating the adsorption kinetics of particles at fluid interfaces as was demostrated by Maass et al. [355]. They studied the adsorption of silica particles decorated with lipids at the water/oil interface which follows a bimodal kinetics process, with the characteristic time of the first process being in a time-scale close to 1 hour. During the first step, G' increases due to the formation of a layer with strong inter-particle interactions. On the other hand, the second step, spanned during several hours, is characterized by slight increase of both G' and G'' as result of the accumulation of material at the interface. The accumulation of material proceeds until the steady state is reached, characterized by values of the storage and loss moduli of the layers which are several orders of magnitude higher than those what are commonly reported for pristine surfactant monolayers [249].

7. Actuated and active particles confined at fluid interfaces

In his famous lecture "There's Plenty of Room at the Bottom", Nobel laureate Richard P. Feynman was already urging scientists of his and later eras to design techniques that would allow precise control of matter at the atomic and micrometer scale [356]. More than sixty years have passed since those early days, and the advances in this direction have been extraordinary, driven by the urgent need to design tiny remotely piloted vehicles to transport and protect drugs to where they must be released. In this regard, any design must meet three main requirements, similar to any microorganism capable of swimming. The first one is that the propulsion of the microscopic vehicles must be powerful enough to overcome the thermal agitation of the medium. The second requirement is that the transport strategies must be adapted to a scale at which the frictional forces exceed the inertial forces. This means that directed transport requires the continuous application of an external action, and that the simplest reciprocal motion, e.g., that used by the scallop to propel itself, is completely inefficient, as pointed out by Purcell in his famous scallop theorem [357]. The final requirement that these microsubmarines must meet is that their shell must be sufficiently robust and/or adaptable to withstand the harshness of the intended environment [358]. Despite the explosive development in the study of these motile micro and nanorobots, more sophisticated designs with innovative functionalities are needed. Modular micro-machines composed of cooperative parts, capable of interacting while completing specific actions, capable of propelling in high-velocity flows, physiological conditions, or in confined environments, should be designed to perform new tasks or provide new medical treatments.

In this sense, active and actuated particles have proven to be essential as building blocks in the design of new dynamic assemblies capable of transforming external energy into propulsion and work, with new tunable properties and potential applications in engineering and biotechnology [359,360]. Active particles convert energy from the surrounding medium into propulsion and mechanical work. These systems are completely autonomous, in the sense that they do not require any external intervention and are propelling using methods that resemble those used by biological swimmers. On the other hand, actuated particles can be remotely piloted without disturbing the surrounding medium by remotely controlled electric, magnetic and/or optical fields. This second type of strategy has the advantage of not consuming fuel and being much more switchable. The previous classification helps categorizing different systems and structuring strategies discussed in this review, but it must be considered that in some designs, both actuation mechanisms are coupled [361].

The proximity of a solid or fluid interface has, in most systems, a strong influence on the dynamics exhibited by the propellers. For instance, hydrodynamic interaction with the fluid interface can transform active Brownian motion into circular [362] or rotation into translation [363], while colloid adsorption can hinder diffusion, rotation and transport [170,364]. Once adsorbed at fluid interfaces, the motion of particles is strongly constrained to the interfacial surface. Hence, particle-laden interfaces are model systems for the fabrication and exploration of new static and dynamic planar assemblies, for the study of 2D phase transitions, or for deepening on the behavior of active/actuated particles in confined environments [82,365–367]. The unraveling of the guiding principles of 2D dynamic self-assembly, and the possibility to remotely control and manipulate particles of different sizes without disturbing the surrounding medium, are crucial in the realization of various approaches for the controlled manipulation of self-assembled structures and the fabrication of simple smart monolayer surfaces and Pickering emulsions, capable of undergoing remotely controllable actuations [368]. Understanding the aggregation of magnetic particles is also essential for their use in the fabrication of metamaterials [369], separation agents in, e. g., protein purification protocols [370], or as cell manipulation operators [371] among others. On the other hand, the design of transport strategies along fluid interfaces, so far based on the exploitation of interfacial physical effects, such as surface waves, magnetocapillary or Marangoni effects, has practical implementations in micro- and nanofluidic devices and fluid interfaces inherent to all living organisms - tear film, oral mucosa and saliva, or those stabilized with lung surfactant [367].

7.1. Actuated particles

7.1.1. Magnetic particles

Magnetic colloids are often used as model systems in the study of the dynamics and hydrodynamics of colloidal suspensions, mainly determined by the translational or rotational motion of the constituent particles [372]. Particles with magnetic properties very different from those of the surrounding media are easily manipulated by applying gentle magnetic fields, which rarely perturb the medium, in a controlled manner, so that the generated flows can be directly analyzed.

Magnetic particles are usually classified as ferromagnetic or superparamagnetic:

- Ferromagnetic particles are made up of magnetic fragments of size equal to or larger than the typical size of the material domains. These particles, once magnetized, present a magnetic moment even in the absence of any applied field. If the permanent magnetic moment of the particles is large enough, so that the magnetic interaction energy is greater than the thermal energy, then they tend to form linear structures, rings, or other structures that can reform and reorient in the presence of an external field.
- Superparamagnetic nanoparticles are magnetic grains smaller than the typical size of the material's magnetic domains [373]. In absence of any external field, the characteristic fluctuation times of the small magnetic grains are smaller than the measuring time, so the measured overall magnetization is zero, even when the colloids are composite micro-sized particles containing thousands of nano-grains. The application of a constant field, however, favors one direction along the axis, and the grains acquire a magnetic moment. The process is completely reversible, because the magnetic moments fluctuate again as soon as the field is switched off, so that the corresponding magnetization curves do not present hysteresis. In most of the experimental studies, superparamagnetic particles are magnetized in the linear regime, where the volume susceptibility is constant.
- Superparamagnetic composite particles are colloids, with sizes ranging approximately from 100 nm to several micrometers, made up of an ensemble of tens of thousands of superparamagnetic grains implanted in a non-magnetic matrix, usually silica or a polymer. Therefore, the superparamagnetic behavior of the embedded magnetic grains is transmitted to the composite particle [374]. Under the influence of a constant magnetic field, the particles tend to form linear structures, bundles and chains, aligned along the field direction.

7.1.1.1. Roto-translational mechanism. If a variable magnetic field $H(\omega_f)$, rotating at an angular velocity ω_f, is applied, the torque generated tends to align the magnetic moment of the particle with the direction of the field, forcing the rotation of the particle as a whole [375]. Hence, magnetic particles adsorbed at fluid interfaces can be used as active micro-rheology probes, in the analysis of the kinetics and mechanism of adsorption, in the study of the effect of 2D confinement on static and dynamic self-assembling, or in the design and construction of new micro-swimmers, capable of propelling while confined along the interfacial surface.

When the microsphere rotates around an axis parallel to a near interface, the variation of the friction coefficient with distance from the boundary favors coupling between rotational and translational motions [376]. In the above experimental setup, the boundary conditions determine both the direction of transport and the efficiency of the rotational-translational mechanism. The described mechanism has been widely used in the design of isolated or self-assembled micro-rollers capable of propulsion in confined environments and physiological conditions, in the vicinity of solid and fluid interfaces [363]. The overall hydrodynamic flow, generated by the spinning particle but rectified by the nearby interface, can be used to propel the spinning particles, sometimes following cooperative strategies, and to transport nearby passive objects adsorbed at the interface. The described method, widely used in the transport of superparamagnetic and ferromagnetic beads, can be easily generalized to other rotating particles, including those subjected to rotating electric or optical fields, made up of different materials, coated with different molecules, and floating over different fluid-fluid or solid-fluid interfaces. The effect of rotating magnetic fields on the plane perpendicular to the interface was demonstrated to induce the creation of propelling chains [363] —worms— and carpets [377] of magnetic colloids.

7.1.1.2. Adsorption of magnetic colloids at fluid interfaces. The adsorption of the magnetic particles on the fluid interface usually requires of the addition of small amount of salt or surfactant, which screen the electrostatic repulsion between particles and interface. Furthermore, it can be promoted by the action of gravity or an external field gradient. If a particle passes above the repulsive potential defined in Section 4, and adsorbs at the fluid interface, then its rotation requires a deformation of the fluid interface [364], which is often pinned to the particle surface heterogeneities [86,170]. When the fluid-fluid interfacial tension is high enough, such interfacial deformation becomes energetically very expensive as soon as the particle crosses the interface several nanometers. In addition, the contact line fluctuation is linked to a dissipative torque that also acts against the induced particle rotation, so that the dissipative force associated with the contact line fluctuation also reduces the rotational and translational diffusion coefficients of the adsorbed particles, even when the viscosity of the entering medium is lower [170]. Due to these impediments in rotation around the axes parallel to the fluid interface, the adsorbed particles no longer exhibit coupled roto-translation.

7.1.1.3. Static and dynamic structures of adsorbed magnetic particles. In dynamic self-assembly, the interactions responsible for the formation of structures or patterns between components only emerge when the system is dissipating energy [214]. In magnetic colloidal dispersions, dynamic self-assembly occurs when the field frequencies are sufficiently low that the particles or their assemblies can couple to the dynamic field vector [378]. Under spatially coherently fluctuating magnetic and electric fields, colloidal magnetic and dielectric particles were predicted to self-assemble into complex structures [213,363,379,380]. The time-averaged action of the time-dependent fields gives rise to an effective interaction with attractive and repulsive domains able to generate chains, membranes and colloidal foams. The application of time varying magnetic fields develops dynamic self-assembled structures that span from unstable fronts, flocks and ribbons of ferromagnetic micro-rollers [381], microtubes of ferromagnetic Janus particles [382] or worms, walkers, carpets and sheets of superparamagnetic colloids [213,363,379,380].

For particles of sizes larger than tenths of nanometers the adsorption energy is typically more than thousands of k_BT, thus, once adsorbed, they remain tightly confined at the fluid interface. In this context, the combination of the tunable and confined character of superparamagnetic particles adsorbed at a fluid-fluid interface make them model systems for the engineering of smart static and dynamic planar structures, with no 3D counterpart. The formed structures, strongly determined by the relative orientation between the applied field and the confining interface, can be used in the study of 2D phase transitions, melting processes, crystallization, etc. or in the design of interfacial microswimmers.

7.1.1.3.1. Static self-assembly of adsorbed magnetic particles. When a constant magnetic field is applied perpendicular to a laden planar fluid interface, the induced moments of the adsorbed magnetic particles are also oriented perpendicular to the confining boundary. In this configuration, the interparticle interactions are repulsive, and neighboring particles tend to separate. If the surface density is high, then the particles try to maximize the interparticle distance, forming 2D hexagonal structures that exhibit an algebraic decay of the translational order and a long-range orientational order [383]. As the field strength decreases, the interaction of the particles decreases and the lattice undergoes a continuous melting transition through the three phases predicted by the Kosterlitz-Thouless-Halperin-Nelson-Young (KTHNY) theory (see Section 5.1.1.1) [224]. The limitation in system dimensions also has profound effects on the glass transition [384]. In fluid interfaces laden with different sized magnetic particles, the increase of the field strength promotes the formation of glassy structures with no long-range order and arrested dynamics, together with different types of 2D quasi-

crystallites [383]. In all these processes, the applied field plays the role of an effective inverse temperature.

If the applied field is oriented parallel to the interface, the induced magnetic moments are nearly coplanar with the confining surface and the particles form trapped structures aligned along the imposed direction, with complexity depending on the applied field strength and monolayer concentration [385]. At intermediate particle density and field amplitude, the equilibrium state consists of linear aggregates of one particle thickness. The emerging interactions between the induced linear aggregates depend on the distance between them, but also on the chain lengths and the relative displacement along the chain direction. However, in most possible configurations, the magnetostatic potential between two parallel chains presents a minimum attraction along the lateral direction at short range, when the two chains are almost in contact, followed by an energy barrier and a repulsion region at long range. The energetic barrier is located at a characteristic length, the escape distance, which increases with chain length [386]. As the area fraction increases, the chains are closer together, so some of them are forced together by a zipper mechanism and form ordered hexagonal bundles of zippered chains, in which the particles of adjacent chains are arranged out of register by a distance of radius [385].

Tilting the applied field with respect to the confining surface can transform the hexagonal order of the floating crystals into metastable structures with other planar crystal symmetries, such as oblique, centered-rectangular, rectangular and square lattices [383], and promote the unzipping of chains laterally aggregated [211]. The unzipping propagation is consistent with an Arrhenius process, in which one of the constituting particles jumps over an energy barrier, before entraining adjacent particles in the chain. Throughout this process, the chains maintain their integrity as they continue separating along the perpendicular direction. The subsequent increase in the slope of the applied field results in the partial fragmentation of the chains, the gradual separation of the monomers, and finally the abrupt colloidal explosion. In this system, the different dismantling mechanisms are reversible and are mainly governed by the tilt angle, but are also strongly influenced by thermal energy, particle contact angle and local magnetization [387]. When the number of adsorbed particles is small, then the particles form finite aggregates, that can be used in the study of border and confinement effects [209,218]. Due to the super-paramagnetic character of the components, all the described structures are stable only under the presence of the external field, while immediately disintegrate due to thermal fluctuations once the applied field is switched off.

7.1.1.3.2. Dynamic self-assembly of adsorbed magnetic particles. Floating magnetic particles have been widely used in the bottom-up fabrication of novel and disparate dynamic self-assemblies, strongly determined by the size and magnetic character of the particles, the geometry and dynamics of the applied field, and the rheological properties of the comprising fluids. In pioneering work, Grzybowski et al. used millimeter-sized magnetic disks adsorbed on a liquid-air interface, and rotating synchronously with the applied field, to study the formation of various dynamic structures [214]. The latter, resulting from the equilibrium between hydrodynamic repulsion and averaged magnetic attraction, were strongly determined by the geometry and chirality of the spinners [388]. In a different work, rotating ferromagnetic microdiscs with cosinusoidal edge-height profiles, confined by an externally applied magnetic potential and subjected to a rapidly rotating field, were assembled and disassembled in different configurations dictated by the directionality of capillary interactions, which were ultimately determined by the profile of the particles and the rotational speed of the applied field [389]. Snezhko et al. reported snake-like structures formed by antiferromagnetically aligned segments, themselves composed of ferromagnetic microfloaters. These objects self-assemble dynamically, upon application of an oscillating field perpendicular to the air/water interface, through coupling between surface waves generated at the fluid interface and magnetic interactions [365]. At the liquid-liquid interface, the oscillating chains generated a hydrodynamic flow in both media that promoted the formation of aster-like structures, organized in 2D periodic arrays at sufficiently high surface concentrations. When energized with an in-plane alternating field, the particles formed monolayers of equal-sized spinners, single-particle-thick linear aggregates, and pulsed clusters [390].

Under low frequency planar rotating fields Melle et al. showed using a microscopic model that paramagnetic microparticles on a plane formed rotating chains of given length and shape as a balance of magnetic dipolar interactions and hydrodynamic drag [391,392]. Abdi et al. extended the analysis to high frequency fields, where —they showed— the chains break and can form clusters, using computer simulations of a microscopic model in the overdamped regime with hydrodynamics treated in the far-field approximation [393]. In these high frequency conditions, the application of in-plane rotating fields at the confining interface induces an attractive interaction between adsorbed magnetic particles, which ultimately promotes dynamic self-assembly into finite hexagonal lattices. Under external magnetic fields rotating on the plane of a fluid-fluid or solid-fluid interface at high frequencies, paramagnetic colloids were shown to form 2D structures with different morphology depending on the polarization of the external actuation, as rationalized in terms of effective averaged particle-particle interactions. Circularly polarized fields were shown to form isotropic clusters —carpets— and crystals of rotating particles [394], whereas elliptically polarized fields can generate both chains and carpets depending on the ellipticity of the actuation [394]. The inclusion of a component perpendicular to the confining boundary induces the transition from planar carpets to separate chains, capable of transporting passive charges through the flow generated by the rotating constituents [211].

7.1.1.3.3. Magnetic interfacial swimmers. Some of the dynamic self-assemblies, formed from the equilibrium of viscous, inertial, capillary, and magnetic forces, can be used as models of numerous intriguing issues, such as the organization in biological structures or the transport of matter in the low Reynolds number regime [395]. In bulk, the main strategies are based on local generation of flow fields through forced rotation of non-perfectly symmetric objects, helical shapes in most designs that mimic some existing natural systems, the roto-translation coupling strategy described above, and the controlled actuation of flexible filaments. On the other hand, controlled transport of microparticles along fluid interfaces has traditionally been induced through strategies that make use of auto-phoresis, capillarity phenomena, or spatial symmetry breaking. For example, the interfacial snake and aster structures described above spontaneously break spatial symmetry at relatively high field frequency, inducing unbalanced surface flows that lead to propulsion and can be used to transport passive charges. At low frequency, it is the presence of a nearby non-magnetic object that introduces the imbalance of the generated fluxes necessary for propulsion [396]. In asters, the latter can be generated by applying an in-plane magnetic field, which promotes the formation of asymmetric extended objects [365].

Using a different strategy, Lumay et al. exploit the balance between field-induced dipole repulsion and capillary attractions to generate propulsion [209]. In the proposed design, three magnetic millimeter spheres adsorbed on a planar water-air interface were energized by both a vertical field and an in-plane oscillating field, so the three spheres form a sequence of triangular configurations that satisfy the time reversibility breakdown required in the low Reynolds regime. At moderate values of the Reynolds number, the energized arrays formed by particles of different sizes follow a non-reciprocal deformation sequence, as the one described by the Najafi-Golestanian microswimmer [397]. Larger magnetocapillary arrays showed metachronal waves at the periphery when subjected to a precessing magnetic field [398]. Recently, Fei et al. applied static or time-varying fields to force magnetic Janus particles adsorbed on curved fluid interfaces to move to the zones where the magnetic moments align parallel to the field [399].

Other alternative propulsion strategies do not rely on the use of hydrodynamic interactions. In these, adsorbed or non-adsorbed colloids

are transported by the action of a moving magnetic potentials generated by a variety of self-assembled structures of magnetic particles. The adsorbed magnetic colloids can be collectively transported across modulated energy landscapes generated by dynamic self-assembled monolayers of differently sized particles, located at different positions with respect to the interface [9]. On the other hand, the subtle balance between magnetic and viscous torques allows the transport of the submerged colloids under straight tracks of adsorbed particles, which function as if they were microassembly lines or Tyrolean traverses [400].

7.1.2. Dielectric colloidal particles adsorbed at a fluid-fluid interface under the action of an external electric field

The response of adsorbed colloidal particles at a fluid interface to an electric field depends on the strength and frequency of the field, as well as on the dielectric properties, electrical conductivity and geometry of both the particles and the surrounding media [401]. The use of an electric field to manipulate colloids and induce self-assembly has some advantages, compared to magnetic field, since the strength and frequency of the former are more tunable, both spanning on several orders of magnitude. However, electric fields, especially DC fields, can cause Faradaic reactions and electrical breakdown that can degrade the sample [402]. Moreover, the implied results are more difficult to interpret, as the electric field interacts with particles, the surrounding media and mobile and immobile charges [403] -consider, for example, the controversial discussion around the long-range interaction described by Nikolaides et al. [404] and Aveyard et al. [189]. To avoid, at least partially, these impediments, high-frequency AC electric fields are often preferred [405].

In the presence of a uniform electric field, charged particles surrounded by an electrolyte are pushed by the field towards the oppositely charged electrode, in a process called electrophoresis [406]. If the applied field is not uniform, which can be promoted or stressed by the proximity of the fluid interface, and the dielectric constant of the particle is different from that of the surrounding media, then the particle experiences a dielectrophoretic force resulting from the electric stress acting on the particle surface [407]. In addition, particles exhibit dipole-dipole interactions that promote the formation of field-induced chains, bundles and 2D lattices at fluid interfaces, while anisotropic particles undergo field-induced alignment [405]. At low frequency, the interaction between the applied field and the polarization of the ionic double layers surrounding the particles can also give rise to nonlinear electro-osmotic flows [408]. All emerging phenomena have been widely used to generate controllable Janus droplets [406], to separate particles on the surface of droplets [406], in the destabilization of Pickering emulsions, or to desorb particles from fluid interfaces [409]. On the other hand, the applied field can induce free charge accumulation at interfaces and local electrical stresses, coupled to interface deformation and flow generation of either fluid [410]. These electrohydrodynamic flows have also been used extensively in the collection and transport of adsorbed particles at fluid interfaces [402,405]. When charged particles adsorbed at a fluid interface are upon the influence of an external electric field, the interface deforms via the electro-dipping force that emerges from the interaction between the surface charge of the particles and the two media. The vertical component of this force, positive or negative depending on the dielectric constant and particle contact angle, is balanced by interfacial tension [411], while the lateral interaction between two adsorbed particles is always repulsive [412].

To our knowledge, all studies concerning adsorbed dielectric particles subjected to the action of external electric fields have been performed on Pickering droplets, but none of them have been carried out on planar charged interfaces. Only in the electrocapillary wave technique is an external AC electric field applied locally through a knife-edge electrode placed just above the interface. However, the field is not used here to arrange or transport adsorbed colloidal particles, but to excite the fluid interface in a Langmuir trough, and measure the rheological properties of the laden particle interfaces [30]. In a similar experimental setup, recently designed by Jia et al., the application of the external field triggers charge injection, allowing modulation of the charge-induced repulsive force, along with the corresponding reversible induction of the repulsion-dominated colloid assembly or dispersion of aggregated particles [413].

7.1.3. Active particles

Active systems, those that can convert convert chemical [414], thermal [415], or electromagnetic [416] energy into mechanical propulsion, are present at a wide range of scales, in assemblies of living organisms such as bacterial colonies and bird flocks or in collectivities of artificial components. In the last decade, the manipulation of active colloids has generated significant experimental and theoretical attention, because the study of self-propelled microparticle suspensions opens the door to the understanding of systems far from equilibrium and to the development of disruptive technologies. The self-propulsion capability of synthetic chemical powered active colloids is supported by different mechanisms, from induced-charge electrophoresis [408], or bubble propulsion [417], to catalytic local reactions and self-phoresis [380]. In autophoresis, a chemical reaction is catalyzed at the particle surface, leading to the generation of asymmetric gradients (thermal, surface tension, ionic and/or chemical) around the particles. The occurrence of these gradients, which may be coupled to each other and/or induced by an external field, such as a light source, ultimately leads to the movement of the particle relative to the solution, due to the action of phoretic forces and the triggering of hydrodynamic flows [418]. These induced flows can also be used to generate long-range hydrodynamic attractions that trigger the assembly of microscale particles [372]. In these experiments, the inherent asymmetry of Janus microbeads, spheres consisting of two different (chemically or thermally) active and passive material faces, is often used to promote a preferred direction of motion.

Active particles have potential applications in the engineering of smart lab-on-a-chips, in the transport of drugs [419], cells [420], pollutants [421] or cargoes [422], in the detection of chemicals as well as in the study of active crystals and glasses [423]. In these systems, individual particle active motion is coupled to Brownian rotational diffusion, similar to what is observed in run-and-tumble systems, while the collective behavior exhibits a variety of complex phenomena, such as local clustering [424], melting of clusters [425], swarming [416], active self-assembly [426] as well as segregation of active and passive species [427], mimicking on many occasions the collective behaviors exhibited by many biological systems. All these phenomena can be to some extent controlled using magnetic [361] and optical fields [428] or by modifying the swimmer geometry. Ensembles of active particles dispersed in a fluid, near fixed obstacles [429] or a solid-liquid interface [430], where particles exhibit alignment interaction [431] and circular trajectories [432], have been widely studied in the last years, and numerous reviews of the subject can be found in the literature [380].

7.1.3.1. Active particles adsorbed at fluid interfaces. Fluid-fluid interfaces are often ignored in most fundamental research, even though they are present in many real systems. However, the dynamics of phoretic colloids is particularly sensitive to the proximity of solid and liquid interfaces [8,38]. Proximity of a fluid interface induces orientation of the active particles laterally and propulsion parallel to the interface, allowing for a robust guidance mechanism along the fluid interface [433], while restricting rotation out of the swimming plane [434]. The hydrodynamic interaction with the fluid-fluid boundary favors the appearance of circular trajectories, like those observed for solid interfaces, but in the reverse direction [362].

When trapped at a fluid interface, active Janus particles exhibit strongly enhanced persistence length and velocity, compared to those observed in the bulk [418], due to the implicit constraints of particle reorientation, slowed down due to local pinning of the three-phase

contact line [185,430]. The above constrictions lead, in some cases, to circular trajectories that deviate significantly from random rectilinear motion by Brownian rotational motion [435]. Since the rotation of the particles about the axes tangent to the interface is strongly hindered by local pinning of the three-phase contact line and the capillary forces, the motion of active Janus particles is strongly determined by the fastened orientation of the particle with respect to the fluid interface, resulting in heterogeneous populations of non-moving and moving particles [430].

The activity of adsorbed particles often induces local surface tension gradients, which give rise to Marangoni stresses. Marangoni surfers use external energy inputs or chemical reactions to create local gradients of temperature and surfactant concentration, propelling themselves at high velocity toward regions of higher surface tension, along directions partially determined by the symmetry of surfers [418]. In principle, Marangoni navigation requires asymmetries in the surface tension gradient of the interface around the particles. However, even symmetric particles exhibit rapid translational and rotational motions when placed at a water-air interface, generated by a convective instability that provokes the spontaneous rupture of the initial axial symmetry. In the above systems, the propulsion mechanism is strongly dictated by the degree of exposition of the catalytic surface to aqueous phase [418]. The interplay between motility, capillary interactions and induced Marangoni flows promotes in some systems instability and rupture of thin films [436], while in others it favors the existence of self-assembled dynamic and stationary states [437,438]. In another type of experiments, where micro-sized floating objects are illuminated with light, the applied radiation is adsorbed by the Janus particles and converted into mechanical work thanks to the coupling between the temperature and surface tension gradients. The micro-machines powered through this mechanism have the advantage of being long-lived and easily switchable, while the linear and angular velocities are easily controlled by the laser power and the surfactant concentration at the interface [418].

7.2. Theory and simulation of dynamic self-assembly

The self-assembly of colloidal particles at liquid-liquid interfaces can occur as a result of a wide range of processes and interactions, both in equilibrium and out of equilibrium. From a theoretical standpoint, systems in thermodynamic equilibrium have been thoroughly studied over many years and are understood using classical concepts of thermodynamics and statistical physics, requiring the minimization of the appropriate thermodynamic potential of the system. At least in principle, the knowledge of interparticle interactions allows us to program the most stable structures that will be spontaneously formed by self-assembly.

Here we focus our attention on the theoretical description of aggregation processes at interfaces that occur out of thermodynamic equilibrium, be it by actuation with external fields or due to collective processes stemming from individual consumption of energy from the environment. A common general theoretical framework which dictates the emergence of such self-assembled structures and their properties is still missing. In search for a deeper understanding of such phenomena, on the one hand microscopic models have been developed to analyze and characterize non-equilibrium structures. On the other hand, numerous investigations have been devoted to find a thermodynamic principle to characterize the emergence of steady structures out of equilibrium.

7.2.1. Self-assembly under time-dependent external fields

In the previously noted work of Grzybowski and co-workers [214], the dynamic structures formed by rotating ferromagnetic disks at a fluid interface were explained as a process governed by the equilibrium between magnetic particle attraction and hydrodynamic repulsion with inertial effects [439]. These systems were also investigated using magneto-hydrodynamic models defined through boundary value problems [440]. The method uses the Navier-Stokes equation, which includes multi-body interactions exerted on the fluid due to the rotations of magnetic particles. The numerical solution of the model permitted the calculation of the energy dissipation rates of the self-assembled steady states of rotating particles. In Ref. [441], the sole effect of hydrodynamics on the collective behavior of spinning discs was studied with the help of simulations of fluid particle dynamics, a technique that allows to properly account for hydrodynamic interactions between particles. The authors concluded that hydrodynamics alone can generate a rich phase behavior of spinners, including a fluid state, clustering, hexatic ordering and glassy states [441]. The formation of clusters of spinning magnetic particles at liquid-liquid interfaces was also investigated using Lattice Boltzmann simulations, which properly accounts for the hydrodynamics (of an incompressible flow) generated by the rotating particles [442]. Using this technique, they demonstrated that hydrodynamics can cause the separation into a particle-rich region and a particle-poor region [442]. Götze and Gompper analyzed the effects of confinement on the assembly and dynamics of magnetic discs driven by a rotating field using multiparticle collision dynamics simulations, which naturally includes both hydrodynamics and thermal effects [443,444].

As mentioned previously, Snezhko et al. [365,396,445] also demonstrated that the coupling between the collective response of ferromagnetic colloidal particles under alternating magnetic fields and the surface waves generated at liquid-air interfaces is responsible for the formation of dynamical self-assembled dynamical patterns. The structure and dynamics of such structures was theoretically described through both a continuum phenomenological approach and also a microscopic model which couple the dynamics of surface waves with the Navier-Stokes equations for the flow [445]. It was shown later on that such structures could be used as self-propelling agents [396]. The transport on self-assembled dynamical structures was also studied in the work by Martínez-Pedrero et al. [446], where Brownian dynamics simulations were used to investigate the dynamics of two types of superparamagnetic particles of different size in a fluid-fluid interface under precessing fields. The authors demonstrated that under such actuation, self-assembled lattices formed by one type of particle could be created and, simultaneously, transport of the other type could be established from node to node of the lattice.

7.2.2. Clustering and phase separation of active particles

So far, the theoretical modelling of active particle systems used to study their collective emergerging effects, e.g., self-assembly, has been mostly done considering highly simplified models. In these models, hydrodynamic interactions are often neglected or considered in an effective manner, and in most cases the systems considered are restricted to move on a plane. However, some of the conclusions drawn from these studies should be general, in the sense that they should be applicable to processes where such restrictions are not imposed, and have been used to predict and interpret experimental behavior of active particles at liquid interfaces.

The sole capacity of particles to self-propel was shown to induce the formation of dynamic clusters (living crystals), even if their mutual interactions are repulsive and no alignment interactions are included [447–450]. This is reflected in long-lived density fluctuations and anomalous clustering. While a system of N passive particles in a volume V exhibits number fluctuations of $\Delta N \sim \sqrt{N}$, the number fluctuations in active particle systems scales as $\Delta N \sim N^{\alpha}$, where α can become of order 1 in two dimensional systems [451,452]. The principle of such cluster formation can be explained qualitatively. Active particles follow a diffusive dynamics with long persistence length in absence of other particles. When they collide with other particles their velocity is reduced due to excluded volume interaction, since it impedes motion induced by the active force. If the characteristic time to reorient and escape from the collision is larger than the characteristic time to encounter another particle clustering will occur.

In fact, self-mobility alone was shown to induce the separation of particles into a dense and dilute fluid phases (Motility Induced Phase

Separation, MIPS). This athermal transition was suggested by Tailleur and Cates [447] using theoretical arguments on a one-dimensional system and later on it was shown using computer simulations of discs moving in a 2D plane [448–450]. Experimental evidence of clustering and phase separation of such active systems was given later on [453,454]. The nature of the transition to the mobility induced phase separated state has been widely investigated from a theoretical persepective [447,455–461]. In case of active brownian particles with no alignment interactions, the pressure exerted by the system was demonstrated to be a state function independent of the interaction with the walls [455–457], and pressure-volume non-equilibrium phase diagrams were obtained. The MIPS transition was found to satisfy the characteristic properties of an equilibrium first-order liquid-gas phase transition [461]. The origin of phase separation was attributed to mechanical [455,456] and diffusive instabilities [447,459,460]. To control the size of the dynamic clusters, systems of active brownian particles moving on a plane and interacting through a short range attraction and a long-range soft repulsion have been studied using computer simulations [462].

In practice, most active and actuated particles used in experiment develop aligning interactions both with other particles and the container walls. These can be originated, for example, from hydrodynamic interactions [463], steric interactions for geometrically anisotropic particles [464], or electrostateic interactions [416]. Such interactions can lead to the emergence of swarming collective motions of particles, as demonstrated by analysis of the Vicsek model [465] and generalized versions of it. In these models, the direction of an active particle is determined by the average direction of the neighboring particles and a phase transition is obtained at high enough concentrations from a fluid of isotropically directed particles to a state where all particles move in the same direction in the form of bands [466,467]. Solon and co-workers demonstrated that systems of active particles with aligning interactions cannot be described by an equation of state, since the pressure that they exert depends on the specific nature of the interaction with the wall, which is not a function of state [457,458]. This result evidences the difficulty of building a general theory to describe the macroscopic out-of-equilibrium behavior of active particle systems.

7.2.3. *Seeking a principle for non-equilibrium self-assembly*

In equilibrium, the self-assembly of a subset of particles of the system occurs as a process to minimize the overall free energy. For self-assembly processes out of equilibrium there is a constant energy dissipation and entropy production and in general there is not a thermodynamical potential which becomes a minimum at steady states. In this context, the quest for a general thermodynamic criterion to predict the evolution of non-equilibrium systems and identify steady states —in particular self-assembled states— has motivated a great number of investigations over the years.

In analogy to the second law of thermodynamics, Onsager proposed the principle of least dissipation to understand the evolution of non-equilibrium systems [468]. Built upon the seminal work of Rayleigh, Onsager formulates his variational principle in terms of a dissipation function which contains the rate of change of entropy and the hydrodynamic dissipation. Onsager's principle has been very influential over the years, with recent applications being discussed [469].

Based on Onsager's work, Prigogine introduced the minimal entropy production theorem to understand steady states out of thermal equilibrium. This theorem asserts that in systems out of equilibrium the rate of production of entropy is a minimum [470]. In dynamical self-assembled states of particles, this theorem would constraint the possible structures in the steady state to those which dissipate the least amount of energy and consequently minimize the rate of entropy production. The theorem is derived in the linear regime where Onsager's reciprocal relations hold, and under the assumption of local thermodynamic equilibrium [470]. However, most of non-equilibrium steady structures, including those of particles at interfaces under time-dependent actuations, occur far from thermal equilibrium and the theorem cannot be applied. In particular, Grzybowski and co-workers studied experimentally how dissipation dictates the selection of given non-equilibrium structures of rotating magnets at an interface, and concluded that the system does not always evolve into the least dissipative structure, minimizing the entropy production as the minimum entropy production claims. Rather, they observed the existence of alternative more dissipative structures although with a probability which decays exponentially with the dissipation rate [471]. To understand steady states far from equilibrium where local thermodynamic equilibrium cannot be applied, Evans and Baranyai proposed an alternative approach in terms of an alternative variational principle [472], although it was found to be only approximately valid [473]

Other approaches have attempted to describe non-equilibrium stationary states using extensions of the concept of entropy. Dewar investigated the emergence of non-equilibrium self organization processes using Jaynes' formalism of statistical mechanics [474,475], based on the path information entropy $S_I = -\sum_\Gamma p_\Gamma \log p_\Gamma$. Here, Γ represent the microscopic phase-space paths, with probability p_Γ, and the sum extends to all possible paths [474,475]. Attard formulated a theory to describe non-equilibrium stationary states introducing a second entropy or transition entropy, defined in terms of the number of molecular configurations associated with a transition between macrostates at a given time [476]. The author then argues that the nonequilibrium steady states of systems under fixed thermodynamic gradients are defined by the maximization of this entropy, providing the optimum rate of change or flux in a given system.

Recently, Arango-Restrepo et al. [477,478] investigated the formation of self-assembled structures under non-equilibrium conditions. They show that the architecture of the formed structures is determined by the entropy production in the process of formation. Furthermore, they demonstrate that such structures are characterized by being extreme values of the entropy production as a function of a structural parameter, and test their findings against experimental results of gelation processes and of Liesgang ring formation [477]. The same authors proposed a criterion to identify the formation of self-assembled structures under nonequilibrium conditions [478]. They propose an effective potential function which takes into account the energy required to change the configuration of the system and its stationary probability. Using a phenomenological approach, they determine that the effective potential becomes a minimum at the stationary structures formed by self-assembly in nonequilibrium conditions. The criterium is successfully tested against experiments of Liesgang rings formation and also against experiments of self-assembly of colloidal particles at interfaces under time-dependent field actuations. In particular, they show that the minimization of the effective potential can predict the most stable structure given an external actuation [478].

8. Potential applications of particle-laden fluid interfaces

Colloidal particles confined at fluid interfaces offer many opportunities on the design of materials. From a practical perspective, the stabilization of interfaces by using particles allows obtaining emulsions and foams with enhanced stability in relation to those stabilized by molecular and polymer surfactants. The combination of quasi-2D confinement of particles adsorbed at fluid interfaces with the advances in the synthesis of new colloids, makes possible to take advantage of the microscopic complexity of colloidal interface-dominated materials for the design of new functional materials with tunable macroscopic properties, which can open new avenues in different technological applications [44].

The controlled and guided exploitation of particle-laden fluid interfaces requires addressing the relationship existing between different correlated aspects, such as the characteristics of the particles, the degree of adsorption, the structure of the emerging assemblies and their magnetic, electrical or rheological properties. Some examples of the

potential applications of particle-laden interfaces are given in this section, while more specific details can be found in the literature [1,2,41,285].

8.1. Particles at fluid interfaces for the stabilization of emulsions and foams

The correlation between the interfacial properties of particle-laden fluid interfaces, and their ability to stabilize emulsions and foams emerges as a very important issue in different technological and industrial fields, ranging from the design and manufacture of new food and cosmetics products to wastewater or oil recovery treatments [19,20,100,237]. The use of particle-laden fluid interfaces for the stabilization of dispersed systems is widespread because they provide novel rheological properties to the fluid interface. As a consequence, they improve long-term stability in foams and emulsions because of the reduction of the interfacial area upon the quasi-irreversible trapping of particles, and the mechanical stability provided by the formation of a rigid protective shell overlaying the external surface of droplets or bubbles, which contribute to hinder, at least partially, the different destabilization processes occurring in dispersed systems, e.g., creaming (or sedimentation), flocculation, coalescence, and Ostwald ripening [14,479]. Therefore, it is possible to assume that the stability and properties of emulsions and foams are closely correlated to the interfacial and mechanical properties of single particulate interfaces, and that the layers of adsorbed particles help to dampen the external mechanical perturbations and thus contribute to minimize destabilization and rupture events of dispersed systems [100,280].

Currently it has become obvious that the increase of the surface density of particles adsorbed at fluid interfaces is critical for the enhancement of the stability of emulsions and foams [295,480]. Processes such as jamming and clogging of colloidal monolayers may induce an arrest of the interfacial dynamics, which in turn minimizes the coarsening processes due to the reduction of the interfacial tension, and enhances the interfacial stability. The stability of emulsions and foams is also associated with the rheological properties of the layers [58,59,236,237,481]. Thus, at high interfacial coverages, strong interparticle interactions tend to promote the formation of particle-laden interfaces with a mainly elastic behavior, controlling the film thinning phenomena [482]. According to the Gibbs criteria, which define the stability of dispersed systems in terms of the ratio between the interfacial tension and elasticity, emulsions and foams are stable only when $\varepsilon' > \gamma/2$. However, this criterion only applies to emulsions and foams formed by spherical droplets or bubbles [236].

The close correlation between stability and surface rheology was confirmed by Sullivan and Kilpatrick [483], who found that the formation of rigid, stagnant particle films via the formation of particle bridges, especially when the interfacial coverage is relatively low, results in dispersed systems with increased stability. Besides, the formation of particle zips between close interfaces helps droplets or bubbles to aggregate forming stable flocs, avoiding, at least partially, the coalescence phenomena [238,480]. The increase of both the shear viscosity and the dilational moduli also plays an important role in the control of the drainage phenomena, which are especially relevant for the stability of foams [296]. The impact of the latter is clearly shown in the studies by Cervantes-Martínez et al. [481]. They found that the resistance against compressive stresses presented by particle-laden fluid interfaces minimizes shrinkage of small bubbles and improves foam stability. Despite the extensive research efforts on seeking correlations between the dilatational rheological properties of particle-laden interfaces and their ability for dispersed system stabilization, the current understanding is far from clear, as evidenced by the studies by Santini et al. [4,60,61,107]. They found no correlation between the stability of dispersed systems and the rheological response of the single interfaces. A similar conclusion was reached at when fluid interfaces are stabilized with layers of silica nanoparticles decorated with palmitic acid [61,106]. The above mixture leads to the formation of very rigid interfaces, with very high values of dilational viscoelastic modulus (> 100 mN/m). However, this is not enough to ensure the stabilization of the foams [61]. A different study showed no correlation between the stability of emulsions stabilized by the above mentioned mixtures and the properties of the single water/oil interface [106].

The potential role of the dilatational modulus in controlling the stability of foams and emulsions is inferred from the above discussion, at least under some experimental conditions. However, the shear modulus also plays a very important role on the stability of dispersed systems, mainly due to its correlation to the interfacial structure and packing [276,289]. Brugger et al. [320] found that emulsions stabilized using poly(N-isopropylacrylamide) particles were stable only when the particle-laden interface exhibited an elastic character, whereas viscous interfaces, with high G" values, were easily destabilized. This coincides with the rapid destabilization shown by asphaltene-stabilized emulsions [484]. Apparently, the increase of the interfacial shear viscosity enhances the coalescence rate (on the order of seconds) between droplets in close contact, whereas the coalescence is hindered when the droplets are coated by a layer with a microstructure dominated for the elastic properties of the single interfaces. The differences in the coalescence rate observed as a function of the viscoelastic properties of single interfaces are commonly related to the existence of a high shear yield stress ($\sim 10^4$ Pa), which in turn is closely correlated to the film shear yield point and the film thickness. The increase of the elastic stiffness prevents the mobility and rupture of the particle layer, and hence the formation of a solid-like film may introduce an energetic barrier against coalescence.

The morphology and size distribution of the droplets and bubbles can be modulated by changing the size or contact angle of the adsorbed particles. These parameters also play a very important role on the control of the stability of emulsions and foams. It should be stressed that the stabilization of emulsions and foams requires partial wetting of the particles for both fluid phases. This leads to the formation of oil/water dispersions in the case of hydrophilic particles ($\theta < 90°$), whereas water/oil dispersions are formed when the interface is stabilized by hydrophobic particles ($\theta > 90°$). The change of the particle wettability by the addition of surfactant can be used in the modulation of the stability of emulsions and foams [243] as demonstrated Binks et al. [111]. They found that mixtures of silica nanoparticles and a bicatenary cationic surfactant can stabilize different types of emulsions, with the surfactant concentration being the control parameter dictating the transition between the different emulsion types. In these mixtures, the degree of hydrophobicity of the particles, and consequently their contact angle at the fluid interface, varies as result of their association with the surfactant molecules, with the inversion point appearing in dispersions stabilized with particles of similar affinity for both interfaces, i.e., for $\theta = 90°$ [100]. The addition of a low surfactant concentrations is not enough to modify significantly particle hydrophobicity, which remains mainly hydrophilic with a contact angle lower than 90°. Hence, the stabilization of oil in water (o/w) emulsions should be expected, while the increase of the surfactant concentration enhances the particle hydrophobicity, resulting in a trapping of the particles at the interface with $\theta > 90°$, and hence the formation of water in oil (w/o) emulsions is found. Further increases in surfactant concentration lead to the re-hydrophilization of the particles, which leads again to the formation of o/w emulsions [485]. Similar transitions were found by using chemically modified particles [486]. The modification of the particle wettability has been also exploited for modulating foam stability [487,488]. However, to the best of our knowledge, the study of the transition from aqueous foams to free aqueous droplets surrounded by a particle shell, e.g., dry water or liquid marbles, has not been systematically done, e.g., by changing the hydrophobicity of the particles. However, there is strong evidence for the formation of dry water and liquid marbles by the use of hydrophobic particles [489,490].

Fig. 17 shows an idealized picture of the possible correlations

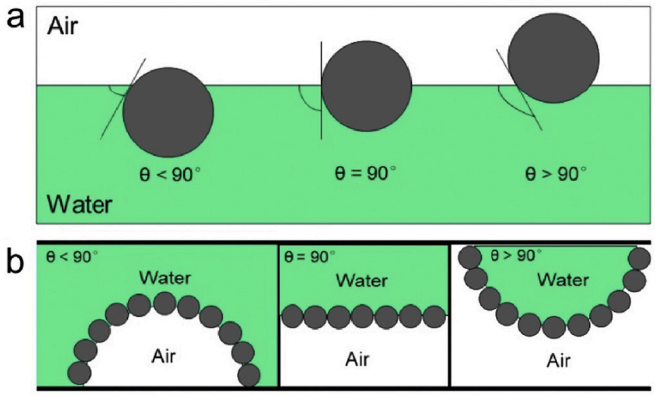

Fig. 17. (a) Idealized representation of the particle position at the water/vapor interface as a function of the wettability. (b) Bending behavior of particle-laden fluid interfaces as function of the particle contact angle. Reprinted from Yu et al. [491], Copyright (2021), with permission from Elsevier.

existing between the contact angle of particles trapped at fluid interface and the interfacial curvature in relation to the stabilization of water/vapor interfaces.

It should be noted that the existence of a non-uniform wetting of the particles at the interface modifies the interfacial energetic landscape, which can change the ability of particles for stabilizing emulsions and foams [102,207,272]. Furthermore, the deformation of the contact line promoted by the weight of large adsorbates may introduce an additional contribution to the destabilization of the dispersed systems as result of the gravitational forces [186].

Particle-stabilized foams and Pickering emulsions have been widely used as templates for the manufacture of solid porous materials, the so-called solid foams. This type of systems can be obtained from the dispersed precursor systems following two different approaches: (i) sintering and drying the wet system, or (ii) direct solidification of the bulk liquid phase [487,491]. Gonzenbach et al. [488] exploited these strategies to obtain solid foams using precursor liquid foams stabilized by mixtures of particles and different short-length surfactant. A similar approach was followed by Zabiegaj et al. [3,4] for the fabrication of particle stabilized solid foams using carbon and alumina particles. Alumina-based aqueous foams were also used by Santos et al. [492] in the preparation of macroporous refractory ceramics by adding calcium aluminate cement as a binder. The addition of the binder allows reducing the time required for setting the solid structure, improving its mechanical strength. Similar results were found by Finhana et al. [493].

8.2. Colloidosomes

Colloidosomes are solid capsules formed by a shell of densely packed particles with their size ranging from the sub-micrometer scale to millimeter scale. They have as main properties their controllable permeability and mechanical strength [2,494]. The most common methodology for the fabrication of colloidosomes is based on the assembly of colloidal particles into emulsion droplets that are locked together by sintering or electrostatic binding of oppositely charged polyelectrolytes, avoiding the destruction of the shell by transferring them to a different fluid [2,40].

Dinsmore et al. [494] prepared colloidosomes by self-assembly of carboxylated polystyrene latex microparticles on the surface of oil-in-water and water-in-oil of emulsions droplets. After the assembly of the particles on the surface of the droplet, they were bound by heating the system just about the glass transition of polystyrene (around 105°C). During this step, glycerol was added to the aqueous phase to prevent water evaporation. The high temperature required for sintering becomes a major drawback in the preparation of colloidosomes, which can be partially overcome by using particles with a lower glass transition [495]. The sintering process can also be performed locally by heating using laser irradiation, as demonstrated López-de-Luzuriaga et al. [496]. By self-assembly of spherical gold nanoparticles at the interface of oleic acid (OA) nanodroplets formed in n-hexane, followed by laser irradiation, they fabricated plasmonic gold colloidosomes with collective plasmonic absorptions tunable in surface, size and shape.

The assembly of oppositely charged polyelectrolytes on particles has also been exploited to prepare colloidosomes and avoid the use of high temperatures. Gordon et al. [497] used this methodology for the assembly of latex particles in toluene/water systems by introducing poly (L-lysine) into the aqueous phase. During the assembly, the poly(L-lysine) chains adsorb on the latex surface, which allows locking them in a superstructure. The formed colloidosomes were strong enough to withstand the osmotic stresses that occur during their transference to a different solvent. Another possibility to fix the particles in colloidosomes is the use of polyelectrolyte multilayers obtained by the Layer-by-Layer (LbL) method [498,499].

Colloidosomes can be also obtained using an internal phase containing a gelling agent. Gelation of the internal phase of water-in-oil colloidosomes generates a solid-like structure, which provides the colloidosomes enough stability and structural strength to prevent their collapse upon solvent exchange processes [500]. Cayre et al. [500] fabricated colloidosomes through the assembly of amine-functionalized polystyrene latex on water droplets containing agarose dispersed in sunflower oil at 70°C. Afterwards, the gelation of the aqueous droplets took place by reducing the temperature from 70 to 20°C. The gelling agent can be replaced by wax to obtain solid capsules. This requires preparing wax-in-water emulsions stabilized by colloidal particles, at high temperature, and then the obtained dispersions must be cooled down to crystallize the oil phase [299].

The stability of the colloidosomes can be improved by polymerization after their preparation, within or on the surface of the Pickering precursor emulsions, which favors the particle entrapment at the interface. This approach was followed by Chen et al. [501] on the preparation of paraffin in water emulsions stabilized by functionalized silica particles in such a way that atom transfer radical polymerization (ATRP) can be induced on their surface. Thus, after preparing the Pickering emulsions, a polymerization process was induced by the addition of 2-hydroxyethyl methacrylate in the medium, which allows obtaining colloidosomes cross-linked by a poly(hydroxyethyl methacrylate) network. An alternative approach is to perform the polymerization inside the droplets by including vinyl monomers. This strategy was used by Bon et al. [502], who stabilized droplets containing styrene and divinylbenzene, using poly(methyl methacrylate) particles as reactors for the copolymerization process. This procedure allowed the formation of colloidosomes with sizes in the range of 5-30 μm reinforced by a polystyrene core. Precipitation of a preformed polymer in the inner core of the Pickering emulsion can be exploited as an alternative to polymerization, as was demonstrated by Cayre et al. [503]. They prepared oil-in-water emulsions stabilized with silica and gold particles. In this work, a linear poly(methyl methacrylate) was dissolved in the oil phase, a mixture of dichloromethane/n-hexadecane. After preparing the emulsions dichloromethane was evaporated, at 40°C. As the polymer is less soluble in hexadecane than in the mixture, the evaporation induced its precipitation on the inner walls of the capsules, blocking the inorganic particles at the interface. The reduction of the amount of polymer leads to a degradation of the mechanical properties of the obtained colloidosomes [504]. In the literature, there are many other examples following similar methods to improve the stability of the colloidosomes obtained [505].

The methodologies discussed above, designed to improve the mechanical strength of colloidosomes, often involve heating steps that should be avoided in certain applications, e.g., encapsulation of biological compounds. This limitation may be overcome by choosing particles suitable for obtaining a covalently cross-linked structure at room

temperature [506]. There are many examples in the literature of colloidosomes reinforced by chemical cross-linking. This idea was used by Croll et al. [507] for the fabrication of colloidosomes upon the assembly of poly-(divinylbenzene-alt-maleic anhydride) microspheres at an oil/water interface, followed by cross-linking via amide or ionic bonds. In the formation of microcapsules, the length of the cross-linker is critical, as low molecular weight species are often too small to span the gap between adjacent particles. Covalent cross-linking was also used in the reinforcement of colloidosomes formed by quantum dots [508]. Skaff et al. [509] obtained cross-linked CdSe/ZnS capsules by a ring-opening metathesis polymerization of norbornene attached to the quantum dots, which allows the quantum dots to be arrested in a superstructure at room temperature. Another strategy used to exploit ionic crosslinking was developed by Arumugan et al. [510] for the fabrication of magnetic colloidosomes stabilized with FePt particles. Here, complexation of terpyridine tethered to the particle surface with Fe(II) metal ion lead to nanoparticle networks at the liquid−liquid interface.

Sharh et al. [511] prepared thermo-sensitive colloidosomes by cross-linking primary amine functionalized PNIPAM particles with glutaraldehyde. These colloidosomes undergo a strong reduction of the size with the increase of the temperature. The combination of covalent cross-linking and steric stabilization is also very popular, as evidenced the study by Walsh et al. [512]. They fabricated colloidosomes of polystyrene latex stabilized by the adsorption of poly(ethylene imine) quaternized with 4-vinylbenzyl chloride, which can be cross-linked by using different bis-epoxy polymeric cross-linkers. A similar approach was followed for the fabrication of colloidosomes by using different organoclays [513,514] and silica particles [515]. Yuan et al. [516] reported another design that combined covalent cross-linking with steric stabilization, by decorating polystyrene particles with a poly(2-dimethylaminoethyl methacrylate)-poly(methyl methacrylate) diblock copolymer. The later can be cross-linked at the oil/water interface though a quaternization process, using 1,2-bis(2-iodoethyloxy)ethane.

8.3. *Coffee ring suppression*

Particles homogeneously dispersed within liquid droplets may lead to the formation of ring-like deposits upon evaporation of the solvent, resulting in the so-called coffee-ring effect [113,234]. The formation of this type of deposits is often undesirable in application such as inkjet printing, and the fabrication of micro- and nanostructures, or coatings, where a more homogenous deposition of the material is required [517–524]. In the last years, the use of colloidal particles trapped at water/vapor interfaces has been very common for a complete suppression, or partial mitigation, of the formation of the coffee-rings when sessile droplets are droplets are evaporated [48,149]. This is the result of the competition between adsorption at the fluid/fluid interface and at the solid/fluid interface occurring during droplet evaporation. Therefore, by modulating the properties of the particles dispersed within the evaporating droplet it is possible to modify their adsorption to the interfaces involved, which in turn provides a large degree of control over the morphology of the deposits obtained. The latter is the result of an intricate balance between particle−particle, particle−fluid/fluid interface, and particle−substrate interactions [338].

There are several methodological approaches enabling the reduction of the coffee-ring effect in the deposition droplets containing colloidal particle suspensions. Bigioni et al. [525] controlled the order of the self-assembled particle array on the solid surface by pushing the particles towards the fluid/fluid interface. This was possible by a combination of a rapid evaporation of the solvent, faster than the diffusion of the particles in the bulk, which favors particle segregation towards the liquid/vapor interface, and the appearance of attractive capillary interaction between particles once they reach to the fluid interface. This leads to the the formation of particle network with a high degree of long-range order, preventing partially the deposition of the coffe-ring on the solid surface. Selective segregation of the particles towards the fluid interface can be also stimulated by the use of a mixture solvent/co-solvent [526]. The combination of water with a co-solvent, with higher vapor pressure, leads to segregation of the co-solvent near to the liquid/vapor interfacial region, which favors the transport of hydrophobic particles to the liquid/vapor interface where they self-assemble into an ordered array. Surfactant-mediated interactions can be also be exploited to modulate the deposition patterns of particles on solid surfaces [338]. In this case, it was possible to adjust the electrostatic and hydrophobic particle−particle, particle−interface, and particle−substrate interactions to create deposits with very different morphologies, from rings to disks. The use of particles with high hydrophobicity (decorated with intermediate concentration of oppositely charged surfactants) leads to the formation of deposits with the highest homogeneity, which is associated with the formation of a skin of colloidal particles at the water/vapor interface during evaporation. On the other side, the deposition of particles decorated with very low and very high surfactant concentrations (highly hydrophilic particles) results in the formation of ring-like deposits.

Another possibility for the suppression of the coffee-ring effects, proposed by Li et al. [527], is based on the capture and self-assembly of a rapidly descending liquid/vapor interface. This method requires the use of an environmental chamber, designed to allow control of the temperature and the relative humidity. High temperature evaporation hinders the deposition in the border of the three-phase contact line, promoting the formation of homogeneous deposits. This happens because at high temperature the rate of descent of the liquid/vapor interface is faster than the diffusion of the colloidal particle, which favors that a part of the particles can be retained by the fluid interface. Thus, the jamming of the particles at the fluid interface leads to an enhancement of the interfacial viscosity in relation to that of the bulk, which introduces an additional resistance to the capillary outflow and leads to the formation of uniform deposits.

Particle shape anisotropy can be also exploited to modulate the morphology of the deposits obtained upon evaporation [528]. Spherical or slightly deformed colloidal particles are usually transported very efficiently to the three-phase contact line because of the evaporation-driven capillary flow, whereas ellipsoidal particles are deposited homogeneously during solvent evaporation. This difference is due to the fact that ellipsoidal particles can be entrained towards the edge of the evaporating droplets due to the outward capillary flow, until they are trapped by the descending liquid/vapor interface, where they undergo strong attractive inter-particle force. These phenomena are accompanied by a strong increase of the interfacial viscosity, associated with the adsorption of ellipsoidal particles that introduces an additional resistance to the outward capillary flow. In colloidal suspensions of spherical particles, the situation changes significantly, as the particles can be desorbed from the descending interface due to the weakness of the inter-particle attraction. The above mechanism based on the balance between capillary and hydrodynamic forces, is quite general. Thus, in systems where the interfacial forces are greater than the hydrodynamic ones, the formation of stable particle networks at the interface is favored and, therefore, their migration towards the three-contact line is hindered. On the contrary, when the hydrodynamic forces overcome the capillary forces, the particles are easily transported to the contact line, where they form heterogeneous deposits [529].

Parthasarathy et al. [530] explored the evaporation of droplets of highly diluted suspensions containing particles of diameters from 3 to 10 microns to study the pattern formation on solid substrates. They stated that the process is governed by the combined effect of gravity and interfacial hydrodynamic forces, such that when the gravity driven deposition exceeds capillary driven transport, it is possible to suppress the coffee ring formation. They also found the existence of a transition in the morphology of the evaporative patterns, from mono- to multilayers, with the increase of the particle diameter and the initial particle concentration of the suspension. Furthermore, they described an order-disorder transition, which disappears at relatively high particle

concentrations. This transition was strongly determined by the organization of the particles at the edge of the deposits.

A more recent approach for minimizing the coffee-ring effect involved the direct spreading of particles at the liquid/vapor interface of the evaporating droplet. This leads to a situation in which the particles can assemble at the interface during the evaporation enabling the formation of a uniform film. This occurs in three steps: (i) spreading of the particles at the surface of the evaporating droplet; (ii) assembly of the particles at the liquid/vapor interface, and (iii) settling of the particle film onto the substrate upon evaporation. This approach can be exploited for the fabrication of low interfacial tensions inks containing colloidal particles and a high interfacial tension liquid, e.g., water or ethanol/water mixtures [531,532].

Recently, Nath and Ray [533] demonstrated the power of the lattice Boltzmann method to predict the 3D-microstructures obtained after evaporation of droplets containing nanoparticles. For Péclet number above the unity, non-uniform coffee ring deposits are obtained in the vicinity of the pinning regions. Besides, the increase of the pattern dimensions and the difference between the pattern and substrate surface energies lead to the formation of deposits with stereoscopic morphologies.

8.4. Fluid interfaces laden with active/actuated particles

Laden fluid interfaces of tunable colloids are promising candidates for designing new smart materials with remarkable properties. For example, Pickering emulsions stabilized with magnetic particles can be destabilized at will simply by approaching a magnet or applying a homogeneous magnetic field. [368,399], and magnetic needles can be used as probes for rheological characterization of fluid interfaces [184]. Guided motion of active and actuated adsorbed particles can be used in the transport of adsorbed matter at the microscale, in confined environments, in the enhancement of mass transport or in the modulation of interfacial properties. However, chaotic flows generated at low Reynolds numbers by dispersions of active colloids [534] can also be harnessed to promote mixing in the microscale or in water remediation. Although the uptake of these emerging applications in commercial technologies is still low, we anticipate that adsorbed active colloids will soon be regularly employed in micro- and nanofluidic devices and at the fluid interfaces inherent in all living organisms, and that out-of-equilibrium assemblies will be used as piloted carriers for precise and targeted interfacial drug transport at biological fluid interfaces, such as oral mucosa and saliva, tear films or those stabilised by lung surfactants [535].

9. Concluding remarks

The impact of particle-laden fluid interfaces in different problems with interest for academia and industry has stimulated to researchers with very different backgrounds to deepen on the understanding of the main forces driving the assembly of colloidal micro- and nano-particles at fluid interfaces as well as of the physico-chemical behavior of the obtained layers. This is essential for opening new avenues allowing the explotaition of the power of particle-laden fluid interfaces in applications, e.g., the fabrication of interface-dominated systems such as foams, emulsions and thin films. Also reconfigurable devices, or the modulation of processes with technological interest, e.g. ink-jet printing, where the broken symmetry of fluid interfaces becomes an ideal platform for the confining of materials to fabricate materials with reduced dimensionality will benefit from particle laden interfaces. Therefore, the analysis of different aspects allowing the modulation of the assembly of particles at the interface, mainly the particle wettability and the inter-particle interactions, and the understanding of the response of particle-laden interface upon the application of external stimuli (mechanical, thermal, magnetic or electric) become of paramount importance.

The behavior of particle-laden fluid interfaces is governed by a complex interplay between the individual and collective behavior of the trapped colloids which confer novel mechanical (shear and dilational) and functional properties to the fluid interface. These properties emerge strongly dependent on the specific chemistry, moprhology, wettability and charge of the considered colloids as well as on the modification of their surface by addition of surfactants or covalent binding of other types of molecules. Nowadays, there is a reasonably good understanding on the behavior of single hard particles at fluid interfaces. However, the current knowledge on the behavior of soft particles as well as of particle-mediated interactions and the collective behavior of particle-laden fluid interfaces remain relatively poor. Therefore, it is necessary to move the research on particle-laden interfaces to such topics. In fact, the interactions are responsible of the ability of particle for migrating, being dispersed or assembly at the interface, resulting in specific ordered structures which in turn define the mechanical behavior of the particle-laden interface. This is very important because defines the high stability of Pickering emulsions and particle-stabilized foams. Furthermore, the dynamical behavior of particles trapped at fluid interfaces also requires further studies. In fact, colloid adsorbed at fluid interfaces show very different motion pathways than colloids in the bulk. The characterization of the dynamical aspects are not only important itself, and the potential application of particles as microrheological traces requires to understand the motion of individual particles. On the other side, the understanding of the dynamics of particle-laden interfaces becomes very important because they play a very important role on the behavior on active colloids trapped at fluid interfaces. These offers very interesting dynamic behavior and phase transitions which deserveds further attention.

This review has tried to present a broad perspective to the study of particle-laden interface, which makes this review an excellent guide for researchers and technologist addressing for first time problems related to particle-laden interface as well as for experienced researcher trying to exploit the whole potential of particle-laden fluid interfaces for opening new avenues in nanoscience and nanotechnology.

CRediT authorship contribution statement

Eduardo Guzmán: Conceptualization, Methodology, Software, Data curation, Writing – original draft, Writing – review & editing, Investigation, Visualization, Funding acquisition. **Fernando Martínez-Pedrero:** Conceptualization, Methodology, Software, Data curation, Writing – original draft, Writing – review & editing, Investigation, Visualization, Funding acquisition. **Carles Calero:** Writing – original draft, Writing – review & editing, Investigation. **Armando Maestro:** Writing – original draft, Writing – review & editing, Investigation. **Francisco Ortega:** Supervision, Validation, Writing – review & editing, Resources, Investigation, Funding acquisition. **Ramón G. Rubio:** Supervision, Validation, Investigation, Writing – review & editing, Resources, Project administration, Funding acquisition.

Declaration of Competing Interest

The authors declare no conflict of interest. The funders had no role in the design of the study; in the collection, analyses, or interpretation of data; in the writing of the manuscript, or in the decision to publish the results.

Acknowledgements

This work was funded by MICINN under grants PID2019-105343GB-I00 and PID2019-106557GB-C21, and by EU in the framework of the European Innovative Training Network-Marie Sklodowska-Curie Action NanoPaInt (grant agreement 955612). We thank Patricia Guisado-Barrado for her help in adapting Fig. 3.

References

[1] Shi S, Russell TP. Nanoparticle assembly at liquid–liquid interfaces: from the nanoscale to mesoscale. Adv. Mater. 2018;30:1800714.
[2] Forth J, Kim PY, Xie G, Liu X, Helms BA, Russell TP. Building reconfigurable devices using complex liquid–fluid interfaces. Adv. Mater. 2019;31:1806370.
[3] Zabiegaj D, Santini E, Ferrari M, Liggieri L, Ravera F. Carbon based porous materials from particle stabilized wet foams. Colloids Surf. A Physicochem. Eng. Asp. 2015;473:24–31.
[4] Zabiegaj D, Santini E, Guzmán E, Ferrari M, Liggieri L, Buscaglia V, et al. Nanoparticle laden interfacial layers and application to foams and solid foams. Colloids Surf. A Physicochem. Eng. Asp. 2013;438:132–40.
[5] Binks BP, Vishal B. Particle-stabilized oil foams. Adv. Colloid Interf. Sci. 2021; 2021:102404.
[6] Guzman E, Orsi D, Cristofolini L, Liggieri L, Ravera F. Two-dimensional DPPC based emulsion-like structures stabilized by silica nanoparticles. Langmuir. 2014; 30:11504–12.
[7] Giner-Casares JJ, Reguera J. Directed self-assembly of inorganic nanoparticles at air/liquid interfaces. Nanoscale. 2016;8:16589–95.
[8] Martínez-Pedrero F. Static and dynamic behavior of magnetic particles at fluid interfaces. Adv. Colloid Interf. Sci. 2020;284:102233.
[9] Martínez-Pedrero F, Ortega F, Rubio RG, Calero C. Magnetic microparticles: collective transport of magnetic microparticles at a fluid interface through dynamic self-assembled lattices. Adv. Funct. Mater. 2020;30:2070333.
[10] Bresme F, Oettel M. Nanoparticles at fluid interfaces. J. Phys. Condens. Matter 2007;19:413101.
[11] Ji X, Wang X, Zhang Y, Zang D. Interfacial viscoelasticity and jamming of colloidal particles at fluid–fluid interfaces: a review. Rep. Prog. Phys. 2020;83: 126601.
[12] Binks BP. Particles as surfactants—similarities and differences. Curr. Opin. Colloid Interface Sci. 2002;7:21–41.
[13] Garbin V. Colloidal particles: Surfactants with a difference. Phys. Today 2013;66: 68.
[14] Binks BP. Colloidal particles at a range of fluid–fluid interfaces. Langmuir. 2017; 33:6947–63.
[15] Fernandez-Rodriguez MA, Binks BP, Rodriguez-Valverde MA, Cabrerizo-Vilchez MA, Hidalgo-Alvarez R. Particles adsorbed at various non-aqueous liquid-liquid interfaces. Adv. Colloid Interf. Sci. 2017;247:208–22.
[16] Vogel N, Retsch M, Fustin C-A, del Campo A, Jonas U. Advances in colloidal assembly: the design of structure and hierarchy in two and three dimensions. Chem. Rev. 2015;115:6265–311.
[17] Velev OD, Gupta S. Materials fabricated by micro- and nanoparticle assembly – the challenging path from science to engineering. Adv. Mater. 2009;21: 1897–905.
[18] Lotito V, Zambelli T. Approaches to self-assembly of colloidal monolayers: a guide for nanotechnologists. Adv. Colloid Interf. Sci. 2017;246:217–74.
[19] Ramsden W, Gotch F. Separation of solids in the surface-layers of solutions and suspensions (observations on surface-membranes, bubbles, emulsions, and mechanical coagulation). Preliminary account. Proc. Roy. Soc. London 1904;72: 156–64.
[20] Pickering SU. CXCVI.—Emulsions. J. Chem. Soc. Trans. 1907;91:2001–21.
[21] Ouchi T, Nakamura R, Suzuki T, Minami H. Preparation of Janus particles composed of hydrophobic and hydrophilic polymers. Ind. Eng. Chem. Res. 2019; 58:20996–1002.
[22] Martín-Roca J, Jiménez M, Ortega F, Calero C, Valeriani C, Rubio RG, et al. Rotating Micro-Spheres for adsorption monitoring at a fluid interface. J. Colloid Interface Sci. 2022;614:378–88.
[23] Maestro A, Guzmán E, Ortega F, Rubio RG. Contact angle of micro- and nanoparticles at fluid interfaces. Curr. Opin. Colloid Interface Sci. 2014;19: 355–67.
[24] Zanini M, Isa L. Particle contact angles at fluid interfaces: pushing the boundary beyond hard uniform spherical colloids. J. Phys. Condens. Matter 2016;28: 313002.
[25] Ballard N, Law AD, Bon SAF. Colloidal particles at fluid interfaces: behaviour of isolated particles. Soft Matter 2019;15:1186–99.
[26] Garbin V. Collapse mechanisms and extreme deformation of particle-laden interfaces. Curr. Opin. Colloid Interface Sci. 2019;39:202–11.
[27] Maestro A. Tailoring the interfacial assembly of colloidal particles by engineering the mechanical properties of the interface. Curr. Opin. Colloid Interface Sci. 2019; 39:232–50.
[28] Thijssen JHJ, Vermant J. Interfacial rheology of model particles at liquid interfaces and its relation to (bicontinuous) Pickering emulsions. J. Phys. Condens. Matter 2017;30:023002.
[29] Correia EL, Brown N, Razavi S. Janus particles at fluid interfaces: stability and interfacial rheology. Nanomaterials. 2021;11:374.
[30] Liggieri L, Santini E, Guzmán E, Maestro A, Ravera F. Wide-frequency dilational rheology investigation of mixed silica nanoparticle–CTAB interfacial layers. Soft Matter 2011;7:7699–709.
[31] Maestro A, Santini E, Zabiegaj D, Llamas S, Ravera F, Liggieri L, et al. Particle and particle-surfactant mixtures at fluid interfaces: assembly, morphology, and rheological description. Adv Condes Matter Phys. 2015;2015:917516.
[32] Maestro A, Santini E, Guzmán E. Physico-chemical foundations of particle-laden fluid interfaces. Eur. Phys J E. 2018;41:97.
[33] Maestro A, Guzmán E. Colloids at fluid interfaces. Processes. 2019;7:942.
[34] Guzmán E, Abelenda-Núñez I, Maestro A, Ortega F, Santamaria A, Rubio RG. Particle-laden fluid/fluid interfaces: physico-chemical foundations. J. Phys. Condens. Matter 2021;33:333001.
[35] Deshmukh OS, van den Ende D, Stuart MC, Mugele F, Duits MHG. Hard and soft colloids at fluid interfaces: Adsorption, interactions, assembly & rheology. Adv. Colloid Interf. Sci. 2015;222:215–27.
[36] Mendoza AJ, Guzmán E, Martínez-Pedrero F, Ritacco H, Rubio RG, Ortega F, et al. Particle laden fluid interfaces: Dynamics and interfacial rheology. Adv. Colloid Interf. Sci. 2014;206:303–19.
[37] Villa S, Boniello G, Stocco A, Nobili M. Motion of micro- and nano- particles interacting with a fluid interface. Adv. Colloid Interf. Sci. 2020;284:102262.
[38] Fei W, Gu Y, Bishop KJM. Active colloidal particles at fluid-fluid interfaces. Curr. Opin. Colloid Interface Sci. 2017;32:57–68.
[39] Guzmán E, Santini E. Lung surfactant-particles at fluid interfaces for toxicity assessments. Curr. Opin. Colloid Interface Sci. 2019;39:24–39.
[40] Dasgupta S, Auth T, Gompper G. Nano- and microparticles at fluid and biological interfaces. J. Phys. Condens. Matter 2017;29:373003.
[41] Wei P, Luo Q, Edgehouse KJ, Hemmingsen CM, Rodier BJ, Pentzer EB. 2D particles at fluid–fluid interfaces: assembly and templating of hybrid structures for advanced applications. ACS Appl. Mater. Interfaces 2018;10:21765–81.
[42] Jena KC, Scheu R, Roke S. Surface impurities are not responsible for the charge on the oil/water interface: a comment. Angew. Chem. Int. Ed. 2012;51:12938–40.
[43] Dugyala VR, Muthukuru JS, Mani E, Basavaraj MG. Role of electrostatic interactions in the adsorption kinetics of nanoparticles at fluid–fluid interfaces. Phys. Chem. Chem. Phys. 2016;18:5499–508.
[44] McGorty R, Fung J, Kaz D, Manoharan VN. Colloidal self-assembly at an interface. Mater. Today 2010;13:34–42.
[45] Ward AFH, Tordai L. Time-dependence of boundary tensions of solutions i. the role of diffusion in time-effects. J. Chem. Phys. 1946;14:453–61.
[46] Wang H, Singh V, Behrens SH. Image charge effects on the formation of pickering emulsions. J. Phys. Chem. Lett. 2012;3:2986–90.
[47] Kettlewell SL, Schmid A, Fujii S, Dupin D, Armes SP. Is latex surface charge an important parameter for foam stabilization? Langmuir. 2007;23:11381–6.
[48] Van Oss CJ, Chaudhury MK, Good RJ. Interfacial Lifshitz-van der Waals and polar interactions in macroscopic systems. Chem. Rev. 1988;88:927–41.
[49] Israelachvili J. Intermolecular and Surface Forces Waltham, MA. USA: Academic Press; 1985.
[50] Schwenke K, Isa L, Del Gado E. Assembly of nanoparticles at liquid interfaces: crowding and ordering. Langmuir. 2014;30:3069–74.
[51] Ravera F, Santini E, Loglio G, Ferrari M, Liggieri L. Effect of nanoparticles on the interfacial properties of liquid/liquid and liquid/air surface layers. J. Phys. Chem. B 2006;110:19543–51.
[52] Garbin V, Crocker JC, Stebe KJ. Forced desorption of nanoparticles from an oil–water interface. Langmuir. 2012;28:1663–7.
[53] Berg JC. An introduction to Interfaces and Colloids: The Bridge to Nanoscience. Singapore, Singapore: World Scientific; 2010.
[54] Joos P. Dynamic Surface Phenomena. Boca Ratón, FL, USA: CRC Press; 1999.
[55] Díez-Pascual AM, Compostizo A, Crespo-Colín A, Rubio RG, Miller R. Adsorption of water-soluble polymers with surfactant character.: Adsorption kinetics and equilibrium properties. J. Colloid Interface Sci. 2007;307:398–404.
[56] Höfling F, Dietrich S. Enhanced wavelength-dependent surface tension of liquid-vapour interfaces. Europhys. Lett. 2015;109:46002.
[57] Safran SA. Statistical thermodynamics of Surfaces, Interfaces and membranes. Boca Raton, FL, USA: CRC Press; 2002.
[58] Maestro A, Rio E, Drenckhan W, Langevin D, Salonen A. Foams stabilised by mixtures of nanoparticles and oppositely charged surfactants: relationship between bubble shrinkage and foam coarsening. Soft Matter 2014;10:6975–83.
[59] Arriaga LR, Drenckhan W, Salonen A, Rodrigues JA, Íñiguez-Palomares R, Rio E, et al. On the long-term stability of foams stabilised by mixtures of nano-particles and oppositely charged short chain surfactants. Soft Matter 2012;8:11085–97.
[60] Santini E, Ravera F, Ferrari M, Alfè M, Ciajolo A, Liggieri L. Interfacial properties of carbon particulate-laden liquid interfaces and stability of related foams and emulsions. Colloids Surf. A Physicochem. Eng. Asp. 2010;365:189–98.
[61] Santini E, Guzmán E, Ravera F, Ciajolo A, Alfè M, Liggieri L, et al. Soot particles at the aqueous interface and effects on foams stability. Colloids Surf. A Physicochem. Eng. Asp. 2012;413:216–23.
[62] Noskov BA, Bykov AG. Dilational rheology of monolayers of nano- and micropaticles at the liquid-fluid interfaces. Curr. Opin. Colloid Interface Sci. 2018;37:1–12.
[63] Yazhgur PA, Noskov BA, Liggieri L, Lin SY, Loglio G, Miller R, et al. Dynamic properties of mixed nanoparticle/surfactant adsorption layers. Soft Matter 2013; 9:3305–14.
[64] Santini E, Krägel J, Ravera F, Liggieri L, Miller R. Study of the monolayer structure and wettability properties of silica nanoparticles and CTAB using the Langmuir trough technique. Colloids Surf. A Physicochem. Eng. Asp. 2011;382: 186–91.
[65] Akanno A, Guzmán E, Fernández-Peña L, Llamas S, Ortega F, Rubio RG. Equilibration of a polycation–anionic surfactant mixture at the water/vapor interface. Langmuir. 2018;34:7455–64.
[66] Du K, Glogowski E, Emrick T, Russell TP, Dinsmore AD. Adsorption energy of nano- and microparticles at liquid−liquid interfaces. Langmuir. 2010;26: 12518–22.
[67] Miller R, Aksenenko EV, Fainerman VB. Dynamic interfacial tension of surfactant solutions. Adv. Colloid Interf. Sci. 2017;247:115–29.
[68] Henderson D. A simple equation of state for hard discs. Mol. Phys. 1975;30: 971–2.

[69] Miller R, Fainerman VB, Kovalchuk VI, Grigoriev DO, Leser ME, Michel M. Composite interfacial layers containing micro-size and nano-size particles. Adv. Colloid Interf. Sci. 2006;128-130:17–26.
[70] Llamas S, Guzmán E, Akanno A, Fernández-Peña L, Ortega F, Campbell RA, et al. Study of the liquid/vapor interfacial properties of concentrated polyelectrolyte–surfactant mixtures using surface tensiometry and neutron reflectometry: equilibrium, adsorption kinetics, and dilational rheology. J. Phys. Chem. C 2018;122:4419–27.
[71] Miller R, Fainerman VB, Makievski AV, Kragel J, Grigoriev DO, Kazakov VN, et al. Dynamics of protein and mixed proteinr/surfactant adsorption layers at the water/fluid interface. Adv. Colloid Interf. Sci. 2000;86:39–82.
[72] Hua X, Bevan MA, Frechette J. Competitive adsorption between nanoparticles and surface active ions for the oil–water interface. Langmuir. 2018;34:4830–42.
[73] Sundaram S, Ferri JK, Vollhardt D, Stebe KJ. Surface phase behavior and surface tension evolution for lysozyme adsorption onto clean interfaces and into DPPC monolayers:theory and experiment. Langmuir. 1998;14:1208–18.
[74] Groot R, Stoyanov S. Equation of state of surface-adsorbing colloids. Soft Matter 2011;6:1682–92.
[75] Deshmukh OS, Maestro A, Duits MHG, van den Ende D, Stuart MC, Mugele F. Equation of state and adsorption dynamics of soft microgel particles at an air–water interface. Soft Matter 2014;10:7045–50.
[76] Iwamatsu M. A generalized Young's equation to bridge a gap between the experimentally measured and the theoretically calculated line tensions. J. Adhes. Sci. Technol. 2018;32:2305–19.
[77] Davies GB, Krüger T, Coveney PV, Harting J. Detachment energies of spheroidal particles from fluid-fluid interfaces. J. Chem. Phys. 2014;141:154902.
[78] Oettel M, Dietrich S. Colloidal interactions at fluid interfaces. Langmuir. 2008;24:1425–41.
[79] Fokkink LGJ, Ralston J. Contact angles on charged substrates. Colloids Surf. A Physicochem. Eng. Asp. 1989;36:69–76.
[80] Maestro A, Guzmán E, Santini E, Ravera F, Liggieri L, Ortega F, et al. Wettability of silica nanoparticle–surfactant nanocomposite interfacial layers. Soft Matter 2012;8:837–43.
[81] Davies GB, Krüger T, Coveney PV, Harting J. Detachment energies of spheroidal particles from fluid-fluid interfaces. J. Chem. Phys. 2014;141:154902.
[82] Pieranski P. Two-dimensional interfacial colloidal crystals. Phys. Rev. Lett. 1980;45:569–72.
[83] Wi HS, Cingarapu S, Klabunde KJ, Law BM. Nanoparticle adsorption at liquid–vapor surfaces: influence of nanoparticle thermodynamics, wettability, and line tension. Langmuir. 2011;27:9979–84.
[84] Lin Y, Skaff H, Emrick T, Dinsmore AD, Russell TP. Nanoparticle assembly and transport at liquid-liquid interfaces. Science. 2003;299:226–9.
[85] Srivastava S, Nykypanchuk D, Fukuto M, Gang O. Tunable nanoparticle arrays at charged interfaces. ACS Nano 2014;8:9857–66.
[86] Kaz DM, McGorty R, Mani M, Brenner MP, Manoharan VN. Physical ageing of the contact line on colloidal particles at liquid interfaces. Nat. Mater. 2012;11:138–42.
[87] Kaz DM, McGorty R, Mani M, Brenner MP, Manoharan VN. Physical ageing of the contact line on colloidal particles at liquid interfaces. Nat. Mater. 2012;11:138–42.
[88] Vella D, Mahadevan L. The "Cheerios effect". Am. J. Phys. 2005;73:817–25.
[89] Galatola P, Fournier J-B. Capillary force acting on a colloidal particle floating on a deformed interface. Soft Matter 2014;10:2197–212.
[90] Zang DY, Rio E, Delon G, Langevin D, Wei B, Binks BP. Influence of the contact angle of silica nanoparticles at the air–water interface on the mechanical properties of the layers composed of these particles. Mol. Phys. 2011;109:1057–66.
[91] Ortega F, Ritacco H, Rubio RG. Interfacial microrheology: Particle tracking and related techniques. Curr. Opin. Colloid Interface Sci. 2010;15:237–45.
[92] Guzmán E, Tajuelo J, Pastor JM, Rubio MÁ, Ortega F, Rubio RG. Shear rheology of fluid interfaces: Closing the gap between macro- and micro-rheology. Curr. Opin. Colloid Interface Sci. 2018;37:33–48.
[93] Garbin V, Crocker JC, Stebe KJ. Nanoparticles at fluid interfaces: Exploiting capping ligands to control adsorption, stability and dynamics. J. Colloid Interface Sci. 2012;387:1–11.
[94] Ivanov IB, Kralchevsky PA, Nikolov AD. Film and line tension effects on the attachment of particles to an interface: I. Conditions for mechanical equilibrium of fluid and solid particles at a fluid interface. J. Colloid Interface Sci. 1986;112:97–107.
[95] Hirth JP, Jossang T, Lothe J. Dislocation energies and the concept of line tension. J. Appl. Phys. 1966;37:110–6.
[96] Coertjens S, Moldenaers P, Vermant J, Isa L. Contact angles of microellipsoids at fluid interfaces. Langmuir. 2014;30:4289–300.
[97] Bresme F, Quirke N. Nanoparticulates at liquid/liquid interfaces. Phys. Chem. Chem. Phys. 1999;1:2149–55.
[98] Dong L, Johnson DT. Adsorption of acicular particles at liquid−fluid interfaces and the influence of the line tension. Langmuir. 2005;21:3838–49.
[99] McBride SP, Law BM. Influence of line tension on spherical colloidal particles at liquid-vapor interfaces. Phys. Rev. Lett. 2012;109:196101.
[100] Aveyard R, Binks BP, Clint JH. Emulsions stabilised solely by colloidal particles. Adv. Colloid Interf. Sci. 2003;100-102:503–46.
[101] Zeng M, Mi J, Zhong C. Wetting behavior of spherical nanoparticles at a vapor–liquid interface: a density functional theory study. Phys. Chem. Chem. Phys. 2011;13:3932–41.
[102] Maestro A, Bonales LJ, Ritacco H, Rubio RG, Ortega F. Effect of the spreading solvent on the three-phase contact angle of microparticles attached at fluid interfaces. Phys. Chem. Chem. Phys. 2010;12:14115–20.
[103] Nonomura Y, Komura S. Surface activity of solid particles with extremely rough surfaces. J. Colloid Interface Sci. 2008;317:501–6.
[104] Maestro A, Deshmukh OS, Mugele F, Langevin D. Interfacial assembly of surfactant-decorated nanoparticles: on the rheological description of a colloidal 2D glass. Langmuir. 2015;31:6289–97.
[105] Ravera F, Ferrari M, Liggieri L, Loglio G, Santini E, Zanobini A. Liquid–liquid interfacial properties of mixed nanoparticle–surfactant systems. Colloids Surf. A Physicochem. Eng. Asp. 2008;323:99–108.
[106] Santini E, Guzmán E, Ferrari M, Liggieri L. Emulsions stabilized by the interaction of silica nanoparticles and palmitic acid at the water–hexane interface. Colloids Surf. A Physicochem. Eng. Asp. 2014;460:333–41.
[107] Zabiegaj D, Santini E, Guzmán E, Ferrari M, Liggieri L, Ravera F. Carbon soot-ionic surfactant mixed layers at water/air interfaces. J. Nanosci. Nanotechnol. 2015;15:3618–25.
[108] Vialetto J, Anyfantakis M. Exploiting additives for directing the adsorption and organization of colloid particles at fluid interfaces. Langmuir. 2021;31:9302–35.
[109] Cappelli S, de Jong AM, Baudry J, Prins MWJ. Interparticle capillary forces at a fluid–fluid interface with strong polymer-induced aging. Langmuir. 2017;33:696–705.
[110] Binks BP, Rodrigues JA, Frith WJ. Synergistic interaction in emulsions stabilized by a mixture of silica nanoparticles and cationic surfactant. Langmuir. 2007;23:3626–36.
[111] Binks BP, Isa L, Tyowua AT. Direct measurement of contact angles of silica particles in relation to double inversion of pickering emulsions. Langmuir. 2013;29:4923–7.
[112] Deleurence R, Parneix C, Monteux C. Mixtures of latex particles and the surfactant of opposite charge used as interface stabilizers – influence of particle contact angle, zeta potential, flocculation and shear energy. Soft Matter 2014;10:7088–95.
[113] Perrin L, Pajor-Swierzy A, Magdassi S, Kamyshny A, Ortega F, Rubio RG. Evaporation of nanosuspensions on substrates with different hydrophobicity. ACS Appl. Mater. Interfaces 2018;10:3082–93.
[114] Magdassi S, Grouchko M, Berezin O, Kamyshny A. Triggering the sintering of silver nanoparticles at room temperature. ACS Nano 2010;4:1943–8.
[115] Howes PD, Chandrawati R, Stevens MM. Colloidal nanoparticles as advanced biological sensors. Science. 2014;346:1247390.
[116] Zang D, Stocco A, Langevin D, Wei B, Binks BP. An ellipsometry study of silica nanoparticle layers at the water surface. Phys. Chem. Chem. Phys. 2009;11:9522–9.
[117] Reed KM, Borovicka J, Horozov TS, Paunov VN, Thompson KL, Walsh A, et al. Adsorption of sterically stabilized latex particles at liquid surfaces: effects of steric stabilizer surface coverage, particle size, and chain length on particle wettability. Langmuir. 2012;28:7291–8.
[118] Bradley LC, Chen W-H, Stebe KJ, Lee D. Janus and patchy colloids at fluid interfaces. Curr. Opin. Colloid Interface Sci. 2017;30:25–33.
[119] Fernandez-Rodriguez MA, Chen L, Deming CP, Rodriguez-Valverde MA, Chen S, Cabrerizo-Vilchez MA, et al. A simple strategy to improve the interfacial activity of true Janus gold nanoparticles: a shorter hydrophilic capping ligand. Soft Matter 2016;12:31–4.
[120] Arnaudov LN, Cayre OJ, Cohen Stuart MA, Stoyanov SD, Paunov VN. Measuring the three-phase contact angle of nanoparticles at fluid interfaces. Phys. Chem. Chem. Phys. 2010;12:328–31.
[121] Hunter TN, Jameson GJ, Wanless EJ. Determination of contact angles of nanosized silica particles by multi-angle single-wavelength ellipsometry. Austr J Chem. 2007;60:651–5.
[122] Isa L, Lucas F, Wepf R, Reimhult E. Measuring single-nanoparticle wetting properties by freeze-fracture shadow-casting cryo-scanning electron microscopy. Nature Comm. 2011;2:438.
[123] Snoeyink C, Barman S, Christopher GF. Contact angle distribution of particles at fluid interfaces. Langmuir. 2015;31:891–7.
[124] Agod A, Deák A, Hild E, Hórvölgyi Z, Kálmán E, Tolnai G, et al. Contact angle determination of nanoparticles: Real experiments and computer simulations. J. Adhes. 2004;80:1055–72.
[125] Guo Y, Tang D, Du Y, Liu B. Controlled fabrication of hexagonally close-packed Langmuir–Blodgett silica particulate monolayers from binary surfactant and solvent systems. Langmuir. 2013;29:2849–58.
[126] Grigoriev DO, Krägel J, Dutschk V, Miller R, Möhwald H. Contact angle determination of micro- and nanoparticles at fluid/fluid interfaces: the excluded area concept. Phys. Chem. Chem. Phys. 2007;9:6447–54.
[127] Grigoriev DO, Möhwald H, Shchukin DG. Theoretical evaluation of nano- or microparticulate contact angle at fluid/fluid interfaces: analysis of the excluded area behavior upon compression. Phys. Chem. Chem. Phys. 2008;10:1975–82.
[128] Clint JH, Taylor SE. Particle size and interparticle forces of overbased detergents: A Langmuir trough study. Colloids Surf. A Physicochem. Eng. Asp. 1992;65:61–7.
[129] Paunov VN, Binks BP, Ashby NP. Adsorption of charged colloid particles to charged liquid surfaces. Langmuir. 2002;18:6946–55.
[130] Aveyard R, Clint JH, Nees D, Paunov VN. Compression and structure of monolayers of charged latex particles at air/water and octane/water interfaces. Langmuir. 2000;16:1969–79.
[131] Gijsenbergh P, Pepicelli M, Wirth CL, Vermant J, Puers R. A polymer microdevice for tensiometry of insoluble components. Procedia Eng. 2014;87:80–3.
[132] Bigui W, Qing C, Caiyun Y. Wettability determined by capillary rise with pressure increase and hydrostatic effects. J. Colloid Interface Sci. 2012;376:307.

[133] Depalo A, Santomaso AC. Wetting dynamics and contact angles of powders studied through capillary rise experiments. Colloids Sur A. 2013;436:371–9.
[134] Washburn EW. The dynamics of capillary flow. Phys. Rev. 1921;17:273–83.
[135] Diggins D, Fokkink LGJ, Ralston J. The wetting of angular quartz particles: Capillary pressure and contact angles. Colloids Surf. A Physicochem. Eng. Asp. 1990;44:299–313.
[136] White LR. Capillary rise in powders. J. Colloid Interface Sci. 1982;90:536–8.
[137] Liu Z, Yu X, Wan L. Influence of contact angle on soil–water characteristic curve with modified capillary rise method. Transp. Res. Rec. 2013;2349:32–40.
[138] Yan N, Maham Y, Masliyah JH, Gray MR, Mather AE. Measurement of contact angles for fumed silica nanospheres using enthalpy of immersion data. J. Colloid Interface Sci. 2000;228:1–6.
[139] Gillies G, Büscher K, Preuss M, Kappl M, Butt H-J, Graf K. Contact angles and wetting behaviour of single micron-sized particles. J. Phys. Condens. Matter 2005;17. S445-S64.
[140] Paunov VN. Novel method for determining the three-phase contact angle of colloid particles adsorbed at air-water and oil-water interfaces. Langmuir. 2003; 19:7970–6.
[141] Paunov VN, Cayre OJ. Supraparticles and “Janus” particles fabricated by replication of particle monolayers at liquid surfaces using a gel trapping technique. Adv. Mater. 2004;16:788–91.
[142] Vogel N, Ally J, Bley K, Kappl M, Landfester K, Weiss CK. Direct visualization of the interfacial position of colloidal particles and their assemblies. Nanoscale. 2014;6:6879–85.
[143] Geisel K, Isa L, Richtering W. Unraveling the 3D localization and deformation of responsive microgels at oil/water interfaces: a step forward in understanding soft emulsion stabilizers. Langmuir. 2012;28:15770–6.
[144] Isa L. Freeze-fracture shadow-casting (FreSCA) cryo-SEM as a tool to investigate the wetting of micro- and nanoparticles at liquid-liquid interfaces. Chimia. 2013; 67:231–5.
[145] van Rijssel J, van der Linden M, Meeldijk JD, van Dijk-Moes RJA, Philipse AP, Erné BH. Spatial distribution of nanocrystals imaged at the liquid-air interface. Phys. Rev. Lett. 2013;111:108302.
[146] Lucić V, Förster F, Baumeister W. Structural studies by electron tomography: from cells to molecules. Annu. Rev. Biochem. 2005;74. 833-8sg65.
[147] Hild E, Szeszták T, Völgyes D, Hórvölgyi Z. Characterisation of silica nanoparticulate layers with scanning-angle reflectometry. Progress in Colloid and Polymer Science125. Berlin, Heidelberg, Germany: Springer; 2004. p. 61–7.
[148] Kubowicz S, Hartmann MA, Daillant J, Sanyal MK, Agrawal VV, Blot C, et al. Gold nanoparticles at the liquid–liquid interface: X-ray study and Monte Carlo simulation. Langmuir. 2009;25:952–8.
[149] Calzolari DCE, Pontoni D, Deutsch M, Reichert H, Daillant J. Nanoscale structure of surfactant-induced nanoparticle monolayers at the oil–water interface. Soft Matter 2012;8:11478–83.
[150] Lin Y, Böker A, Skaff H, Cookson D, Dinsmore AD, Emrick T, et al. Nanoparticle assembly at fluid interfaces:structure and dynamics. Langmuir. 2005;21:191–4.
[151] Smits J, Prasad Giri R, Shen C, Mendonça D, Murphy B, Huber P, et al. Assessment of nanoparticle immersion depth at liquid interfaces from chemically equivalent macroscopic surfaces. J. Colloid Interface Sci. 2022;611:670–83.
[152] Reguera J, Ponomarev E, Geue T, Stellacci F, Bresme F, Moglianetti M. Contact angle and adsorption energies of nanoparticles at the air–liquid interface determined by neutron reflectivity and molecular dynamics. Nanoscale. 2015: 5665–73.
[153] Hórvölgyi Z, Németh S, Fendler JH. Spreading of hydrophobic silica beads at water—air interfaces. Colloids Surf. A Physicochem. Eng. Asp. 1993;71:327–35.
[154] Daly R, Sader JE, Boland JJ. The dominant role of the solvent–water interface in water droplet templating of polymers. Soft Matter 2013;9:7960–5.
[155] Daly R, Sader JE, Boland JJ. Existence of micrometer-scale water droplets at solvent/air interfaces. Langmuir. 2012;28:13218–23.
[156] Mohammadi R, Amirfazli A. Contact angle measurement for dispersed microspheres using scanning confocal microscopy. J. Dispers. Sci. Technol. 2005; 25:567–74.
[157] Kelleher CP, Wang A, Guerrero-García GI, Hollingsworth AD, Guerra RE, Krishnatreya BJ, et al. Charged hydrophobic colloids at an oil–aqueous phase interface. Phys. Rev. E 2015;92:062306.
[158] Aloi A, Vilanova N, Albertazzi L, Voets IK. iPAINT: a general approach tailored to image the topology of interfaces with nanometer resolution. Nanoscale. 2016;8: 8712–6.
[159] Aloi A, Vilanova N, Isa L, de Jong AM, Voets IK. Super-resolution microscopy on single particles at fluid interfaces reveals their wetting properties and interfacial deformations. Nanoscale. 2019;11:6654–61.
[160] Hadjiiski A, Dimova R, Denkov ND, Ivanov IB, Borwankar R. Film trapping technique:precise method for three-phase contact angle determination of solid and fluid particles of micrometer size. Langmuir. 1996;12:6665–75.
[161] Horozov TS, Braz DA, Fletcher PDI, Binks BP, Clint JH. Novel film-calliper method of measuring the contact angle of colloidal particles at liquid interfaces. Langmuir. 2008;24:1678–81.
[162] Geisel K, Henzler K, Guttmann P, Richtering W. New insight into microgel-stabilized emulsions using transmission X-ray microscopy: nonuniform deformation and arrangement of microgels at liquid interfaces. Langmuir. 2015; 31:83–9.
[163] Weon BM, Lee JS, Kim JT, Pyo J, Je JH. Colloidal wettability probed with X-ray microscopy. Curr. Opin. Colloid Interface Sci. 2012;17:388–95.
[164] Squires TM, Mason TG. Fluid mechanics of microrheology. Annu. Rev. Fluid Mech. 2010;42:413–38.
[165] Watarai T, Iwai T. Experimental study on air-liquid interface effect of Brownian dynamics using spectral-domain low-coherence dynamic light scattering. Opt. Rev. 2014;21:378–81.
[166] Cheung DL. Molecular simulation of nanoparticle diffusion at fluid interfaces. Chem. Phys. Lett. 2010;495:55–9.
[167] Negishi M, Sakaue T, Yoshikawa K. Mismatch of bulk viscosity reduces interfacial diffusivity at an aqueous-oil system. Phys. Rev. E 2010;81:020901.
[168] Rezvantalab H, Drazer G, Shojaei-Zadeh S. Molecular simulation of translational and rotational diffusion of Janus nanoparticles at liquid interfaces. J. Chem. Phys. 2015;142:014701.
[169] Boniello G, Blanc C, Fedorenko D, Medfai M, Mbarek NB, In M, et al. Brownian diffusion of a partially wetted colloid. Nat. Mater. 2015;14:908–11.
[170] Boniello G, Blanc C, Fedorenko D, Medfai M, Mbarek NB, In M, et al. Brownian diffusion of a partially wetted colloid. Nat. Mater. 2015;14:908–11.
[171] Fischer TM, Dhar P, Heinig P. The viscous drag of spheres and filaments moving in membranes or monolayers. J. Fluid Mech. 2006;558:451–75.
[172] Peng Y, Chen W, Fischer TM, Weitz DA, Tong P. Short-time self-diffusion of nearly hard spheres at an oil–water interface. J. Fluid Mech. 2009;618:243–61.
[173] Wirth CL, Furst EM, Vermant J. Weak electrolyte dependence in the repulsion of colloids at an oil–water interface. Langmuir. 2014;30:2670–5.
[174] Orsi D, Guzmán E, Liggieri L, Ravera F, Ruta B, Chushkin Y, et al. 2D dynamical arrest transition in a mixed nanoparticle-phospholipid layer studied in real and momentum spaces. Sci. Rep. 2015;5:17930.
[175] Mazoyer S, Ebert F, Maret G, Keim P. Dynamics of particles and cages in an experimental 2D glass former. Eur Phys Lett. 2009;88:66004.
[176] Mazoyer S, Ebert F, Maret G, Keim P. Correlation between dynamical heterogeneities, structure and potential-energy distribution in a 2D amorphous solid. Eur. Phys J E. 2011;34:101.
[177] Morse DC. Theory of constrained Brownian motion. In: Rice SA, editor. Advances in chemical physics. Hoboken, NJ, U.S.A: John Wiley & Sons; 2004.
[178] Galvan-Miyoshi J, Delgado J, Castillo R. Diffusing wave spectroscopy in Maxwellian fluids. Eur. Phys J E. 2008;26:369–77.
[179] Keim P, Maret G, Herz U, von Grünberg HH. Harmonic lattice behavior of two-dimensional colloidal crystals. Phys. Rev. Lett. 2004;21:215504.
[180] Prasad V, Weeks ER. Two-dimensional to three-dimensional transition in soap films demonstrated by microrheology. Phys. Rev. Lett. 2009;102:178302.
[181] Shlomovitz R, Evans AA, Boatwright T, Dennin M, Levine AJ. Measurement of monolayer viscosity using noncontact microrheology. Phys. Rev. Lett. 2013;110: 137802.
[182] Maestro A, Jones D, de Rojas Sánchez, Candela C, Guzman E, Duits MHG, et al. Tuning interfacial properties and processes by controlling the rheology and structure of poly(N-isopropylacrylamide) particles at air/water interfaces. Langmuir. 2018;34:7067–76.
[183] Tajuelo J, Guzmán E, Ortega F, Rubio RG, Rubio MA. Phase diagram of fatty acid langmuir monolayers from rheological measurements. Langmuir. 2017;33: 4280–90.
[184] Tajuelo J, Rubio MA. A magnetic rod interfacial shear rheometer driven by a mobile magnetic trap. J. Rheol. 2016;60:1095.
[185] Wang X, In M, Blanc C, Nobili M, Stocco A. Enhanced active motion of Janus colloids at the water surface. Soft Matter 2015;11:7376–84.
[186] Kralchevsky PA, Nagayama K. Capillary interactions between particles bound to interfaces, liquid films and biomembranes. Adv. Colloid Interf. Sci. 2000;85: 145–92.
[187] Loudet JC, Alsayed AM, Zhang J, Yodh AG. Capillary interactions between anisotropic colloidal particles. Phys. Rev. Lett. 2005;94:018301.
[188] Botto L, Lewandowski EP, Cavallaro M, Stebe KJ. Capillary interactions between anisotropic particles. Soft Matter 2012;8:9957–71.
[189] Aveyard R, Binks BP, Clint JH, Fletcher PDI, Horozov TS, Neumann B, et al. Measurement of long-range repulsive forces between charged particles at an oil-water interface. Phys. Rev. Lett. 2002;88:246102.
[190] Park BJ, Furst EM. Attractive interactions between colloids at the oil–water interface. Soft Matter 2011;7:7676–82.
[191] Masschaele K, Park BJ, Furst EM, Fransaer J, Vermant J. Finite ion-size effects dominate the interaction between charged colloidal particles at an oil-water interface. Phys. Rev. Lett. 2010;105:048303.
[192] Lee D-G, Cicuta P, Vella D. Self-assembly of repulsive interfacial particles via collective sinking. Soft Matter 2017;13:212–21.
[193] Xia Y, Gates B, Yin Y, Lu Y. Monodispersed colloidal spheres: old materials with new applications. Adv. Mater. 2000;12:693–713.
[194] Williams DF, Berg JC. The aggregation of colloidal particles at the air—water interface. J. Colloid Interface Sci. 1992;152:218–29.
[195] Dias CS, Yunker PJ, Yodh AG, Araújo NAM, Gama MmTd. Interaction anisotropy and the KPZ to KPZQ transition in particle deposition at the edges of drying drops. Soft Matter 2018;14:1903–7.
[196] Yunker PJ, Lohr MA, Still T, Borodin A, Durian DJ, Yodh AG. Effects of particle shape on growth dynamics at edges of evaporating drops of colloidal suspensions. Phys. Rev. Lett. 2013;110:035501.
[197] Dias CS, Araújo NAM, Gama MmTd. Kinetic roughening of aggregates of patchy colloids with strong and weak bonds. Eur Phys Lett. 2014;107:56002.
[198] Israelachvili JN. Intermolecular and surfaces forces. Amsterdam, The Netherlands: Elsevier; 2011.
[199] Dias CS, Araújo NAM, Telo da Gama MM. Adsorbed films of three-patch colloids: Continuous and discontinuous transitions between thick and thin films. Phys. Rev. E 2014;90:032302.
[200] Hurd AJ. The electrostatic interaction between interfacial colloidal particles. J. Phys. A 1985;18. L1055-L60.

[201] Bleibel J, Domínguez A, Oettel M. Colloidal particles at fluid interfaces: Effective interactions, dynamics and a gravitation–like instability. Eur Phys J Special Topics. 2013;222:3071–87.
[202] Frydel D, Dietrich S, Oettel M. Charge renormalization for effective interactions of colloids at water interfaces. Phys. Rev. Lett. 2007;99:118302.
[203] Kralchevsky PA, Denkov ND, Danov KD. Particles with an undulated contact line at a fluid interface:interaction between capillary quadrupoles and rheology of particulate monolayers. Langmuir. 2001;17:7694–705.
[204] EAV Nierop, Stijnman MA, Hilgenfeldt S. Shape-induced capillary interactions of colloidal particles. Eur Phys Lett. 2005;72:671–7.
[205] Bowden N, Terfort A, Carbeck J, Whitesides GM. Self-assembly of mesoscale objects into ordered two-dimensional arrays. Science. 1997;276:233–5.
[206] Gennes Pgd, Brochard-Wyart F, Quere D. Capillarity and Wetting Phenomena: Drops, Bubbles, Pearls, Waves. New York, NY, USA: Springer Verlag; 2003.
[207] Stamou D, Duschl C, Johannsmann D. Long-range attraction between colloidal spheres at the air-water interface: The consequence of an irregular meniscus. Phys. Rev. E 2000;62:5263–72.
[208] Grzelczak M, Vermant J, Furst EM, Liz-Marzán LM. Directed self-assembly of nanoparticles. ACS Nano 2010;4:3591–605.
[209] Vandewalle N, Obara N, Lumay G. Mesoscale structures from magnetocapillary self-assembly. Eur. Phys J E. 2013;36:127.
[210] Berke AP, Turner L, Berg HC, Lauga E. Hydrodynamic attraction of swimming microorganisms by surfaces. Phys. Rev. Lett. 2008;101:038102.
[211] Martínez-Pedrero F, González-Banciella A, Camino A, Mateos-Maroto A, Ortega F, Rubio RG, et al. Static and dynamic self-assembly of pearl-like-chains of magnetic colloids confined at fluid interfaces. Small. 2021;17:2101188.
[212] Lauga E, DiLuzio WR, Whitesides GM, Stone HA. Swimming in circles: motion of bacteria near solid boundaries. Biophys. J. 2006;90:400–12.
[213] Sing CE, Schmid L, Schneider MF, Franke T, Alexander-Katz A. Controlled surface-induced flows from the motion of self-assembled colloidal walkers. Proc. Natl. Acad. Sci. 2010;107:535–40.
[214] Grzybowski BA, Stone HA, Whitesides GM. Dynamic self-assembly of magnetized, millimetre-sized objects rotating at a liquid–air interface. Nature. 2000;405:1033–6.
[215] Dörr A, Hardt S, Masoud H, Stone HA. Drag and diffusion coefficients of a spherical particle attached to a fluid–fluid interface. J. Fluid Mech. 2016;790:607–18.
[216] Erni P. Deformation modes of complex fluid interfaces. Soft Matter 2011;7:7586–600.
[217] Maestro A, Zaccone A. Nonaffine deformation and tunable yielding of colloidal assemblies at the air–water interface. Nanoscale. 2017;9:18343–51.
[218] Martínez-Pedrero F, Benet J, Rubio JEF, Sanz E, Rubio RG, Ortega F. Field-induced sublimation in perfect two-dimensional colloidal crystals. Phys. Rev. E 2014;89:012306.
[219] Chen W, Tan S, Zhou Y, Ng TK, Ford WT, Tong P. Attraction between weakly charged silica spheres at a water-air interface induced by surface-charge heterogeneity. Phys. Rev. E 2009;79:041403.
[220] Li-Destri G, Ruffino R, Tuccitto N, Marletta G. In situ structure and force characterization of 2D nano-colloids at the air/water interface. Soft Matter 2019;15:8475–82.
[221] Zang DY, Stocco A, Langevin D, Wei BB, Binks BP. An ellipsometry study of silica nanoparticle layers at the water surface. PhysChem Chem Phys. 2009;11:9522–9.
[222] Bonales LJ, Rubio JEF, Ritacco H, Vega C, Rubio RG, Ortega F. Freezing transition and interaction potential in monolayers of microparticles at fluid interfaces. Langmuir. 2011;27:3391–400.
[223] Parolini L, Law AD, Maestro A, Buzza DMA, Cicuta P. Interaction between colloidal particles on an oil–water interface in dilute and dense phases. J. Phys. Condens. Matter 2015;27:194119.
[224] Kosterlitz JM, Thouless DJ. Long range order and metastability in two dimensional solids and superfluids. (Application of dislocation theory). J. Phys. C Solid State Phys. 1972;5. L124-L6.
[225] Bonales LJ, Martínez-Pedrero F, Rubio MA, Rubio RG, Ortega F. Phase behavior of dense colloidal binary monolayers. Langmuir. 2012;28:16555–66.
[226] Rahman SE, Laal-Dehghani N, Barman S, Christopher GF. Modifying interfacial interparticle forces to alter microstructure and viscoelasticity of densely packed particle laden interfaces. J. Colloid Interface Sci. 2019;536:30–41.
[227] Reynaert S, Moldenaers P, Vermant J. Control over colloidal aggregation in monolayers of latex particles at the oil−water interface. Langmuir. 2006;22:4936–45.
[228] Firouzi D, Russel MK, Rizvi SN, Ching CY, Selvaganapathy PR. Development of flexible particle-laden elastomeric textiles with improved penetration resistance to hypodermic needles. Mat Des. 2018;156:419–28.
[229] Guzmán E, Fernández-Peña L, Akanno A, Llamas S, Ortega F, Rubio G. Two different scenarios for the equilibration of polycation—anionic solutions at water–vapor interfaces. Coatings. 2019;9:438.
[230] Whitby CP, Wanless EJ. Controlling pickering emulsion destabilisation: a route to fabricating new materials by phase inversion. Materials. 2016;9:626.
[231] Shen AQ, Gleason B, McKinley GH, Stone HA. Fiber coating with surfactant solutions. Phys. Fluids 2002;14:4055–68.
[232] Scheid B, Delacotte J, Dollet B, Rio E, Restagno F, Von Nierop E, et al. The role of surface rheology in liquid film formation. Europhys. Lett. 2010;90:24002.
[233] Levich VG. Physicochemical Hydrodynamics. Harlow, UK: Longman Higher Education; 1963.
[234] Perrin L, Akanno A, Guzman E, Ortega F, Rubio RG. Pattern formation upon evaporation of sessile droplets of polyelectrolyte/surfactant mixtures on silicon wafers. Int. J. Mol. Sci. 2021;22:7953.
[235] Langevin D. Influence of interfacial rheology on foam and emulsion properties. Adv. Colloid Interf. Sci. 2000;88:209–22.
[236] Stocco A, Rio E, Binks BP, Langevin D. Aqueous foams stabilized solely by particles. Soft Matter 2011;7:1260–7.
[237] Stocco A, Drenckhan W, Rio E, Langevin D, Binks BP. Particle-stabilised foams: an interfacial study. Soft Matter 2009;5:2215–22.
[238] Stancik EJ, Kouhkan M, Fuller GG. Coalescence of Particle-Laden Fluid Interfaces. Langmuir. 2004;20:90–4.
[239] Leal-Calderón LG. Flow induced coalescence of drops in a viscous fluid. Phys. Fluids 2004;16:1833–51.
[240] Guzmán E, Llamas S, Maestro A, Fernández-Peña L, Akanno A, Miller R, et al. Polymer–surfactant systems in bulk and at fluid interfaces. Adv. Colloid Interf. Sci. 2016;233:38–64.
[241] Guzman E, Liggieri L, Santini E, Ferrari M, Ravera F. Mixed DPPC-cholesterol Langmuir monolayers in presence of hydrophilic silica nanoparticles. Colloids Surf B. 2013;105:284–93.
[242] Guzman E, Liggieri L, Santini E, Ferrari M, Ravera F. Influence of silica nanoparticles on dilational rheology of DPPC-palmitic acid Langmuir monolayers. Soft Matter 2012;8:3938–48.
[243] Tambe DE, Sharma MM. The effect of colloidal particles on fluid-fluid interfacial properties and emulsion stability. Adv. Colloid Interf. Sci. 1994;52:1–63.
[244] Fuller GG, Vermant J. Complex fluid-fluid interfaces: rheology and structure. Ann. Rev. Chem. Biomol. Eng. 2012;3:519–43.
[245] Noskov BA. Fast adsorption at the liquid-gas interface. Adv. Colloid Interf. Sci. 1996;69:63–129.
[246] Maestro A, Guzmán E, Chuliá R, Ortega F, Rubio RG, Miller R. Fluid to soft-glass transition in a quasi-2D system: thermodynamic and rheological evidences for a Langmuir monolayer. Phys. Chem. Chem. Phys. 2011;13:9534–9.
[247] Beltramo PJ, Gupta M, Alicke A, Liascukiene I, Gunes DZ, Baroud CN, et al. Arresting dissolution by interfacial rheology design. Proc. Natl. Acad. Sci. U. S. A. 2017;114:10373–8.
[248] Kotsmar C, Pradines V, Alahverdjieva VS, Aksenenko EV, Fainerman VB, Kovalchuk VI, et al. Thermodynamics, adsorption kinetics and rheology of mixed protein–surfactant interfacial layers. Adv. Colloid Interf. Sci. 2009;150:41–54.
[249] Safouane M, Langevin D, Binks BP. Effect of particle hydrophobicity on the properties of silica particle layers at the air-water interface. Langmuir. 2007;23:11546–53.
[250] Zahn K, Wille A, Maret G, Sengupta S, Nielaba P. Elastic properties of 2D colloidal crystals from video microscopy. Phys. Rev. Lett. 2003;90:155506.
[251] Kirby SM, Anna SL, Walker LM. Effect of surfactant tail length and ionic strength on the interfacial properties of nanoparticle–surfactant complexes. Soft Matter 2018;14:112–23.
[252] Zang DY, Rio E, Langevin D, Wei B, Binks BP. Viscoelastic properties of silica nanoparticle monolayers at the air-water interface. Eur. Phys J E. 2010;31:125–34.
[253] Kobayashi T, Kawaguchi M. Surface dilational moduli of latex-particle monolayers spread at air–water interface. J. Colloid Interface Sci. 2013;390:147–50.
[254] Bykov AG, Noskov BA, Loglio G, Lyadinskaya VV, Miller R. Dilational surface elasticity of spread monolayers of polystyrene microparticles. Soft Matter 2014;10:6499–505.
[255] del Río OI, Kwok DY, Wu R, Alvarez JM, Neumann AW. Contact angle measurements by axisymmetric drop shape analysis and an automated polynomial fit program. Colloids Surf. A Physicochem. Eng. Asp. 1998;143:197–210.
[256] Bykov AG, Loglio G, Miller R, Noskov BA. Dilational surface elasticity of monolayers of charged polystyrene nano- and microparticles at liquid/fluid interfaces. Colloids Surf. A Physicochem. Eng. Asp. 2015;485:42–8.
[257] Vella D, Aussillous P, Mahadevan L. Elasticity of an interfacial particle raft. Europhys. Lett. 2004;68:212–8.
[258] Hilles H, Monroy F, Bonales LJ, Ortega F, Rubio RG. Fourier-transform rheology of polymer Langmuir monolayers: Analysis of the non-linear and plastic behaviors. Adv. Colloid Interf. Sci. 2006;122:67–77.
[259] Langevin D. Light Scattering by Liquid Surfaces and Complementary Techniques. New York, N.Y., U.S.A.: Marcel Dekker, Inc.; 1992.
[260] Gray JJ, Bonnecaze RT. Rheology and dynamics of sheared arrays of colloidal particles. J. Rheol. 1998;42:1121–51.
[261] Trappe V, Weitz DA. Scaling of the viscoelasticity of weakly attractive particles. Phys. Rev. Lett. 2000;85:449–53.
[262] Cicuta P, Stancik EJ, Fuller GG. Shearing or compressing a soft glass in 2D: Time-concentration superposition. Phys. Rev. Lett. 2003;90:236101.
[263] Yu K, Zhang H, Biggs S, Xu Z, Cayre OJ, Harbottle D. The rheology of polyvinylpyrrolidone-coated silica nanoparticles positioned at an air-aqueous interface. J. Colloid Interface Sci. 2018;527:346–55.
[264] Imperiali L, Liao K-H, Clasen C, Fransaer J, Macosko CW, Vermant J. Interfacial rheology and structure of tiled graphene oxide sheets. Langmuir. 2012;28:7990–8000.
[265] Barman S, Christopher GF. Simultaneous interfacial rheology and microstructure measurement of densely aggregated particle laden interfaces using a modified double wall ring interfacial rheometer. Langmuir. 2014;30:9752–60.
[266] Barman S, Christopher GF. Role of capillarity and microstructure on interfacial viscoelasticity of particle laden interfaces. J. Rheol. 2015;60:35–45.
[267] Reynaert S, Moldenaers P, Vermant J. Interfacial rheology of stable and weakly aggregated two-dimensional suspensions. Phys. Chem. Chem. Phys. 2007;9:6463–75.

[268] Wijmans CM, Dickinson E. Simulation of interfacial shear and dilatational rheology of an adsorbed protein monolayer modeled as a network of spherical particles. Langmuir. 1998;14:7278–86.
[269] Muntz I, Thijssenar JHJ. Interfacial Shear Rheology without an Interfacial Geometry. 2020.
[270] Wilson HJ, Davis RH. Shear stress of a monolayer of rough spheres. J. Fluid Mech. 2002;452:425–41.
[271] Brown E, Zhang H, Forman NA, Maynor BW, Betts DE, DeSimone JM, et al. Shear thickening and jamming in densely packed suspensions of different particle shapes. Phys. Rev. E 2011;84:031408.
[272] San-Miguel A, Behrens SH. Influence of Nanoscale Particle Roughness on the Stability of Pickering Emulsions. Langmuir. 2012;28:12038–43.
[273] Zanini M, Marschelke C, Anachkov SE, Marini E, Synytska A, Isa L. Universal emulsion stabilization from the arrested adsorption of rough particles at liquid-liquid interfaces. Nat. Commun. 2017;8:15701.
[274] Zang D, Langevin D, Binks BP, Wei B. Shearing particle monolayers: Strain-rate frequency superposition. Phys. Rev. E 2010;81:011604.
[275] Cheng H-L, Velankar SS. Controlled jamming of particle-laden interfaces using a spinning drop tensiometer. Langmuir. 2009;25:4412–20.
[276] Vandebril S, Vermant J, Moldenaers P. Efficiently suppressing coalescence in polymer blends using nanoparticles: role of interfacial rheology. Soft Matter 2010;6:3353–62.
[277] Krishnaswamy R, Majumdar S, Ganapathy R, Agarwal VV, Sood AK, Rao CNR. Interfacial rheology of an ultrathin nanocrystalline film formed at the liquid/liquid interface. Langmuir. 2007;23:3084–7.
[278] Orsi D, Baldi G, Cicuta P, Cristofolini L. On the relation between hierarchical morphology and mechanical properties of a colloidal 2D gel system. Colloids Surf. A Physicochem. Eng. Asp. 2012;413:71–7.
[279] Erni P, Jerri HA, Wong K, Parker A. Interfacial viscoelasticity controls buckling, wrinkling and arrest in emulsion drops undergoing mass transfer. Soft Matter 2012;8:6958–67.
[280] Binks BP. Particles as surfactants—similarities and differences. Curr. Opin. Colloid Interface Sci. 2002;7:21–41.
[281] Leahy BD, Pocivavsek L, Meron M, Lam KL, Salas D, Viccaro PJ, et al. Geometric stability and elastic response of a supported nanoparticle film. Phys. Rev. Lett. 2010;105:058301.
[282] Kassuga TD, Rothstein JP. Buckling of particle-laden interfaces. J. Colloid Interface Sci. 2015;448:287–96.
[283] Basavaraj MG, Fuller GG, Fransaer J, Vermant J. Packing, flipping, and buckling transitions in compressed monolayers of ellipsoidal latex particles. Langmuir. 2006;22:6605–12.
[284] Razavi S, Cao KD, Lin B, Lee KYC, Tu RS, Kretzschmar I. Collapse of particle-laden interfaces under compression: buckling vs particle expulsion. Langmuir. 2015;31:7764–75.
[285] Park BJ, Lee D. Particles at fluid–fluid interfaces: From single-particle behavior to hierarchical assembly of materials. MRS Bull. 2014;39:1089–98.
[286] Kumar A, Park BJ, Tu F, Lee D. Amphiphilic Janus particles at fluid interfaces. Soft Matter 2013;9:6604–17.
[287] Brown ABD, Smith CG, Rennie AR. Fabricating colloidal particles with photolithography and their interactions at an air-water interface. Phys. Rev. E 2000;62:951–60.
[288] Bowden N, Arias F, Deng T, Whitesides GM. Self-assembly of microscale objects at a liquid/liquid interface through lateral capillary forces. Langmuir. 2001;17:1757–65.
[289] Madivala B, Fransaer J, Vermant J. Self-assembly and rheology of ellipsoidal particles at interfaces. Langmuir. 2009;25:2718–28.
[290] Lewandowski EP, Cavallaro M, Botto L, Bernate JC, Garbin V, Stebe KJ. Orientation and self-assembly of cylindrical particles by anisotropic capillary interactions. Langmuir. 2010;26:15142–54.
[291] Bradley LC, Chen W-H, Lee D. Anisotropic particles at fluid-fluid interfaces (experiment). In: Wu N, Lee D, Striolo A, editors. Anisotropic Particle Assemblies. Amsterdam, The Netherlands: Elsevier; 2018. p. 201–31.
[292] Botto L, Yao L, Leheny RL, Stebe KJ. Capillary bond between rod-like particles and the micromechanics of particle-laden interfaces. Soft Matter 2012;8:4971.
[293] Kim F, Kwan S, Akana J, Yang P. Langmuir-Blodgett Nanorod Assembly. J. Am. Chem. Soc. 2001;123:4360–1.
[294] Hernández-López JL, Alvizo-Páez ER, Moya SE, Ruiz-García J. Trapping, pattern formation, and ordering of polyelectrolyte/single-wall carbon nanotube complexes at the air/water and air/solid interfaces. J. Phys. Chem. B 2006;110:23179–91.
[295] Stancik EJ, Widenbrant MJO, Laschitsch AT, Vermant J, Fuller GG. Structure and dynamics of particle monolayers at a liquid-liquid interface subjected to extensional flow. Langmuir. 2002;18:4372–5.
[296] Cui Z. Weakly sheared active suspensions: Hydrodynamics, stability, and rheology. Phys. Rev. E 2011;83:031911.
[297] de Gennes PG. Soft matter. Rev. Mod. Phys. 1992;64:645–8.
[298] Park BJ, Brugarolas T, Lee D. Janus particles at an oil–water interface. Soft Matter 2011;7:6413–7.
[299] Jiang S, Granick S. Janus balance of amphiphilic colloidal particles. J. Chem. Phys. 2007;127:161102.
[300] Aveyard R. Can Janus particles give thermodynamically stable Pickering emulsions? Soft Matter 2012;8:5233–40.
[301] Ondarçuhu T, Fabre P, Raphaël E, Veyssié M. Specific properties of amphiphilic particles at fluid interfaces. J Phys France. 1990;51:1527–36.
[302] Razavi S, Lin B, Lee KYC, Tu RS, Kretzschmar I. Impact of surface amphiphilicity on the interfacial behavior of Janus particle layers under compression. Langmuir. 2019;35:15813–24.
[303] Park BJ, Choi C-H, Kang S-M, Tettey KE, Lee C-S, Lee D. Geometrically and chemically anisotropic particles at an oil–water interface. Soft Matter 2013;9:3383–8.
[304] Cheung DL, Bon SAF. Stability of Janus nanoparticles at fluid interfaces. Soft Matter 2009;3969-76.
[305] Isa L, Samudrala N, Dufresne ER. Adsorption of sub-micron amphiphilic dumbbells to fluid interfaces. Langmuir. 2014;30:5057.
[306] Rezvantalab H, Shojaei-Zadeh S. Designing patchy particles for optimum interfacial activity. Phys. Chem. Chem. Phys. 2014;16:8283–93.
[307] Kadam R, Zilli M, Maas M, Rezwan K. Nanoscale Janus particles with dual protein functionalization. Part. Part. Syst. Charact. 2018;35:1700332.
[308] Fernández-Rodríguez MÁ, Rahmani S, Yu CKJ, Rodríguez-Valverde MÁ, Cabrerizo-Vílchez MÁ, Michel CA, et al. Synthesis and interfacial activity of PMMA/PtBMA Janus and homogeneous nanoparticles at water/oil interfaces. Colloids Surf. A Physicochem. Eng. Asp. 2018;536:259–65.
[309] Yin T, Yang Z, Dong Z, Lin M, Zhang J. Physicochemical properties and potential applications of silica-based amphiphilic Janus nanosheets for enhanced oil recovery. Fuel. 2019;237:344–51.
[310] Rezvantalab H, Connington KW, Shojaei-Zadeh S. Shear-induced interfacial assembly of Janus particles. Phys Rev Fluids. 2016;1:074205.
[311] Rezvantalab H, Shojaei-Zadeh S. Tilting and tumbling of janus nanoparticles at sheared interfaces. ACS Nano 2016;10:5354–61.
[312] Paiva FL, Hore MJA, Secchi A, Calado V, Maia J, Khani S. Dynamic Interfacial Trapping of Janus Nanorod Aggregates. Langmuir. 2020;36:4184–93.
[313] Wang H, Yang X, Fu Z, Zhao X, Li Y, Li J. Rheology of nanosilica-compatibilized immiscible polymer blends: formation of a “heterogeneous network” facilitated by interfacially anchored hybrid nanosilica. Macromolecules. 2017;50:9494–506.
[314] Senff H, Richtering W. Influence of cross-link density on rheological properties of temperature-sensitive microgel suspensions. Colloid Polym. Sci. 2000;278:830–40.
[315] Guan Y, Zhang Y. PNIPAM microgels for biomedical applications: from dispersed particles to 3D assemblies. Soft Matter 2011;7:6375–84.
[316] Schwall CT, Banerjee IA. Micro- and nanoscale hydrogel systems for drug delivery and tissue engineering. Materials (Basel). 2009;2:577–612.
[317] Debord JD, Lyon LA. Synthesis and characterization of pH-responsive copolymer microgels with tunable volume phase transition temperatures. Langmuir. 2003;19:7662–4.
[318] Style RW, Isa L, Dufresne ER. Adsorption of soft particles at fluid interfaces. Soft Matter 2015;11:7412–9.
[319] Butt H-J. Capillary Forces:Influence of Roughness and Heterogeneity. Langmuir. 2008;24:4715–21.
[320] Brugger B, Vermant J, Richtering W. Interfacial layers of stimuli-responsive poly-(N-isopropylacrylamideco-methacrylicacid) (PNIPAM-co-MAA) microgels characterized by interfacial rheology and compression isotherms. Phys. Chem. Chem. Phys. 2010;12:14573–8.
[321] Garbin V, Jenkins I, Sinno T, Crocker JC, Stebe KJ. Interactions and Stress Relaxation in Monolayers of Soft Nanoparticles at Fluid-Fluid Interfaces. Phys. Rev. Lett. 2015;114:108301.
[322] Schmidt S, Liu T, Rütten S, Phan KH, Möller M, Richtering W. Influence of microgel architecture and oil polarity on stabilization of emulsions by stimuli-sensitive core-shell poly(N-isopropylacrylamide-co-methacrylic acid) microgels: Mickering versus Pickering behavior? Langmuir. 2011;27:9801–6.
[323] Destribats M, Lapeyre V, Wolfs M, Sellier E, Leal-Calderon F, Ravaine V, et al. Soft microgels as Pickering emulsion stabilisers: role of particle deformability. Soft Matter 2011;7:7689–98.
[324] Scheidegger L, Fernández-Rodríguez MÁ, Geisel K, Zanini M, Elnathan R, Richtering W, et al. Compression and deposition of microgel monolayers from fluid interfaces: particle size effects on interface microstructure and nanolithography. Phys. Chem. Chem. Phys. 2017;19:8671–80.
[325] Plamper FA, Richtering W. Functional microgels and microgel systems. Acc. Chem. Res. 2017;50:131–40.
[326] Bochenek S, Scotti A, Richtering W. Temperature-sensitive soft microgels at interfaces: air–water versus oil–water. Soft Matter 2021;17:976–88.
[327] Pinaud F, Geisel K, Massé P, Catargi B, Isa L, Richtering W, et al. Adsorption of microgels at an oil–water interface: correlation between packing and 2D elasticity. Soft Matter 2014;10:6963–74.
[328] Brugger B, Rosen BA, Richtering W. Microgels as stimuli-responsive stabilizers for emulsions. Langmuir. 2008;24:12202–8.
[329] Geisel K, Isa L, Richtering W. The compressibility of pH-sensitive microgels at the oil–water interface: higher charge leads to less repulsion. Angew. Chem. Int. Ed. 2014;53:4905–9.
[330] Rey M, Hou X, Tang JSJ, Vogel N. Interfacial arrangement and phase transitions of PNiPAm microgels with different crosslinking densities. Soft Matter 2017;13:8717–27.
[331] Vialetto J, Nussbaum N, Bergfreund J, Fischer P, Isa L. Influence of the interfacial tension on the microstructural and mechanical properties of microgels at fluid interfaces. J. Colloid Interface Sci. 2022;608:2584–92.
[332] Brugger B, Richtering W. Emulsions stabilized by stimuli-sensitive poly(n-isopropylacrylamide)-co-methacrylic acid polymers: microgels versus low molecular weight polymers. Langmuir. 2008;24:7769–77.
[333] Cohin Y, Fisson M, Jourde K, Fuller GG, Sanson N, Talini L, et al. Tracking the interfacial dynamics of PNiPAM soft microgels particles adsorbed at the air-water interface and in thin liquid films. Rheol. Acta 2013;52:445–54.

[334] Murray BS. Microgels at fluid-fluid interfaces for food and drinks. Adv. Colloid Interf. Sci. 2019;271:101990.
[335] Rey M, Fernández-Rodríguez MÁ, Steinacher M, Scheidegger L, Geisel K, Richtering W, et al. Isostructural solid–solid phase transition in monolayers of soft core–shell particles at fluid interfaces: structure and mechanics. Soft Matter 2016; 12:3545–57.
[336] Cohin Y, Fisson M, Jourde K, Fuller GG, Sanson N, Talini L, et al. Tracking the interfacial dynamics of PNiPAM soft microgels particles adsorbed at the air–water interface and in thin liquid films. Rheol. Acta 2013;52:445–54.
[337] Huang S, Gawlitza K, von Klitzing R, Steffen W, Auernhammer GK. Structure and rheology of microgel monolayers at the water/oil interface. Macromolecules. 2017;50:3680–9.
[338] Anyfantakis M, Geng Z, Morel M, Rudiuk S, Baigl D. Modulation of the coffee-ring effect in particle/surfactant mixtures: the importance of particle–interface interactions. Langmuir. 2015;31:4113–20.
[339] Fujii S, Ryan AJ, Armes SP. Long-range structural order, moiré patterns, and iridescence in latex-stabilized foams. J. Am. Chem. Soc. 2006;128:7882–6.
[340] Velikov KP, Durst F, Velev OD. Direct observation of the dynamics of latex particles confined inside thinning water−air films. Langmuir. 1998;14:1148–55.
[341] Bykov AG, Noskov BA, Loglio G, Lyadinskaya VV, Miller R. Dilational surface elasticity of spread monolayers of polystyrene microparticles. Soft Matter 2014; 10:6499–505.
[342] Costa L, Li-Destri G, Thomson NH, Konovalov O, Pontoni D. Real space imaging of nanoparticle assembly at liquid–liquid interfaces with nanoscale resolution. Nano Lett. 2016;16:5463–8.
[343] Anyfantakis M, Vialetto J, Best A, Auernhammer GK, Butt H-J, Binks BP, et al. Adsorption and crystallization of particles at the air–water interface induced by minute amounts of surfactant. Langmuir. 2018;34:15526–36.
[344] Vialetto J, Rudiuk S, Morel M, Baigl D. From bulk crystallization of inorganic nanoparticles at the air/water interface: tunable organization and intense structural colors. Nanoscale. 2020;12:6279–84.
[345] Li C, Xu Y, Li X, Ye Z, Yao C, Chen Q, et al. Unexpected Dual Action of Cetyltrimethylammonium Bromide (CTAB) in the self-assembly of colloidal nanoparticles at liquid–liquid interfaces. Adv. Mater. Interfaces 2020;7:2000391.
[346] Park Y-K, Yoo S-H, Park S. Assembly of highly ordered nanoparticle monolayers at a water/hexane interface. Langmuir. 2007;23:10505–10.
[347] Kim JY, Kwon SJ, Chang J-B, Ross CA, Hatton TA, Stellacci F. Two-dimensional nanoparticle supracrystals: a model system for two-dimensional melting. Nano Lett. 2016;16:1352–8.
[348] Isa L, Calzolari DCE, Pontoni D, Gillich T, Nelson A, Zirbs R, et al. Core–shell nanoparticle monolayers at planar liquid–liquid interfaces: effects of polymer architecture on the interface microstructure. Soft Matter 2013;9:3789–97.
[349] Whitby CP, Fornasiero D, Ralston J, Liggieri L, Ravera F. Properties of fatty amine–silica nanoparticle interfacial layers at the hexane–water interface. J. Phys. Chem. C 2012;116:3050–8.
[350] Da C, Zhang X, Alzobaidi S, Hu D, Wu P, Johnston KP. Tuning surface chemistry and ionic strength to control nanoparticle adsorption and elastic dilational modulus at air-brine interface. Langmuir. 2021;37:5795–809.
[351] Huerre A, Cacho-Nerin F, Poulichet V, Udoh CE, De Corato M, Garbin V. Dynamic organization of ligand-grafted nanoparticles during adsorption and surface compression at fluid–fluid interfaces. Langmuir. 2018;34:1020–8.
[352] Orsi D, Cristofolini L, Baldi G, Madsen A. Heterogeneous and anisotropic dynamics of a 2D Gel. Phys. Rev. Lett. 2012;108:105701.
[353] Sollich P, Lequeux F, Hébraud P, Cates ME. Rheology of soft glassy materials. Phys. Rev. Lett. 1997;78:2020–3.
[354] Wyss HM, Miyazaki K, Mattsson J, Hu Z, Reichman DR, Weitz DA. Strain-rate frequency superposition: a rheological probe of structural relaxation in soft materials. Phys. Rev. Lett. 2007;98:238303.
[355] Maas M, Ooi CC, Fuller GG. Thin film formation of silica nanoparticle/lipid composite films at the fluid-fluid interface. Langmuir. 2010;26:17867–73.
[356] Feynman R. Infinitesimal machinery. J. Microelectromech. Syst. 1993;2:4–14.
[357] Purcell EM. Life at low Reynolds number. Am. J. Phys. 1977;45:3–11.
[358] Xu H, Medina-Sánchez M, Magdanz V, Schwarz L, Hebenstreit F, Schmidt OG. Sperm-hybrid micromotor for targeted drug delivery. ACS Nano 2018;12:327–37.
[359] Tokarev A, Gu Y, Zakharchenko A, Trotsenko O, Luzinov I, Kornev KG, et al. Reconfigurable anisotropic coatings via magnetic field-directed assembly and translocation of locking magnetic chains. Adv. Funct. Mater. 2014;24:4738–45.
[360] Rosensweig RE. Ferrohydrodynamics: Dover Publications. 2013.
[361] Martinez-Pedrero F, Massana-Cid H, Tierno P. Assembly and transport of microscopic cargos via reconfigurable photoactivated magnetic microdockers. Small. 2017;13:1603449.
[362] Di Leonardo R, Dell'Arciprete D, Angelani L, Iebba V. Swimming with an image. Phys. Rev. Lett. 2011;106:038101.
[363] Martinez-Pedrero F, Ortiz-Ambriz A, Pagonabarraga I, Tierno P. Colloidal microworms propelling via a cooperative hydrodynamic conveyor Belt. Phys. Rev. Lett. 2015;115:138301.
[364] Cappelli S, Xie Q, Harting J, de Jong AM, Prins MWJ. Dynamic wetting: status and prospective of single particle based experiments and simulations. New Biotechnol. 2015;32:420–32.
[365] Snezhko A, Aranson IS. Magnetic manipulation of self-assembled colloidal asters. Nature Mat. 2011;10:698–703.
[366] Zahn K, Maret G. Dynamic criteria for melting in two dimensions. Phys. Rev. Lett. 2000;85:3656–9.
[367] Grosjean G, Hubert M, Collard Y, Pillitteri S, Vandewalle N. Surface swimmers, harnessing the interface to self-propel. Eur. Phys J E. 2018;41:137.
[368] Melle S, Lask M, Fuller GG. Pickering emulsions with controllable stability. Langmuir. 2005;21:2158–62.
[369] Trotsenko O, Tokarev A, Gruzd A, Enright T, Minko S. Magnetic field assisted assembly of highly ordered percolated nanostructures and their application for transparent conductive thin films. Nanoscale. 2015;7:7155–61.
[370] Lim J, Yeap SP, Low SC. Challenges associated to magnetic separation of nanomaterials at low field gradient. Sep. Purif. Technol. 2014;123:171–4.
[371] Lin Z, Fan X, Sun M, Gao C, He Q, Xie H. Magnetically actuated peanut colloid motors for cell manipulation and patterning. ACS Nano 2018;12:2539–45.
[372] Martínez-Pedrero F, Tierno P. Advances in colloidal manipulation and transport via hydrodynamic interactions. J. Colloid Interface Sci. 2018;519:296–311.
[373] Néel L. Théorie du traînage magnétique des ferromagnétiques en grains fins avec application aux terres cuites. Ann géophys 1949;5:99–136.
[374] Melle S. Study of the dynamics in MR suspensions subject to external fields by means of optical techniques: aggregation processes, structure formation and temporal evolution. Madrid: UNED; 2002.
[375] Janssen XJA, Schellekens AJ, van Ommering K, van Ijzendoorn LJ, Prins MWJ. Controlled torque on superparamagnetic beads for functional biosensors. Biosens. Bioelectron. 2009;24:1937–41.
[376] Helgesen G. Magnetic propulsion of microspheres at liquid-glass interfaces. J. Appl. Phys. 2018;123:064902.
[377] Massana-Cid H, Meng F, Matsunaga D, Golestanian R, Tierno P. Tunable self-healing of magnetically propelling colloidal carpets. Nat. Commun. 2019;10: 2444.
[378] Martin JE, Snezhko A. Driving self-assembly and emergent dynamics in colloidal suspensions by time-dependent magnetic fields. Rep. Prog. Phys. 2013;76: 126601.
[379] Osterman N, Poberaj I, Dobnikar J, Frenkel D, Ziherl P, Babić D. Field-induced self-assembly of suspended colloidal membranes. Phys. Rev. Lett. 2009;103: 228301.
[380] Moran JL, Posner JD. Phoretic self-propulsion. Annu. Rev. Fluid Mech. 2017;49: 511–40.
[381] Driscoll M, Delmotte B, Youssef M, Sacanna S, Donev A, Chaikin P. Unstable fronts and motile structures formed by microrollers. Nat. Phys. 2017;13:375–9.
[382] Yan J, Bloom M, Bae SC, Luijten E, Granick S. Linking synchronization to self-assembly using magnetic Janus colloids. Nature. 2012;491:578–81.
[383] Wen W, Zhang L, Sheng P. Planar magnetic colloidal crystals. Phys. Rev. Lett. 2000;85:5464–7.
[384] König H, Hund R, Zahn K, Maret G. Experimental realization of a model glass former in 2D. Eur. Phys J E. 2005;18:287–93.
[385] Faraudo J, Andreu JS, Calero C, Camacho J. Predicting the self-assembly of superparamagnetic colloids under magnetic fields. Adv. Funct. Mater. 2016;26: 3837–58.
[386] Mohebi M, Jamasbi N, Liu J. Simulation of the formation of nonequilibrium structures in magnetorheological fluids subject to an external magnetic field. Phys. Rev. E 1996;54:5407–13.
[387] Martínez-Pedrero F, Ortega F, Codina J, Calero C, Rubio RG. Controlled disassembly of colloidal aggregates confined at fluid interfaces using magnetic dipolar interactions. J. Colloid Interface Sci. 2020;560:388–97.
[388] Grzybowski BA, Whitesides GM. Dynamic aggregation of chiral spinners. Science. 2002;296:718–21.
[389] Wang W, Giltinan J, Zakharchenko S, Sitti M. Dynamic and programmable self-assembly of micro-rafts at the air-water interface. Sci. Adv. 2017;3:e1602522.
[390] Han K, Kokot G, Das S, Winkler RG, Gompper G, Snezhko A. Reconfigurable structure and tunable transport in synchronized active spinner materials. Sci. Adv. 2020;6:eaaz8535.
[391] Melle S, Martin JE. Chain model of a magnetorheological suspension in a rotating field. J. Chem. Phys. 2003;118:9875–81.
[392] Melle S, Calderón OG, Rubio MA, Fuller GG. Microstructure evolution in magnetorheological suspensions governed by Mason number. Phys. Rev. E 2003; 68:041503.
[393] Abdi H, Soheilian R, Erb RM, Maloney CE. Paramagnetic colloids: chaotic routes to clusters and molecules. Phys. Rev. E 2018;97:032601.
[394] Martínez-Pedrero F, González-Banciella A, Camino A, Mateos-Maroto A, Ortega F, Rubio RG, et al. Static and dynamic self-assembly of pearl-like-chains of magnetic colloids confined at fluid interfaces. Small. 2021;17:2101188.
[395] Grzybowski BA, Campbell CJ. Complexity and dynamic self-assembly. Chem. Eng. Sci. 2004;59:1667–76.
[396] Snezhko A, Belkin M, Aranson IS, Kwok WK. Self-assembled magnetic surface swimmers. Phys. Rev. Lett. 2009;102:118103.
[397] Najafi A, Golestanian R. Simple swimmer at low Reynolds number: Three linked spheres. Phys. Rev. E 2004;69:062901.
[398] Collard Y, Grosjean G, Vandewalle N. Magnetically powered metachronal waves induce locomotion in self-assemblies. Commun. Phys. 2020;3:112.
[399] Fei W, Driscoll MM, Chaikin PM, Bishop KJM. Magneto-capillary dynamics of amphiphilic Janus particles at curved liquid interfaces. Soft Matter 2018;14: 4661–5.
[400] Mateos-Maroto A, Ortega F, Rubio RG, Calero C, Martínez-Pedrero F. Modular interfacial microswimmers. Phys Rev Appl. 2021;16:064045.
[401] Mikkelsen A, Wojciechowski J, Rajňák M, Kurimský J, Khobaib K, Kertmen A, et al. Electric field-driven assembly of sulfonated polystyrene microspheres. Materials. 2017;10:329.
[402] Liljeström V, Chen C, Dommersnes P, Fossum JO, Gröschel AH. Active structuring of colloids through field-driven self-assembly. Curr. Opin. Colloid Interface Sci. 2019;40:25–41.

[403] Mittal M, Lele PP, Kaler EW, Furst EM. Polarization and interactions of colloidal particles in ac electric fields. J. Chem. Phys. 2008;129:064513.
[404] Nikolaides MG, Bausch AR, Hsu MF, Dinsmore AD, Brenner MP, Gay C, et al. Electric-field-induced capillary attraction between like-charged particles at liquid interfaces. Nature. 2002;420:299–301.
[405] Dommersnes P, Rozynek Z, Mikkelsen A, Castberg R, Kjerstad K, Hersvik K, et al. Active structuring of colloidal armour on liquid drops. Nature Comm. 2013;4:2066.
[406] Li M, Li D. Redistribution of charged aluminum nanoparticles on oil droplets in water in response to applied electrical field. J. Nanopart. Res. 2016;18:120.
[407] Nudurupati S, Janjua M, Aubry N, Singh P. Concentrating particles on drop surfaces using external electric fields. Electrophoresis. 2008;29:1164–72.
[408] Gangwal S, Cayre OJ, Bazant MZ, Velev OD. Induced-charge electrophoresis of metallodielectric particles. Phys. Rev. Lett. 2008;100:058302.
[409] Nudurupati S, Janjua M, Singh P, Aubry N. Effect of parameters on redistribution and removal of particles from drop surfaces. Soft Matter 2010;6:1157–69.
[410] Dommersnes P, Fossum JO. Surface structuring of particle laden drops using electric fields. Eur Phys J Special Topics. 2016;225:715–28.
[411] Eigenbrod M, Bihler F, Hardt S. Electrokinetics of a particle attached to a fluid interface: Electrophoretic mobility and interfacial deformation. Phys Rev Fluids. 2018;3:103701.
[412] Danov KD, Kralchevsky PA. Forces acting on dielectric colloidal spheres at a water/nonpolar fluid interface in an external electric field. 2. Charged particles. J. Colloid Interface Sci. 2013;405:269–77.
[413] Jia Y, Huang R, Lan Y, Ren Y, Jiang H, Lee D. Reversible aggregation and dispersion of particles at a liquid–liquid interface using space charge injection. Adv. Mater. Interfaces 2019;6:1801920.
[414] Howse JR, Jones RAL, Ryan AJ, Gough T, Vafabakhsh R, Golestanian R. Self-motile colloidal particles: from directed propulsion to random walk. Phys. Rev. Lett. 2007;99:048102.
[415] Jiang H-R, Yoshinaga N, Sano M. Active motion of a janus particle by self-thermophoresis in a defocused laser beam. Phys. Rev. Lett. 2010;105:268302.
[416] Bricard A, Caussin J-B, Desreumaux N, Dauchot O, Bartolo D. Emergence of macroscopic directed motion in populations of motile colloids. Nature. 2013;503:95–8.
[417] Wang R, Guo W, Li X, Liu Z, Liu H, Ding S. Highly efficient MOF-based self-propelled micromotors for water purification. RSC Adv. 2017;7:42462–7.
[418] Dietrich K, Jaensson N, Buttinoni I, Volpe G, Isa L. Microscale Marangoni surfers. Phys. Rev. Lett. 2020;125:098001.
[419] Wang AZ, Langer R, Farokhzad OC. Nanoparticle delivery of cancer drugs. Annu. Rev. Med. 2012;63:185–98.
[420] El-Ali J, Sorger PK, Jensen KF. Cells on chips. Nature. 2006;442:403–11.
[421] Jurado-Sánchez B, Sattayasamitsathit S, Gao W, Santos L, Fedorak Y, Singh VV, et al. Self-propelled activated carbon janus micromotors for efficient water purification. Small. 2015;11:499–506.
[422] Baraban L, Tasinkevych M, Popescu MN, Sanchez S, Dietrich S, Schmidt OG. Transport of cargo by catalytic Janus micro-motors. Soft Matter 2012;8:48–52.
[423] Janssen LMC. Active glasses. J. Phys. Condens. Matter 2019;31:503002.
[424] Buttinoni I, Bialké J, Kümmel F, Löwen H, Bechinger C, Speck T. Dynamical clustering and phase separation in suspensions of self-propelled colloidal particles. Phys. Rev. Lett. 2013;110:238301.
[425] Kümmel F, Shabestari P, Lozano C, Volpe G, Bechinger C. Formation, compression and surface melting of colloidal clusters by active particles. Soft Matter 2015;11:6187–91.
[426] Maggi C, Simmchen J, Saglimbeni F, Katuri J, Dipalo M, De Angelis F, et al. Self-assembly of micromachining systems powered by janus micromotors. Small. 2016;12:446–51.
[427] Stenhammar J, Wittkowski R, Marenduzzo D, Cates ME. Activity-induced phase separation and self-assembly in mixtures of active and passive particles. Phys. Rev. Lett. 2015;114:018301.
[428] Bregulla AP, Yang H, Cichos F. Stochastic localization of microswimmers by photon nudging. ACS Nano 2014;8:6542–50.
[429] Bregulla AP, Yang H, Cichos F. Stochastic localization of microswimmers by photon nudging. ACS Nano 2014;8:6542–50.
[430] Dietrich K, Renggli D, Zanini M, Volpe G, Buttinoni I, Isa L. Two-dimensional nature of the active Brownian motion of catalytic microswimmers at solid and liquid interfaces. New J. Phys. 2017;19:065008.
[431] Simmchen J, Katuri J, Uspal WE, Popescu MN, Tasinkevych M, Sánchez S. Topographical pathways guide chemical microswimmers. Nature Comm. 2016;7:10598.
[432] Palacios LS, Katuri J, Pagonabarraga I, Sánchez S. Guidance of active particles at liquid–liquid interfaces near surfaces. Soft Matter 2019;15:6581–8.
[433] Palacios LS, Katuri J, Pagonabarraga I, Sánchez S. Guidance of active particles at liquid–liquid interfaces near surfaces. Soft Matter 2019;15:6581–8.
[434] Jalilvand Z, Haider H, Cui J, Kretzschmar Ilona. Pt-SiO2 janus particles and the water/oil interface: a competition between motility and thermodynamics. Langmuir. 2020;36:6880–7.
[435] Wang X, In M, Blanc C, Würger A, Nobili M, Stocco A. Janus colloids actively rotating on the surface of water. Langmuir. 2017;33:13766–73.
[436] Pototsky A, Thiele U, Stark H. Stability of liquid films covered by a carpet of self-propelled surfactant particles. Phys. Rev. E 2014;90:030401.
[437] Domínguez A, Malgaretti P, Popescu MN, Dietrich S. Collective dynamics of chemically active particles trapped at a fluid interface. Soft Matter 2016;12:8398–406.
[438] Domínguez A, Popescu MN. Phase coexistence in a monolayer of active particles induced by Marangoni flows. Soft Matter 2018;14:8017–29.
[439] Grzybowski BA, Fitzner K, Paczesny J, Granick S. From dynamic self-assembly to networked chemical systems. Chem. Soc. Rev. 2017;46:5647–78.
[440] Tretiakov KV, Bishop KJM, Grzybowski BA. The dependence between forces and dissipation rates mediating dynamic self-assembly. Soft Matter 2009;5:1279–84.
[441] Goto Y, Tanaka H. Purely hydrodynamic ordering of rotating disks at a finite Reynolds number. Nat. Commun. 2015;6:5994.
[442] Shen Z, Lintuvuori JS. Two-phase crystallization in a carpet of inertial spinners. Phys. Rev. Lett. 2020;125:228002.
[443] Kapral R. Multiparticle collision dynamics: simulation of complex systems on mesoscales. Adv. Chem. Phys. 2008:89–146.
[444] Götze IO, Gompper G. Dynamic self-assembly and directed flow of rotating colloids in microchannels. Phys. Rev. E 2011;84:031404.
[445] Belkin M, Snezhko A, Aranson IS, Kwok WK. Driven magnetic particles on a fluid surface: pattern assisted surface flows. Phys. Rev. Lett. 2007;99:158301.
[446] Martínez-Pedrero F, Ortega F, Rubio RG, Calero C. Collective transport of magnetic microparticles at a fluid interface through dynamic self-assembled lattices. Adv. Funct. Mater. 2020;30:2002206.
[447] Tailleur J, Cates ME. Statistical mechanics of interacting run-and-tumble bacteria. Phys. Rev. Lett. 2008;100:218103.
[448] Fily Y, Marchetti MC. Athermal phase separation of self-propelled particles with no alignment. Phys. Rev. Lett. 2012;108:235702.
[449] Redner GS, Hagan MF, Baskaran A. Structure and dynamics of a phase-separating active colloidal fluid. Phys. Rev. Lett. 2013;110:055701.
[450] Redner GS, Baskaran A, Hagan MF. Reentrant phase behavior in active colloids with attraction. Phys. Rev. E 2013;88:012305.
[451] Toner J, Tu Y, Ramaswamy S. Hydrodynamics and phases of flocks. Ann. Phys. 2005;318:170–244.
[452] Chaté H, Ginelli F, Montagne R. Simple model for active nematics: quasi-long-range order and giant fluctuations. Phys. Rev. Lett. 2006;96:180602.
[453] Palacci J, Sacanna S, Steinberg AP, Pine DJ, Chaikin PM. Living crystals of light-activated colloidal surfers. Science. 2013;339:936–40.
[454] Buttinoni I, Bialké J, Kümmel F, Löwen H, Bechinger C, Speck T. Dynamical clustering and phase separation in suspensions of self-propelled colloidal particles. Phys. Rev. Lett. 2013;110:238301.
[455] Takatori SC, Yan W, Brady JF. Swim pressure: stress generation in active matter. Phys. Rev. Lett. 2014;113:028103.
[456] Takatori SC, Brady JF. Towards a thermodynamics of active matter. Phys. Rev. E 2015;91:032117.
[457] Solon AP, Fily Y, Baskaran A, Cates ME, Kafri Y, Kardar M, et al. Pressure is not a state function for generic active fluids. Nat. Phys. 2015;11:673–8.
[458] Solon AP, Stenhammar J, Wittkowski R, Kardar M, Kafri Y, Cates ME, et al. Pressure and phase equilibria in interacting active Brownian Spheres. Phys. Rev. Lett. 2015;114:198301.
[459] Wittkowski R, Tiribocchi A, Stenhammar J, Allen RJ, Marenduzzo D, Cates ME. Scalar φ4 field theory for active-particle phase separation. Nat. Commun. 2014;5:4351.
[460] Stenhammar J, Tiribocchi A, Allen RJ, Marenduzzo D, Cates ME. Continuum theory of phase separation kinetics for active Brownian particles. Phys. Rev. Lett. 2013;111:145702.
[461] Levis D, Codina J, Pagonabarraga I. Active Brownian equation of state: metastability and phase coexistence. Soft Matter 2017;13:8113–9.
[462] Tung C, Harder J, Valeriani C, Cacciuto A. Micro-phase separation in two dimensional suspensions of self-propelled spheres and dumbbells. Soft Matter 2016;12:555–61.
[463] Lauga E, Powers TR. The hydrodynamics of swimming microorganisms. Rep. Prog. Phys. 2009;72:096601.
[464] Peruani F, Deutsch A, Bär M. Nonequilibrium clustering of self-propelled rods. Phys. Rev. E 2006;74:030904.
[465] Czirók A, Stanley HE, Vicsek T. Spontaneously ordered motion of self-propelled particles. J. Phys. A Math. Gen. 1997;30:1375–85.
[466] Ramaswamy S. The mechanics and statistics of active matter. Ann. Rev. Condens. Matter. Physics. 2010;1:323–45.
[467] Solon AP, Chaté H, Tailleur J. From phase to microphase separation in flocking models: the essential role of nonequilibrium fluctuations. Phys. Rev. Lett. 2015;114:068101.
[468] Onsager L. Reciprocal relations in irreversible processes. I. Physical Rev. 1931;37:405–26.
[469] Doi M. Onsager's variational principle in soft matter. J. Phys. Condens. Matter 2011;23:284118.
[470] Prigogine I, Nicolis G. Self-organisation in nonequilibrium systems: towards a dynamics of complexity. In: Hazewinkel M, Jurkovich R, Paelinck JHP, editors. Bifurcation Analysis: Principles, Applications and Synthesis. Dordrecht: Springer Netherlands; 1985. p. 3–12.
[471] Tretiakov KV, Szleifer I, Grzybowski BA. The rate of energy dissipation determines probabilities of non-equilibrium assemblies. Angew. Chem. Int. Ed. 2013;52:10304–8.
[472] Evans DJ, Baranyai A. Possible variational principle for steady states far from equilibrium. Phys. Rev. Lett. 1991;67:2597–600.
[473] Brey JJ, Santos A, Garzó V. Analysis of the Evans and Baranyai variational principle in dilute gases. Phys. Rev. Lett. 1993;70:2730–3.
[474] Dewar RC. Maximum entropy production and the fluctuation theorem. J. Phys. A Math. Gen. 2005;38. L371-L81.
[475] Dewar R. Information theory explanation of the fluctuation theorem, maximum entropy production and self-organized criticality in non-equilibrium stationary states. J. Phys. A Math. Gen. 2003;36:631–41.

[476] Attard P. The second entropy: a general theory for non-equilibrium thermodynamics and statistical mechanics. Ann. Rep. Section "C" (Physical Chem.). 2009;105:63–173.
[477] Arango-Restrepo A, Rubi JM, Barragán D. The role of energy and matter dissipation in determining the architecture of self-assembled structures. J. Phys. Chem. B 2019;123:5902–8.
[478] Arango-Restrepo A, Barragán D, Rubi JM. A criterion for the formation of nonequilibrium self-assembled structures. J. Phys. Chem. B 2021;125:1838–45.
[479] Lucia A, Toloza AC, Guzmán E, Ortega F, Rubio RG. Novel polymeric micelles for insect pest control: encapsulation of essential oil monoterpenes inside a triblock copolymer shell for head lice control. PeerJ. 2017;5:e3171.
[480] Horozov TS, Aveyard R, Clint JH, Neumann B. Particle zips: vertical emulsion films with particle monolayers at their surfaces. Langmuir. 2005;21:2330–41.
[481] Cervantes-Martinez A, Rio E, Delon G, Saint-Jalmes A, Langevin D, Binks BP. On the origin of the remarkable stability of aqueous foams stabilised by nanoparticles: link with microscopic surface properties. Soft Matter 2008;4:1531–5.
[482] Bhamla MS, Giacomin CE, Balemans C, Fuller GG. Influence of interfacial rheology on drainage from curved surfaces. Soft Matter 2014;10:6917–25.
[483] Sullivan AP, Kilpatrick PK. The effects of inorganic solid particles on water and crude oil emulsion stability. Ind. Eng. Chem. Res. 2002;41:3389–404.
[484] Harbottle D, Chen Q, Moorthy K, Wang L, Xu S, Liu Q, et al. Problematic stabilizing films in petroleum emulsions: shear rheological response of viscoelastic asphaltene films and the effect on drop coalescence. Langmuir. 2014;30:6730–8.
[485] Binks BP, Rodrigues JA. Double inversion of emulsions by using nanoparticles and a di-chain surfactant. Angew. Chem. Int. Ed. 2007;46:5389–92.
[486] Kostakis T, Ettelaie R, Morray SB. Effect of high salt concentrations on the stabilization of bubbles by silica particles. Langmuir. 2006;22:1273–80.
[487] Studart AR, Gonzenbach UT, Tervoort E, Gauckler LJ. Processing routes to macroporous ceramics: a review. J. Am. Ceram. Soc. 2006;89:1771–89.
[488] Gonzenbach UT, Studart AR, Tervoort E, Gauckler LJ. Ultrastable particle-stabilized foams. Angew. Chem. Int. Ed. 2006;118:3606–10. https://doi.org/10.1002/ange.200503676.
[489] Gallo A, Tavares F, Das R, Mishra H. How particle–particle and liquid–particle interactions govern the fate of evaporating liquid marbles. Soft Matter 2021;17:7628–44.
[490] Saczek J, Yao X, Zivkovic V, Mamlouk M, Wang D, Pramana SS, et al. Long-lived liquid marbles for green applications. Adv. Funct. Mater. 2021;31:2011198.
[491] Yu K, Li B, Zhang H, Wang Z, Zhang W, Wang D, et al. Critical role of nanocomposites at air–water interface: From aqueous foams to foam-based lightweight functional materials. Chem. Eng. J. 2021;416:129121.
[492] Santos T, Machado VVS, Borges OH, Salvini VR, Parr C, Pandolfelli VC. Calcium aluminate cement aqueous suspensions as binders for Al2O3-based particle stabilised foams. Ceram. Int. 2021;47:8398–407.
[493] Finhana IC, Machado VVS, Santos T, Borges OH, Salvini VR, Pandolfelli VC. Direct foaming of macroporous ceramics containing colloidal alumina. Ceram. Int. 2021;47:15237–44.
[494] Dinsmore AD, Hsu MF, Nikolaides MG, Marquez M, Bausch AR, Weitz DA. Colloidosomes: selectively permeable capsules composed of colloidal particles. Science. 2002;298:1006–9.
[495] Yow HN, Routh AF. Release profiles of encapsulated actives from colloidosomes sintered for various durations. Langmuir. 2009;25:159–66.
[496] López-de-Luzuriaga JM, Monge M, Quintana J, Rodríguez-Castillo M. Single-step assembly of gold nanoparticles into plasmonic colloidosomes at the interface of oleic acid nanodroplets. Nanoscale Adv. 2021;3:198–205.
[497] Gordon VD, Chen X, Hutchinson JW, Bausch AR, Marquez M, Weitz DA. Self-assembled polymer membrane capsules inflated by osmotic pressure. J. Am. Chem. Soc. 2004;126:14117–22.
[498] Guzmán E, Rubio RG, Ortega F. A closer physico-chemical look to the Layer-by-Layer electrostatic self-assembly of polyelectrolyte multilayers. Adv. Colloid Interf. Sci. 2020;282:102197.
[499] Guzmán E, Mateos-Maroto A, Ruano M, Ortega F, Rubio RG. Layer-by-Layer polyelectrolyte assemblies for encapsulation and release of active compounds. Adv. Colloid Interf. Sci. 2017;249:290–307.
[500] Cayre OJ, Noble PF, Paunov VN. Fabrication of novel colloidosome microcapsules with gelled aqueous cores. J. Mater. Chem. 2004;14:3351–5.
[501] Chen Y, Wang C, Chen J, Liu X, Tong Z. Growth of lightly crosslinked PHEMA brushes and capsule formation using pickering emulsion interface-initiated ATRP. J. Polym. Sci. A. 2009;47:1354–67.
[502] Bon SAF, Cauvin S, Colver PJ. Colloidosomes as micron-sized polymerisation vessels to create supracolloidal interpenetrating polymer network reinforced capsules. Soft Matter 2007;3:194–9.
[503] Cayre OJ, Biggs S. Hollow microspheres with binary porous membranes from solid-stabilised emulsion templates. J. Mater. Chem. 2009;19:2724–8.
[504] Cayre OJ, Biggs S. Hollow microspheres with binary colloidal and polymeric membrane: effect of polymer and particle concentrations. Adv. Powder Technol. 2010;21:19–22.
[505] Yin D, Zhang Q, Yin C, Zhao X, Zhang H. Hollow microspheres with covalent-bonded colloidal and polymeric shell by Pickering emulsion polymerization. Polym. Adv. Technol. 2012;23:273–7.
[506] Thompson KL, Williams M, Armes SP. Colloidosomes: synthesis, properties and applications. J. Colloid Interface Sci. 2015;447:217–28.
[507] Croll LM, Stöver HDH. Mechanism of self-assembly and rupture of cross-linked microspheres and microgels at the oil−water interface. Langmuir. 2003;19:10077–80.
[508] Lin Y, Skaff H, Böker A, Dinsmore AD, Emrick T, Russell TP. Ultrathin cross-linked nanoparticle membranes. J. Am. Chem. Soc. 2003;125:12690–1.
[509] Skaff H, Lin Y, Tangirala R, Breitenkamp K, Böker A, Russell TP, et al. Crosslinked capsules of quantum dots by interfacial assembly and ligand crosslinking. Adv. Mater. 2005;17:2082–6.
[510] Arumugam P, Patra D, Samanta B, Agasti SS, Subramani C, Rotello VM. Self-assembly and cross-linking of FePt nanoparticles at planar and colloidal liquid-liquid interfaces. J. Am. Chem. Soc. 2008;130:10046–7.
[511] Shah RK, Kim J-W, Weitz DA. Monodisperse stimuli-responsive colloidosomes by self-assembly of microgels in droplets. Langmuir. 2010;26:1561–5.
[512] Walsh A, Thompson KL, Armes SP, York DW. Polyamine-functional sterically stabilized latexes for covalently cross-linkable colloidosomes. Langmuir. 2010;26:18039–48.
[513] Cui Y, van Duijneveldt JS. Microcapsules composed of cross-linked organoclay. Langmuir. 2012;28:1753–7.
[514] Williams M, Armes SP, York DW. Clay-based colloidosomes. Langmuir. 2012;28:1142–8.
[515] Williams M, Armes SP, Verstraete P, Smets J. Double emulsions and colloidosomes-in-colloidosomes using silica-based pickering emulsifiers. Langmuir. 2014;30:2703–11.
[516] Yuan Q, Cayre OJ, Fujii S, Armes SP, Williams RA, Biggs S. Responsive core−shell latex particles as colloidosome microcapsule membranes. Langmuir. 2010;26:18408–14.
[517] Majumder M, Rendall C, Li M, Behabtu N, Eukel JA, Hauge RH, et al. Insights into the physics of spray coating of SWNT films. Chem. Eng. Commun. 2010;65:2000–8.
[518] Chung S, Karim MAU, Spencer M, Kwon H-J, Grigoropoulos CP, Alon E, et al. Exploitation of the coffee-ring effect to realize mechanically enhanced inkjet-printed microelectromechanical relays with U-bar-shaped cantilevers. Appl. Phys. Lett. 2014;105:261901.
[519] Sefiane K. On the formation of regular patterns from drying droplets and their potential use for bio-medical applications. J Bionic Eng. 2010;7:S82–93.
[520] Wen JT, Ho CM, Lillehoj PB. Coffee ring aptasensor for rapid protein detection. Langmuir. 2013;29:8440–6.
[521] Kong YL, Tamargo IA, Kim H, Johnson BN, Gupta MK, Koh TW, et al. 3D printed quantum dot light-emitting diodes. Nano Lett. 2014;14:7017–23.
[522] Wu J, Wang R, Yu H, Li G, Xu K, Tien NC, et al. Inkjet-printed microelectrodes on PDMS as biosensors for functionalized microfluidic systems. Lab Chip 2015;15:690–5.
[523] Fang X, Li B, Petersen E, Seo YS, Samuilov VA, Chen Y, et al. Drying of DNA droplets. Langmuir. 2006;22:6308–12.
[524] Jin H, Qian J, Zhou L, Yuan J, Huang H, Wang Y, et al. Suppressing the coffee-ring effect in semitransparent MnO2 film for a high-performance solar-powered energy storage window. ACS Appl. Mater. Interfaces 2016;8:9088–96.
[525] Bigioni TP, Lin X-M, Nguyen TT, Corwin EI, Witten TA, Jaeger HM. Kinetically driven self assembly of highly ordered nanoparticle monolayers. Nature Mat. 2006;5:265–70.
[526] Boley JW, Hyun S-H, White EL, Thompson DH, Kramer RK. Hybrid self-assembly during evaporation enables drop-on-demand thin film devices. ACS Appl. Mater. Interfaces 2016;8:34171–8.
[527] Li Y, Yang Q, Li M, Song Y. Rate-dependent interface capture beyond the coffee-ring effect. Sci. Rep. 2016;6:24628.
[528] Yunker PJ, Still T, Lohr MA, Yodh AG. Suppression of the coffee-ring effect by shape-dependent capillary interactions. Nature. 2011;476:308–11.
[529] Kim D-O, Pack M, Hu H, Kim H, Sun Y. Deposition of colloidal drops containing ellipsoidal particles: competition between capillary and hydrodynamic forces. Langmuir. 2016;32:11899–906.
[530] Parthasarathy D, Thampi SP, Ravindran P, Basavaraj MG. Further insights into patterns from drying particle laden sessile drops. Langmuir. 2021;37:4395–402.
[531] Al-Milaji KN, Secondo RR, Ng TN, Kinsey N, Zhao H. Interfacial self-assembly of colloidal nanoparticles in dual-droplet inkjet printing. Adv. Mater. Interfaces 2018;5:1701561.
[532] Al-Milaji KN, Radhakrishnan V, Kamerkar P, Zhao H. pH-modulated self-assembly of colloidal nanoparticles in a dual-droplet inkjet printing process. J. Colloid Interface Sci. 2018;529:234–42.
[533] Nath G, Ray B. Manipulating the three-phase contact line of an evaporating particle-laden droplet to get desirable microstructures: a lattice Boltzmann study. Phys. Fluids 2021;33:083304.
[534] Bechinger C, Di Leonardo R, Löwen H, Reichhardt C, Volpe G, Volpe G. Active particles in complex and crowded environments. Rev. Mod. Phys. 2016;88:045006.
[535] Bertsch P, Bergfreund J, Windhab EJ, Fischer P. Physiological fluid interfaces: functional microenvironments, drug delivery targets, and first line of defense. Acta Biomater. 2021;130:32–53.